University of Windsor
Scholarship at UWindsor

Electronic Theses and Dissertations

1997

Improving the performance of soil-metal structures subjected to loss of soil support.

Karlos Ernesto. Melgar
University of Windsor

Follow this and additional works at: http://scholar.uwindsor.ca/etd

Recommended Citation
Melgar, Karlos Ernesto., "Improving the performance of soil-metal structures subjected to loss of soil support." (1997). *Electronic Theses and Dissertations.* Paper 2407.

This online database contains the full-text of PhD dissertations and Masters' theses of University of Windsor students from 1954 forward. These documents are made available for personal study and research purposes only, in accordance with the Canadian Copyright Act and the Creative Commons license—CC BY-NC-ND (Attribution, Non-Commercial, No Derivative Works). Under this license, works must always be attributed to the copyright holder (original author), cannot be used for any commercial purposes, and may not be altered. Any other use would require the permission of the copyright holder. Students may inquire about withdrawing their dissertation and/or thesis from this database. For additional inquiries, please contact the repository administrator via email (scholarship@uwindsor.ca) or by telephone at 519-253-3000ext. 3208.

INFORMATION TO USERS

This manuscript has been reproduced from the microfilm master. UMI films the text directly from the original or copy submitted. Thus, some thesis and dissertation copies are in typewriter face, while others may be from any type of computer printer.

The quality of this reproduction is dependent upon the quality of the copy submitted. Broken or indistinct print, colored or poor quality illustrations and photographs, print bleedthrough, substandard margins, and improper alignment can adversely affect reproduction.

In the unlikely event that the author did not send UMI a complete manuscript and there are missing pages, these will be noted. Also, if unauthorized copyright material had to be removed, a note will indicate the deletion.

Oversize materials (e.g., maps, drawings, charts) are reproduced by sectioning the original, beginning at the upper left-hand corner and continuing from left to right in equal sections with small overlaps. Each original is also photographed in one exposure and is included in reduced form at the back of the book.

Photographs included in the original manuscript have been reproduced xerographically in this copy. Higher quality 6" x 9" black and white photographic prints are available for any photographs or illustrations appearing in this copy for an additional charge. Contact UMI directly to order.

UMI

A Bell & Howell Information Company
300 North Zeeb Road, Ann Arbor MI 48106-1346 USA
313/761-4700 800/521-0600

IMPROVING THE PERFORMANCE

OF

SOIL-METAL STRUCTURES

SUBJECTED TO LOSS OF SOIL SUPPORT

by

KARLOS MELGAR

A Thesis Submitted
to the
College of Graduate Studies and Research
through the
Department of Civil and Environmental Engineering
in
Partial Fulfilment of the Requirements
for the
Degree of Master of Applied Science in Civil Engineering
at
The University of Windsor

Windsor, Ontario, Canada
October, 1997

National Library of Canada
Bibliothèque nationale du Canada

Acquisitions and Bibliographic Services
Acquisitions et services bibliographiques

395 Wellington Street
Ottawa ON K1A 0N4
Canada

395, rue Wellington
Ottawa ON K1A 0N4
Canada

Your file Votre référence

Our file Notre référence

The author has granted a non-exclusive licence allowing the National Library of Canada to reproduce, loan, distribute or sell copies of this thesis in microform, paper or electronic formats.

L'auteur a accordé une licence non exclusive permettant à la Bibliothèque nationale du Canada de reproduire, prêter, distribuer ou vendre des copies de cette thèse sous la forme de microfiche/film, de reproduction sur papier ou sur format électronique.

The author retains ownership of the copyright in this thesis. Neither the thesis nor substantial extracts from it may be printed or otherwise reproduced without the author's permission.

L'auteur conserve la propriété du droit d'auteur qui protège cette thèse. Ni la thèse ni des extraits substantiels de celle-ci ne doivent être imprimés ou autrement reproduits sans son autorisation.

0-612-30977-0

Canada

© KARLOS MELGAR, 1997

I hereby declare that I am the sole author of this thesis. I authorise the University of Windsor to lend this thesis to other institutions or individuals for the purpose of scholarly research.

KARLOS MELGAR

I further authorise the University of Windsor to reproduce this thesis by photocopying or by other means, in total or in part, at the request of other institutions or individuals for the purpose of scholarly research.

KARLOS MELGAR

ABSTRACT

Years of dependable service and a multitude of wide ranging installations have led to the corrugated steel pipe industry to play a major role in modern engineering technology. Flexible steel conduits play an important role in the form of culverts, storm sewers, subdrains, spillways, underpasses, conveyor conduits and service tunnels; for highways, railways, airports, municipalities, recreation areas, industrial parks, flood and conservation projects, water pollution abatement and many other programs.

In recent years developments have been made which allow engineers and contractors the use of conventional corrugated structural plates to design and build structures having larger spans and increased permissible live and dead loads.

These structures are generally used for conditions where the depth-of-cover is limited to about 5 to 10 m and the design is constrained by a relatively low, wide-opening.

However, in recent years many accidents and sudden failures have been reported on this type of structure. Such failures often originate from large soil settlements, poor soil compacting practices, and frost-thaw cycles. As a result, many different methods have been proposed to eliminate these problems. In this thesis the use of a Geogrid mesh to reinforce the soil surrounding the corrugated metal structure is proposed. It is the belief of the author that this material (Geogrid), which is widely used in the design and construction of retaining walls, will improve the strength and durability of soil-metal structures.

The study carried out involved building and testing pipe-arches under shallow depth-of cover. The results obtained from these tests served to compare and document the advantage of using reinforced soil structures in contrast to non-reinforced soil structures.

FIRST AND FOREMOST TO GOD

TO MY PARENTS AND SISTERS

ACKNOWLEDGEMENTS

The author wishes to acknowledge Dr. J. B. Kennedy for his important suggestions and encouragement, to him I say: thanks your invaluable advice will be remembered always.

Also, the author likes to thank the staff of the Technical Research Centre and Richard Clark for their continuous help and support during this investigation.

Last but not least, the author likes to thank his parents and sisters for their continuous support and encouragement.

LIST OF CONTENTS

LIST OF TABLES

LIST OF FIGURES

CHAPTER I

INTRODUCTION

1.1 General

A culvert is usually, although not always, differentiated from a bridge by virtue of the fact that the top of the culvert does not form a part of the travelled roadway. More frequently, culverts are differentiated from bridges on the basis of span length. Culverts also differ from bridges in that they are usually designed to flow full under certain conditions, while bridges are designed to pass floating debris or vessels.

There are two types of culverts; these are flexible culverts and rigid culverts. Flexible culverts are either thin-walled steel pipes or galvanised corrugated metal pipes; they rely only partly on the strength of the pipe walls to resist the external loads, and they are designed to deflect under the loads. When deflection takes place, the horizontal diameter of the culvert increases and compresses the soil at the sides and in this manner the passive resistance of the soil is triggered to help support the applied loads. When failure of a flexible culvert does occur it is primarily because of excessive deflection. In contrast to the flexible pipes, rigid culverts are composed of reinforced concrete, cast iron or vitrified clay and their load-carrying ability is primarily a function of the stiffness of the walls of the culverts. When failure does occur it is usually due to rupture of the walls of the culvert.

Corrugated metal plate pipes can be divided generically into two categories, namely, those that are manufactured in closed pipe shapes and those that are assembled on site

from curved corrugated plates. The structures in the former category are referred to as corrugated steel pipe and are normally of smaller diameter than those of the latter category, which are usually referred to as structural plate corrugated steel pipes.

New technology has allowed engineers and designers to use these structures for longer spans and under relatively shallow soil cover conditions. However, under these conditions the surrounding soil may not provide enough support for the structure. This in turn allows the structure to move more freely and therefore increase its deformations. The lack of sufficient support for the structure also gives rise to a considerable increase in the bending moments in the structure as well as in its susceptibility to sudden buckling failure.

Through the years many of these structures have failed because of inadequate support provided by the surrounding soil. Failures of two structures were reported and documented. The first failure occurred in Ohio and the second one in Ontario [33]. What is most unfortunate is that they both involved the loss of lives due to their sudden failures. In 1986 Moore [33] inspected 141 soil steel structures in the county of Elgin, Ontario. Moore found that 56 out of the 141 structures showed some sign of distress. Some of the signs of distress found are:

1. Joint Failure.
2. Excessive deformation of the culvert's crown.
3. Lifting of the invert of the metal structure.
4. Crimp formation.
5. Excessive distortion in some culverts.

Several techniques have been suggested in trying to overcome the side effects of building long span structures under shallow soil cover conditions. These different techniques can be grouped as follows [3]:

1. Techniques that reduce load effects, in particular the thrust , in the conduit wall.
2. Techniques that increase the strength of the conduit wall by reinforcing it.
3. Techniques that increase the strength of the conduit wall by stiffening the soil and thus enhancing the stiffness of the radial support to the conduit wall.

The first two techniques make the structure stronger by means of adding stiffeners or by introducing relieving slabs over the metallic structure [16]. This approach, although widely used proves to be rather expensive and will lead to divert more external load to the metallic structure and less load to the surrounding soil. This in turn will decrease the number of load paths.

On the other hand a less expensive and better method is represented by the third technique, accomplished by cementing the soil [10], using thrust beams [12], or reinforcing the soil by means of flat bars [22]. Many studies have been conducted on scale models that have proved the effectiveness of increasing the strength of the structure and the load bearing capacity of the soil and thus reducing the probability of catastrophic/sudden failure of soil-metal structures.

1.2 Objective and Scope

In general, out of all the different shapes of structural plate corrugated steel pipes that are fabricated, none requires more care and attention than the Pipe-arch. Pipe-arches (see Figure 1.1) are more prone to distress than other soil-steel bridges mainly because the radius of curvature of the haunch segments of the conduit wall is significantly smaller than the radius of curvature of the invert segment, as well as the soil under the haunches is usually very difficult to compact properly. Nevertheless, Pipe-arches have become widely used throughout North America in the construction of highway bridges and drainage structures. With an increasing demand for using this type of structure a need for a more reliable design method exists; one that prevents sudden and/or catastrophic failure of the structure. This study examines and compares the behaviour of reinforced-soil and unreinforced-soil pipe-arches during the following stages:

1. Construction and placement of the structure
2. Loading of structure (externally applied loads)
3. Failure of the soil surrounding the haunches of the structure

To accomplish this, experimental work was carried out to compare and analyse the effect of reinforcing the soil under the conditions mentioned above.

The objectives of this research are as follows:

1. To study the behaviour of unreinforced-soil pipe-arches during the three stages mentioned earlier.

2. To study the behaviour of reinforced-soil pipe-arches during the three stages mentioned earlier.
3. To compare and document the behaviour of unreinforced-soil and reinforced-soil pipe-arches.

Figure 1.1 Pipe-Arch Components

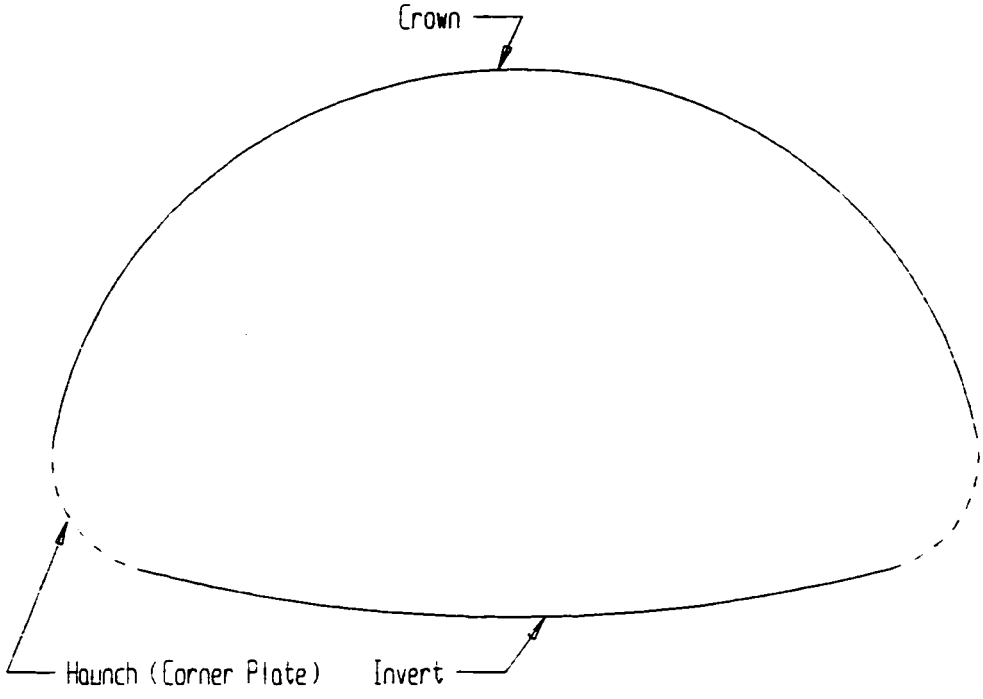

CHAPTER II

LITERATURE REVIEW

This chapter reviews the previous research in the area of soil-metal structures, reinforced earth and buckling of soil-metal structures. Also, previous research in the area of non-biodegradable materials as an alternative to metal strips for reinforcing the soil in soil-metal structures is reviewed.

2.1 Soil-Metal Structures

Soil-metal structures have been built for many years. However, a great number of conflicting theories concerning their analysis and design still remain. Some of the acceptable theories are presented in this section.

M. G. Sprangler (1941) [40] observed that the Martson theory [31] for calculating loads on buried pipes was not adequate for flexible pipe design. Sprangler noted that flexible pipes provided little inherent stiffness in comparison to rigid pipes, yet they perform remarkably well when buried in soil. This significant ability of a flexible pipe to support vertical soil loads is derived from (a) the redistribution of loads around the pipe, and (b) the passive pressures induced as the sides of the pipe move outward against the surrounding soil.

Sprangler incorporated the effects of the surrounding soil on the pipe's deflection. This was accomplished by assuming that the loads applied would be uniformly distributed

on the plane at the top of the pipe. He also assumed a uniform pressure over part of the bottom, depending upon the bedding angle. On the sides, he assumed the horizontal pressure on each side would be proportional to the deflection of the pipe into the soil. The constant of proportionality was defined as shown in Figure 2.1 and was called the modulus of passive resistance of the soil. The modulus would presumably be a constant for a given soil and could be measured in a simple laboratory test. Through analysis he derived the following Iowa formula:

$$\Delta X = \frac{D_L K W_C r^3}{E I + 0.061 e r^4} \qquad (2\text{-}1)$$

where,

D_L = deflection lag factor

K = bedding constant

W_C = Martson's load per unit length of pipe, lb/in

r = mean radius of the pipe, in

E = modulus of elasticity of pipe material, lb/in^2

I = moment of inertia of the pipe wall per unit length, in^4/in

e = modulus of passive resistance of the side fill, $lb/(in^2)(in)$

ΔX = horizontal deflection or change in diameter, in

Reynold K. Watkins (1966) [45], investigated the modulus of passive resistance through model studies and examined the Iowa formula. As a result of Watkins effort, another soil parameter was defined. This was the modulus of soil reaction

$$E' = e\, r \tag{2-2}$$

Consequently, a new formula called the modified Iowa formula was proposed.

$$\Delta X = \frac{D_L\, K\, W_C\, r^3}{E\, I + 0.061\, E'\, r^3} \tag{2-3}$$

Two observations from Watkins' work are of particular note: (a) There is little point in evaluating E' by a model test and then using this modulus to predict ring deflection, since the model gives ring deflection directly. (b) Ring deflection may not be the only performance limit.

Work performed by White (1960) [47] showed that the deflection of underground conduits does not govern the design , but wall strength does. He introduced the so-called "ring compression theory", assuming that the tangential compressive stress σ_c in a conduit wall is less than the yield stress of the wall material as shown:

$$\sigma_c = \frac{W_c\, S}{2\, A_r} \quad < \quad F_y \tag{2-4}$$

where,

W_c = vertical load per unit length of the conduit

S = span or diameter of the conduit

A_r = cross sectional area of the conduit wall

F_y = yield stress of the conduit wall material

The problem with this theory is that it neglects the bending moments in the conduit walls which is reasonably correct under high fills. Although such a condition is met successfully in many installations, it is not applicable if the soil cover is shallow or the surrounding soil to the structure is loose.

A relationship between soil density and conduit deformations was proposed by Watkins (1964) [46]. He found that when soil density exceeds a critical value, wall strength and not the deflections, governs the design.

Brockenbrough (1964) [11] suggested the following equations for a conduit's ultimate design:

$$F_u = F_y \qquad \text{for} \quad S/r < 24 \qquad (2\text{-}5)$$

$$F_u = 40{,}000 - 0.081\,(S/r)^2 \qquad \text{for} \quad 294 < S/r < 500 \qquad (2\text{-}6)$$

$$F_u = \frac{4.93 \times 10^9}{(S/r)^2} \qquad \text{for} \quad S/r > 500 \qquad (2\text{-}7)$$

where,

Fu = ultimate strength of the conduit walls, lbf/in^2

Fy = yield stress of the conduit wall material, lbf/in^2

S = diameter or span, in

r = radius of gyration of the conduit wall, in

Equations (2-5), (2-6), and (2-7) are analogous to the classical equations for column design. Equation (2-5) specifies the ultimate yield of the conduit wall material which represents the wall crushing zone. Interaction between yielding and buckling is represented by equation (2-6). Finally, the zone of ring buckling is specified by equation (2-7).

Lusher and Hoeg (1994) [29] studied the beneficial contributions of the backfill to the performance of the soil-metal structures. They showed three very important contributions: (a) pressure redistribution which activates the lateral earth pressure, (b) deformation restrain which forces the conduit to buckle in a higher mode, and (c) arching in which the vertical pressure on the conduit walls is reduced as it deflects vertically.

Despite all the different theories available and their limitations, one of the most commonly used formulas for designing and analysing shallow cover soil-metal structures is the Iowa formula developed by Sprangler. The Iowa formula has been widely used and successfully applied, particularly for circular conduits.

2.2 Reinforced Earth

Reinforced earth is a construction material comprising soil that has been strengthened by tensile elements such as metal rods and/or strips, non-biodegradable fabrics (geotextiles), geogrids and the like. The fundamental idea of reinforcing the soil is not new; in fact, it goes back to biblical times. However, the present concept of systematic analysis and design was developed by a French engineer, H. Vidal (1966) [43].

Vidal (1966) [44], applied this concept to retaining walls and showed that the cost was below that of conventional walls. Schlosser and Vidal (1979) [38] suggested that soil with reinforcing strips behaves as if it were isotropically cohesive. They considered the reinforcement inside the soil as a substitute for a lateral restraining force enabling the soil to carry vertical stresses.

Juran et al. (1978) [19] tested sand samples reinforced by circular plates made of aluminium discs. In general, it was found that reinforcement stiffened the soil and also increased failure resistance.

Al-Hussaini (1978) [5] carried out a test on an instrumented reinforced earth wall 4.88 m long and 3.66 m high. He found that the lateral earth pressure on the wall facing at the end of the construction could be reasonably approximated by the Rankine theory of earth pressure. However, the line connecting the points of maximum tensile stresses in the reinforcing strips did not coincide with the theoretical Rankine line.

Kennedy et al. (1980) [21] conducted experimental and theoretical work on a reinforced earth retaining wall subjected to vertical surcharge load. Four different

positions of the load were considered. They developed a simplified pattern of distribution for the tensile force along the reinforcing strips.

Laba et al. (1984) [26] studied the effect of horizontal as well as vertical surcharge load on reinforced earth retaining walls. It was concluded that the location of the maximum tensile stresses along the reinforcing strips and the potential failure plane can be approximated by using Culmann's method. It was also stated that the horizontal force towards the wall facing will increase the tensile stresses in the reinforcing strips and the largest increase will take place at a certain depth below the soil surface.

Laba and Kennedy (1986) [25] proposed the stress transfer technique. It was found that the over-stressed regions of the reinforced earth wall transfer stresses to the regions where the reinforcing strips have not yet reached their capacity. This transfer of stresses was found to be influenced by the surcharge load magnitude and its distance from the wall facing.

More recent studies in the USA have revealed that the reinforcing material (metal strips and/or other materials) is capable of resisting frost action effectively [33]. During winter period the forces in the reinforcing material increased because they restricted the outside movement of the wall facing. After the spring thaw, these forces dropped back to a level near the lower range of the previous fall.

In summary, some of the beneficial effects for soil reinforcement are derived from (a) the soil's increased tensile strength and (b) the shear resistance developed due to the friction at the soil reinforcement interfaces. Such reinforcement is comparable to that of concrete structures.

2. 3 Buckling of Conduit Walls of Soil-Metal Structures Under Shallow Cover

Earlier investigators paid little attention to buckling as a potential mode of failure of the conduit wall. Sprangler (1941) [40] believed that the failure of the conduit wall was related either to wall crushing or to deformation of the pipe. Field performance of pipes having diameters less than 3 m and under fairly large depths of soil cover has provided some support for this belief.

In recent years, a general increase in the size of soil-metal structures has prompted further investigation on the phenomenon of failure of the conduit wall. The research performed on this phenomenon has brought to light the fact that buckling is a significant mode of failure, and that it can take place even at small deformations of the conduit. It is now well established that the stability analysis of the conduit wall is an indispensable component of the design process, especially when the spans are large and the depth of soil cover is small.

In determining the buckling stress, f_e, different approaches are studied. One approach is derived from a modification of the buckling formula proposed by Timoshenko and Gere (1961) [42].

$$f_e = \frac{3\,E}{(R/r)^2} \tag{2-8}$$

where,

E = modulus of elasticity of the conduit wall

R = radius of the conduit

r = radius of gyration of the conduit wall

This formula is subjected to the assumption that the soil in a soil-pipe system is non-compressible and with an angle of friction θ tending to zero. In such a case the radial pressure on the pipe is very nearly hydrostatic, and it can be described by equation (2-8).

Watkins (1966) [45] further studied this formula and the effect of Sprangler's assumptions. He proposed that, since the formula is based on the assumption that $\theta = 0$, it has the effect of underestimating the buckling stress on the conduit walls. Watkins developed a soil stiffness parameter, K, to account for the difference between the actual and assumed fluid soil. Watkins suggested that such a parameter could be taken as the ratio of the horizontal to the vertical soil pressure. For cohesionless soils this factor is equal to the active earth pressure $K = K_o$. Thus the equation for buckling becomes:

$$f_e = \frac{3\,E}{(K\,R/r)^2} \qquad (2\text{-}9)$$

Abdel-Sayed et al. (1994) [4] proposed that the parameter K should also depend upon the relative stiffness of the soil with respect to the rigidity of the conduit wall and they proposed the following expression for K:

$$K = B\,(E\,I/E'\,R)^{0.25} \qquad (2\text{-}10)$$

where,

E' = modulus of soil reaction, lbf/in^2

I = moment of inertia per unit length of column wall, in^4

B = 1.22 for the sides and bottom of the conduit, and

$= 1.22 \{ 1 + 2 (E I / E' R)^{0.25} \}$ for the rest of the conduit

Furthermore, the Ontario Highway Bridge Design Code OHBDC [36] adopted this expression for the calculation of K.

A different approach for studying buckling effects in conduit walls was taken by Booy (1957) [9]. He suggested that the buckling formula available for analysing elastically supported curved beams could be used for evaluating the buckling stress of the conduit walls:

$$f_e = (2 / A) (E' I E / R)^{0.5} \qquad (2\text{-}11)$$

where,

A = cross-sectional area of the conduit wall per unit length

Lusher (1966) [28] developed the same buckling formula by studying the buckling of circular beams under radial pressure and simulating the soil effect by springs of constant modulus. He proposed that the modulus of soil reaction is dependent on the thickness of

the soil cover. He also developed an expression for calculating the effective modulus of soil reaction E″.

$$E'' = E' \frac{(1-(R/r+h)^2)}{(1-(R/r+h)^2(1-\nu))} \qquad (2\text{-}12)$$

where,

ν = Poisson's ratio for the soil

h = Thickness of soil cover

r = radius of gyration of the conduit

R = Radius or span of conduit

Subsequently, Meyerhof et al. (1968) [32] simplified this expression to the following form:

$$E'' = E'(1-(R/r+h)^2) \qquad (2\text{-}13)$$

The formula developed for curved beams represents a more accurate formula and it was proved by Abdel-Sayed (1978) [2] that in the case of corrugated sheets in plane strain state of stress it can be used without modification.

2. 4 Metal Strips vs. Non-biodegradable Materials And Geogrids

2.4.1 Metal-Strips

Lee et al. (1973) [27] showed that with a conservative design, 5mm thick galvanised steel strips would be enough to hold a wall about 14 to 15m in height. The reinforcing strips, which are thin and wide placed at regular intervals are often used in the design of retaining walls and other reinforced soil structures.

Kennedy and Laba (1989) [22] proposed a concept of combining conventional soil-steel bridge design with the technique of reinforcing the soil with strips of steel. The steel strips are laid at different levels and tied to relatively thin facia panels.

In most instances galvanised metal strips have proved to be advantageous in providing reinforcement for soil-steel structures. However, galvanised steel is subjected to corrosion. The rate of corrosion depends on several environmental factors. Binquet and Lee (1975) [8] suggested that the average rate of corrosion of galvanised steel strips varies between .025 and .050 mm/yr. So, in the actual design of reinforcement allowance must be made for the rate of corrosion. This allowance is given by the following:

$$t_C = t_d + r \qquad (2\text{-}14)$$

where,

t_C = actual thickness of reinforcing strips to be used in construction

t_d = thickness of strip determined from design calculations

r = added thickness to compensate for corrosion

In recent years, new materials have been developed and studied. These materials are not only resistant to environmental factors but also in some instances they have been found to be stronger and less expensive.

2.4.2 Non-Biodegradable Fabrics And Geogrids

2.4.2.1 Non-biodegradable fabrics

Non-biodegradable fabrics are generally referred to as geotextiles. Since 1970 the use of geotextiles has increased tremendously around the world [14]. The fabrics are usually made from petroleum products, polyester, polyethylene, and polypropylene. They may also be made from Fiberglas. Geotextiles may be woven, knitted, or non-woven.

Woven geotextiles are made of two sets of parallel filaments or strands of yarn systematically interlaced to form a planar structure. Knitted geotextiles are formed by interlocking series of loops of one or more filaments or strands of yarn to form a planar structure. Non-woven geotextiles are formed from filaments or strands of yarn to form a planar structure. These filaments or short fibers are, in the beginning arranged into a loose web. They are then bonded by chemical, thermal and/or mechanical means.

Geotextiles have been used extensively in foundation engineering in many different areas, and are of special interest in the construction and design of highways because of :

1. Separation: Geotextiles help keep various soil layers separate after construction and during the project service period of the structure. For example, in the construction of highways, a clayed subgrade can be separated from a granular base subgrade.
2. Reinforcement: The tensile strength of geofabrics increases the load-bearing capacity of the soil.

Koerner (1990) [24] proposed a step by step procedure for designing retaining walls with geotextile reinforcement. In this procedure the active pressure distribution on the wall was calculated by using Rankine's active pressure formulae:

$$\sigma_a = K_a \gamma_1 z \qquad (2\text{-}15)$$

where,

K_a = Rankine earth pressure coefficient

$= \tan^2 (45 - \phi_1 / 2)$

γ_1 = unit weight of granular backfill

z = vertical spacing of layers at any depth

ϕ_1 = angle of internal friction of the soil

Koerner suggested that by determining the active pressure required the appropriate geotextile fabric could be selected based on the allowable strength of the fabric.

Furthermore, Koerner proposed that the length of each geotextile could be calculated from:

$$L = l_r + l_e \tag{2-16}$$

where,

l_r = (H – z) / tan (45 + ϕ_1 / 2)

l_e = (S_v σ_a [$FS_{(P)}$]) / (2 σ_v ϕ_F)

σ_a = Rankine's active pressure

σ_v = γ_1 + z

ϕ_F = friction angle at reinforcement (soil interface)

ϕ_1 = angle of internal friction of the soil

S_v = vertical spacing between layers of reinforcement

H = total depth of excavation

z = depth from top of soil cover to the layer of reinforcement

$FS_{(P)}$= factor of safety against reinforcement pullout

Koerner determined that the magnitude of $FS_{(P)}$ is generally between 1.3 and 1.5 and that the friction angle ϕ_F can be taken as 2/3 of ϕ_1. Based on the published results presented by Martin et al. (1984) [30] this assumption proved to be conservative.

Many studies have shown that the introduction of reinforcing geotextile materials in the construction of reinforced earth structures has given excellent results. Billard and Wu

(1991) [7] tested a full-scale geotextile reinforced retaining wall, 1.5 m high. It was designed based on the assumption of Rankine active pressure distribution and a factor of safety equal to 1 for a surcharge, q, of 40.7 kN/m^2 on the surface of the backfill. They discovered that the wall actually failed when the surcharge reached 127.5 kN/m^2. This experimental finding proved that the geotextile material had in fact increased the overall load bearing capacity of the soil.

2.4.2.2 Geogrids

Geogrids are high-modulus polymer materials, such as polypropylene and polyethylene and are prepared by tensile drawing. Netlon Ltd. of the United Kingdom was the first producer of geogrids. In 1982, the Tensar Corporation, presently Tensar Earth Technologies, Inc., introduced geogrids in the United States [15].

The major function of geogrids is reinforcement. Geogrids are relatively stiff netlike materials with large openings called apertures. These apertures are large enough to allow interlocking with the surrounding soil and/or rock and perform the function(s) of reinforcement and/or segregation.

In practice geogrids are found to be of two types: (a) biaxial geogrids and (b) uniaxial geogrids.

Uniaxial geogrids are manufactured by stretching a punched sheet of extruded high-density polyethylene in one direction under carefully controlled conditions. This process

aligns the polymer's long chain of molecules in the direction of draw and results in a product with high one-directional tensile strength and modulus.

Biaxial geogrids are manufactured by stretching the punched sheet of polypropylene in two orthogonal directions. This process results in a product with high tensile strength and different moduli in two perpendicular directions. The resulting grid apertures are either square or rectangular.

Geogrids are manufactured so that the open areas of the grids are greater that 50% of the total area. Currently, geogrids are manufactured in many shapes and/or sizes. However grids used for soil reinforcement usually have apertures that are rectangular or elliptical in shape. Carroll (1988) [13] performed experimental test on geogrids used for reinforcing soils and discovered that geogrids develop reinforcing strength at low strain levels, such as 2%.

Geogrids, like geotextiles, are also used as reinforcement in granular backfill for the construction of reinforced earth structures. The design procedure available for geogrid reinforced soil construction is similar to the one used for geotextile materials. In 1990 Thamm et al. [41] tested a full-scale retaining wall reinforced with TENSAR SR2 geogrid. Failure on the wall was caused by applying a load to a concrete slab measuring 2.4 m x 0.9 m. The wall failed when the vertical load on the concrete slab reached 1065 kN. They concluded that the resistance of the wall had considerably increased when compared to a rigid retaining wall.

2.4.2.3 Effects on the Load Bearing Capacity of Soils

Guido et al. (1987) [18] performed tests to determine the load bearing capacity of square foundations on laboratory models with sandy soils (relative density = 50%). Such soils were reinforced with layers of non-woven heat-bonded geotextiles. For these tests several parameters were varied (number of layers of geotextile, strength of geotextile, depth of cover , etc.). In general, results showed that when the geotextile layers are placed within a depth equal to the width of the foundation they increase the load bearing capacity of the foundation.

Sakti and Das (1987) [39] reported some model test results on the bearing capacity of a strip foundation on saturated clay. They used a heat-bonded non-woven geotextile for reinforcement. They concluded that in general the load bearing capacity of the foundation was increased when using geotextile material for reinforcing the soil, specially when the first layer of geotextile material was placed at a depth of 0.35B (B = width of foundation).

Omar et al. (1993) [35] after extensive experimental investigation concluded that geogrids can be used as soil reinforcement to increase the ultimate and allowable bearing capacity of shallow foundations.

In general, the introduction of geogrids and non-biodegradable materials has improved the load bearing capacity of soils. However, this becomes more advantageous when the design involves a structure that will be placed under shallow soil cover conditions. This is usually the case when designing pipe-arches and other soil-metal structures.

Figure 2.1 Basis of Sprangler's Derivation of the Iowa Formula

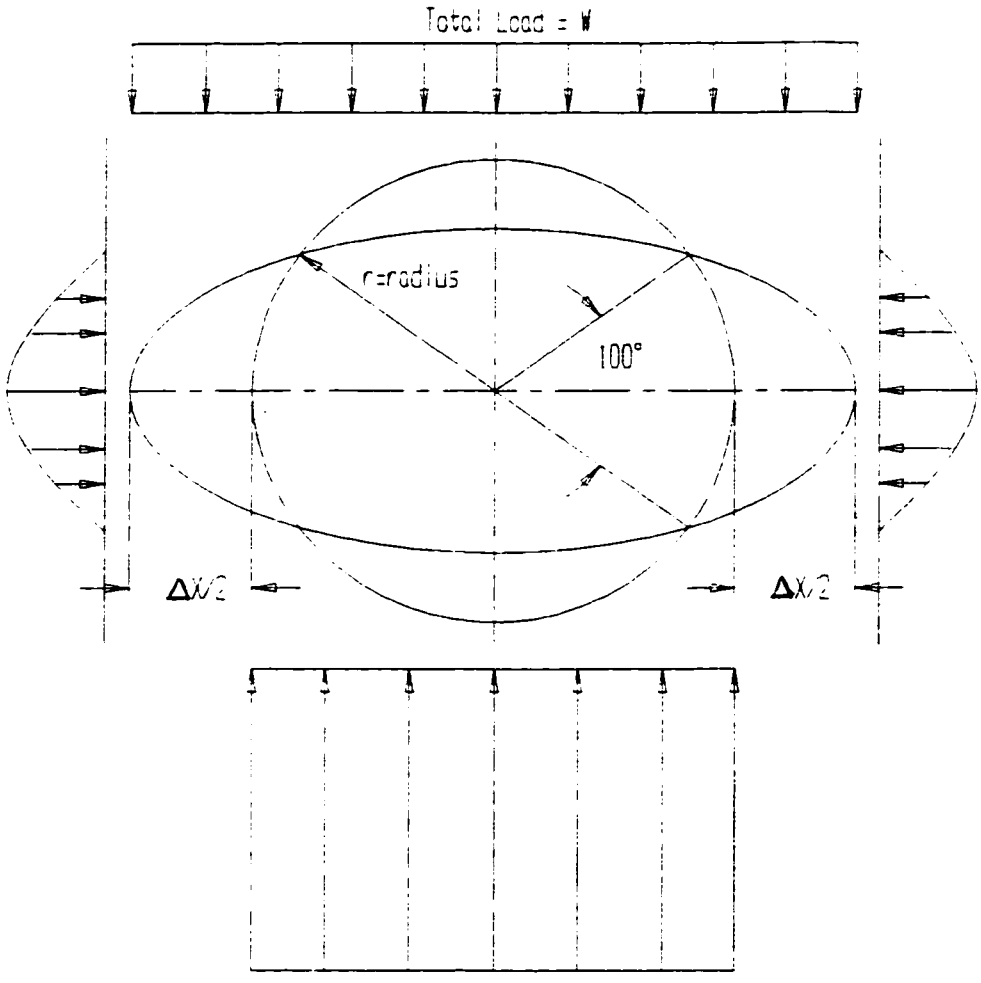

CHAPTER III

EXPERIMENTAL STUDY

3.1 Selection of Prototype Structure

It was noted earlier that soil-metal structures are fabricated in many different shapes and sizes (Figure 3.1). The selection of any particular shape and size of a soil-metal structure often depends on the constraints governing the design. However, out of all the shapes available none represents more risk for sudden failure than the pipe-arch. Specially, those pipe-arches that have large spans and are built under shallow soil cover conditions.

The structure studied here is a scale model of the largest available span of a pipe-arch structure with a corrugation profile of 152 x 51mm (Figure 3.2). Such a prototype structure tends to fail suddenly because of yielding of the soil under the haunches of the structure. The sectional properties for the profile as well as the structural properties of the pipe-arch were obtained from design tables prepared by the American Iron and Steel Institute [1]. These properties are shown in Table 3.1. and Figure 3.3.

3.2 Development of the Model Structure

In designing any soil-metal structure the three most important factors to be considered are (a) dead and live loads; (b) stiffness of surrounding soil and soil cover; (c) wall stiffness of the metal structure. However, for structures under shallow soil cover conditions deflection becomes the main constraint in the design. Therefore, the structural components of the experimental model were selected based on the relative deflection and/or deformation expected from the prototype structure. In order to accomplish this the Sprangler's Iowa formula [40] was used.

By applying the Iowa formula the horizontal deflection experienced by both the prototype and the model can be related. From this relationship the structural components of the model can be derived.

The resulting structure, after several iterations, was a metal pipe-arch made from flat aluminium sheets 1mm in thickness having a corrugation profile as the one described in Figure 3.4 and overall dimensions as shown in Figure 3.5.

The sectional properties for the experimental model were derived mathematically. These included the calculation of moment of inertia, I; area, A; section modulus, S; and radius of gyration, r. In calculating the properties, Wolford's formulas [50] were used:

$$I = C_5\, b\, t^3 + C_6\, b\, d^2\, t \qquad (3\text{-}1)$$

$$S = 2I / (d + t) \qquad (3\text{-}2)$$

where,

I = moment of inertia

S = section modulus

l = length of corrugation

d = depth of corrugation

t = thickness of sheet

C_5 = factor depending on shape or arc-and-tangent type corrugation

C_6 = factor depending on shape or arc-and-tangent type corrugation

3.3 Construction of the Pipe-Arch

Once the appropriate dimensions of the pipe-arch were determined (section 3.2), the next step was to build the structure.

The general procedure described by the American Society and Steel Industry [1] for building actual structural steel plate structures, was adapted to the model structure. Three pipe-arches were built in the following manner:

First, two wooden templates were cut out of 19.0mm thick plywood. These templates were cut according to the dimensions obtained in section 3.2 for the metal structure. The two templates were then attached by using two pieces of 51 x 102mm lumber having a total length of 910mm, as shown in Figures 3.6

The metal arch was made out of 1mm thick galvanised aluminium sheets. Each aluminium sheet had to be cut and corrugated to the required length and corrugation

profile. The metal was corrugated by using a manual corrugation machine such as the one shown in Figure 3.7. This machine allows the user to set the required corrugation profile by means of adjusting the levers located on the sides of the machine. Also, the required curvature of the metal arch can be achieved by using the front and back levers.

After the aluminium sheets had been corrugated and cut, they were then manually attached. This was accomplished by using 9.5mm steel-aluminium rivets and an air rivet gun. The rivets were placed along the span of the structure. Each plate was secured at the crest and valley of the corrugation profile. Typical examples of finished structural plates are shown in Figure 3.8.

Finally, after the structural plates were attached together, they were moulded to the appropriate shape by using the wooden template shown previously in Figure 3.6. Figure 3.9 shows the finished pipe-arch structure.

3.4 Testing Equipment and Components

The equipment used during testing consisted of several reinforcement sheets of geogrid, a plywood-Plexiglas box, instrumentation and measuring devices, a loading system, two rubber pressure tubes, Lake Erie sand, and three pipe-arches. The following sections provide a detailed description of the properties of each piece of equipment.

3.4.1 Properties of the Lake Sand

The backfill used during construction of the structure was clean, fine, dry sand. Such sand is obtained from Lake Erie and is available for commercial use. The properties of the sand were investigated by applying the sand cone method and the direct shear test method. Based on the direct shear test method the angle of internal friction of the sand was calculated to be $\phi = 40°$. The sand cone method revealed that the average dry compacted unit weight of this particular batch of sand is $\gamma_{dry} = 16.8$ kN / m^3, with a saturation ratio S = 92.7% and a moisture content $\omega = 12.03\%$. A brief summary of these findings is provided in Table 3.2.

3.4.2 The Sand Box

The pipe-arches were built inside a plywood-Plexiglas box. The box was made from standard plywood sheets with a thickness of 25mm and supported by 70 x 50 x 5mm steel angles. One side of the box was made out of Plexiglas sheet with a thickness of 12.7mm. Two pairs of steel angles of 60 x 60 x 6mm were used as vertical stiffeners and two pairs of the same size angles were used as post stiffeners for the vertical sides. The overall dimensions of the box are presented in Figure 3.10. The use of Plexiglas facilitated the testing procedure specially regarding observation and control of the structure during construction.

A rectangular hole was cut out from the front face of the box to facilitate placement of the testing equipment. Also, four holes were cut out from the front face and back face of the box to introduce two rubber pressure tubes used during testing.

3.4.3 The Loading Device

The pipe-arches were loaded by applying a strip load. The footprint of the load was equal to the inside width of the Plexiglas box, plus or minus a few millimetres to allow for frictionless motion of a spreader beam during loading. The load was applied by using a 70 kN capacity hydraulic ram fixed vertically to the horizontal spreader beam of the loading structural frame. The load was transferred to the soil by a series of steps: first, the load was transferred from the hydraulic ram to the 950mm long spreader beam made out of 7mm thick steel plates. The beam then transferred the load to a piece of wood 950mm long by 250mm wide and 38mm thick. The wood rested over a rubber mat, 6mm thick, to avoid local failure in transferring the load to the soil. Figure 3.11 shows the general arrangement of the loading device and its overall dimensions.

3.4.4 Instrumentation

In order to measure and record the desired data, twenty electric resistance strain gauges per model were installed. A total of 10 different locations around the

circumference of the pipe-arch were chosen for the gauge locations. Each location had two strain gauges installed, one on the crest of the corrugation and a second one on the valley of the same corrugation profile. Figure 3.12 and 3.13 show these locations and the general arrangement of the strain gauges. The strain gauges with a gauge length equal to 10mm were fabricated by Showa Measuring Instruments, Ltd. The type of gauges used were N11-FA-10-350-23 gauges with a resistance of 349.8 Ω and a gauge factor of 2.11 ± 1%.

The tangential strains detected during loading and backfilling operation were recorded with an Automatic Strain Indicator manufactured by Vishay Inter-Technology. The main components of this machine are: The VIC-22 automatic printer, VIE-25 scan controller, VIE-21 switch and balance unit, and eight digital strain indicators (Figure 3.17).

A total of eight mechanical dial gauges were installed to measure and control the deflection profile of the pipe-arches during the backfilling operation and then loading of the finished structure. The dial gauges were placed inside the structure as shown in Figures 3.14 and 3.15.

Two universal flat load cells were also used during the loading of the structure in order to monitor the applied load. Load cell number 1 had a capacity of 25 kN and can be identified by the serial number equal to S/N 06588-1. Load cell number 2 was of the same capacity as load cell number 1 and its serial number was, S/N 012052-1. The load cells and the beam are shown in Figure 3.16.

3.4.5 The Rubber Pressure Tubes

In order to simulate loss of soil support due to freeze-thaw cycle. A 7 m long piece of flexible pressure hose was used to build two rubber pressure tubes each would hold air inside to a maximum pressure of 2.98 kN/m^2 . The flexible hose used had an inside diameter equal to 130mm and was manufactured by Checker Industrial. This type of flexible hose is capable of holding pressure up to 7.25 kN/m^2. Each rubber tube built from the flexible hose, had a span of 1100mm.

In order to seal the ends of the tubes, four flanges having a diameter of 110mm were made out of stainless steel. These flanges were placed one at each end of the tubes and secured with two 114mm clamps (see Figure 3.18). Once the clamps were secured and tightened, a silicon paste was applied to the outer face of the flanges to seal any spaces between the rubber tubes and the clamps. This last step was necessary to ensure that no air would leak out from the rubber tubes during the backfilling operation and/or initial loading of the structure.

Two holes 10mm in diameter were drilled in each flange. One of the holes was used to attach a 90° shut-off valve to regulate the amount of air pumped into the tubes. The second hole served to install a 14.5 kN/m^2 mechanical dial gauge to monitor the air pressure inside the tube.

3.4.6 The Reinforcement

Sheets of geogrid material were used for reinforcing the soil. Two out of the three structures tested had reinforcing material attached to them by means of small aluminium plates secured to the structure with 9.5mm aluminium/steel rivets. The material used for reinforcement was fabricated by Tensar Polytechnologies, Inc. Such material is commercially available under the name heavy duty hardware net. The size of the mesh was 95 x 65mm. The width of the reinforcing sheet was 950mm (the width of the reinforcement is equal to the span of the pipe-arch). The spacing between layers of reinforcement was kept at approximately 100mm and a total of 8 layers of reinforcement were used on each side of the structure (see Figure 3.19). The span of the reinforcing mesh varied in length depending on the location of any particular layer relative to the metal structure. Figure 3.20 shows the length and general arrangement of the reinforcement layers with respect to the metal structure.

In order to determine the strength of the material being used for reinforcement, a simple test was developed. A test set-up similar to the one shown in Figure 3.21 was employed. In this test small weights were added to an aluminium rod clamped to a piece of geogrid similar to the one shown in Figure 3.22. The piece of geogrid material being tested was in turn clamped to a steel beam by means of aluminium plates and C-clamps. As the weight was increased the elongation of the material was measured and recorded until failure. A total of 30 tests were performed. Table 3.3 shows the average results of the tests performed, also Figure 3.23 shows the load versus elongation obtained for this

material. Finally the data from the experimental tests were checked against the nominal values obtained from Tensar Polytechnologies, Inc. The nominal values were somewhat different from the magnitude of those obtained in the laboratory by about 3 to 4 %.

3.4.7 The Pipe-Arch

A total of three pipe-arches were built as described in section 3.3. One of the three pipe-arches was designed and built with no reinforcement material attached to it. The other two structures were designed and built with geogrid material (used to reinforce the soil) attached to them.

3.5 Testing Procedure (Construction and Set-up)

In this section special attention is given to the testing procedure and the preparation of the soil surrounding the structures tested. These two factors are critical since they determine the structural behaviour of the structure and the reliability of the results.

To ensure that each test provided the most accurate results, the method outlined in this section was rigorously followed and applied to each of the structures tested.

3.5.1 Preparation of Surrounding Soil and Backfill Operation

A good foundation for an underground pipe-arch will maintain the elevation and grade of the invert to a planned position (a) with the pipe-arch in the desired cross-sectional shape, and (b) without concentration of the foundation pressures that tend to produce excessive stresses in the pipe-arch.

Buried pipe-arches must always be relatively yielding compared to the side fill. Therefore, preparing a hard bed for a buried pipe-arch would be equivalent to placing the structure on an anvil for the load to strike. That is why softer foundations are desired. When a load is applied to a structure in a soft foundation, the load creates earth arching. This results in reduction of the load on the structure as well as it provides a natural cushioning effect on the structure.

In practice evaluation of the soil is very important. When a soil contains undesirable soil material such as muck or rock sledges, the soil in the site is excavated and replaced with more desirable soil. For example large rocks or ledge rocks materials of poor or non-uniform bearing capacity are often replaced with sand. Sand is accepted as a suitable fill because it provides uniform and relatively yielding support.

In the laboratory, Lake Erie sand was used as the fill material (see section 3.4.1). A 200mm thick layer (often referred as bedding) was compacted on the bottom of the soil container. Then a 50mm thick layer of sand was pre-shaped to fit the invert radius of the pipe-arch. The structure's bedding was prepared wide enough to permit compacting the reminder of the backfill under the haunches of the structure efficiently. As explained

earlier, this last layer (50mm thick) was left uncompacted to allow relaxation of the structure into the bedding.

Once the structure was in place then the backfill operation started as follows:

For the unreinforced-soil structure:

1. Sand was placed in 100mm thick layers and compacted on each side of the conduit.
2. Compacting was performed in an even manner starting at a point closest to the structure to the point furthest away from the structure. This technique of compacting the soil provided two advantages: an adequate strength of the compacted soil; and second, it prevented pockets of uncompacted soil from being placed next to structure.
3. Two rubber tubes located a few millimetres under the haunches of the structure were filled with air to a constant pressure of 2.9 kN/m^2 during the backfill operation.
4. Once the sand reached the top of the crown of the structure, two more layers, (one 100mm and a second one 75mm) were added and compacted on top of the structure.

For the horizontally reinforced-soil structure:

1. The first layer of reinforcing material attached to the invert of the structure (geogrid) was laid flat over the 200mm thick layer of compacted sand. This layer of geogrid was placed underneath the flexible hose filled with air.
2. A 100mm layer of sand was placed on top of the first layer of geogrid and compacted in the same manner as it was done for the unreinforced-soil structure (Figure 3.24).
3. For every 100mm thick layer of well compacted sand, a layer of geogrid was unrolled and laid flat over the previous layer of sand. This process was repeated until the last

layer of reinforcement that was attached to the crown of the structure was covered with sand (Figure 3.25).

4. Two more layers of sand were placed over the last layer of geogrid. The first was a 100mm thick layer of well compacted sand, and the second was a layer 75mm thick of well compacted sand.
5. The rubber tubes were kept at a constant pressure of 2.9 kN/m^2 during the entire process.
6. Each of the sheets of geogrid was held in place and fully extended during the backfilling operation.

Experience and research have shown that the critical density of backfill to be 85% Standard Proctor density. Therefore, the backfill had to be compacted to a greater density than the critical to assure good performance of the structure. A Standard Proctor density of 90% minimum was maintained during all of the test conducted, by means of a hand-held tamper of 12 kg. in weight, such as the one shown in Figure 3.24.

3.5.2 Testing of the Soil-Metal Structure

The following procedure applies for both the unreinforced-soil and reinforced-soil pipe-arches tested: During backfilling, the structure was monitored by means of strain gauges and dial gauges placed in the structure as described in section 3.4.4. Once the

Automatic Strain Indicator (see section 3.4.4) had been calibrated and set to zero, readings for tangential strain were taken after each layer of soil (100mm thick) had been compacted. At the same time the deformation of the structure was monitored with 8 dial gauges placed inside the structure (see section 3.4.4). This method was repeated until the last layer of soil had been compacted. During the entire process of backfilling the pressure in the flexible hoses located under the haunches was kept constant at 2.9 kN/m^2.

After compacting the soil on the top of the culvert, the loading device (described in section 3.4.4) was set in place. With the aid of the hydraulic jack the load was applied to the structure in equal increments. After each increment readings for deflections, strains and load magnitude were taken and recorded. During the application of the first few increments of live load, the soil surrounding the structure and specially at the haunches was kept undisturbed. The air pressure inside both of the rubber tubes was decreased simultaneously and in small amounts for two of the three structures tested. After each variation in pressure, readings for strains, deflections, and pressure inside the rubber tubes, were taken and recorded.

A third horizontally reinforced-soil pipe-arch was tested in the same manner, except that the pressure inside one of the two rubber tubes was kept constant at 2.9 kN/m^2, while the pressure inside the second rubber tube was decreased in small amounts. Again, strains and deflections were monitored and recorded for this structure.

Table 3.1

Sectional and Structural Properties for Corrugated Sheet an Plate
Corrugation Profile: 152 x 51 mm

Wall Thickness T mm	Area A mm^2 / mm	Tangent Length TL mm	Tangent Angle Degrees	Moment of Inertia I mm^4 / mm	Section Modulus S mm^3 / mm	Radius of Gyration r mm	Corrugation Radius CR mm
5.0	6.1	45.6	45.3	1867	67.0	17.4	28.6

Span mm	Rise mm	End Area m^2	B mm	R(t) mm	R(c) mm	R(b) mm
6250	3910	19.2	1120	3175	840	9630

Table 3.2

Sand Cone Method Test Results on Lake Erie Sand

	Trial 1	Trial 2	Trial 3	Average
Moisture Content	0.012	0.010	0.013	0.012
Dry weight of Sand Excavated (kg)	0.76	0.58	0.70	0.68
Volume of hole Excavated (mm^3)	450000	352000	423000	408333
Dry unit weight of sand Compacted (kN/m^3)	16.9	16.7	16.8	16.8

Table 3.3

Tensile Test Results: Tensar Multinetting

Force N	Gauge Length (mm)	Elongation (%)	
0	39.8	0.0	
22.4	39.8	0.2	
44.8	40.0	0.6	
67.2	40.3	1.3	
69.4	40.7	2.4	
70.3	41.0	3.0	
71.7	41.6	4.5	
76.2	41.7	4.9	
78.4	42.0	5.7	
80.6	42.3	6.4	
82.9	42.3	6.4	(failure)

Figure 3.1 Structural Plate Shapes [3]

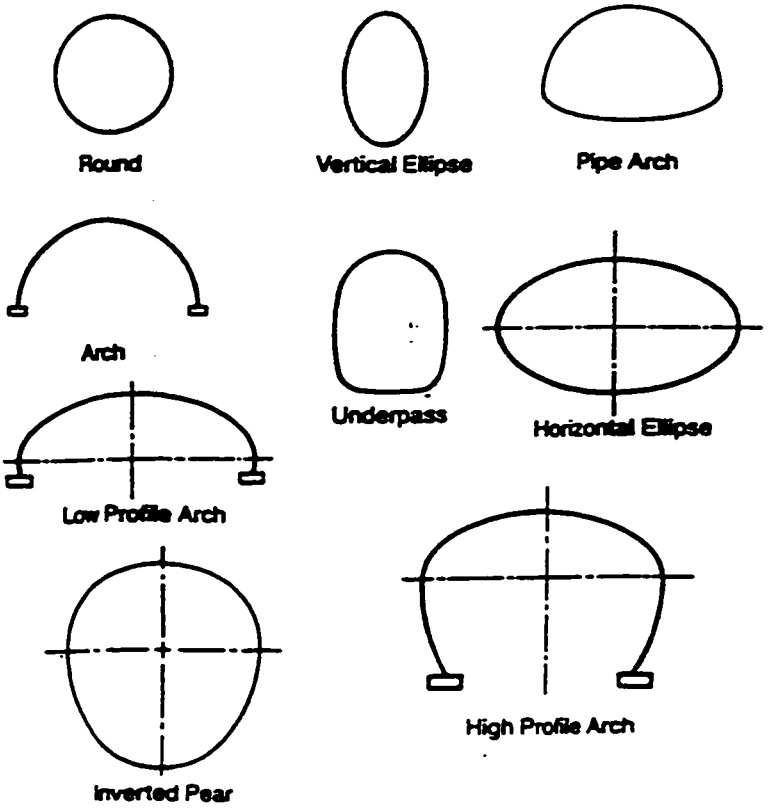

Figure 3.2 Corrugation Profile - Prototype Pipe-Arch (all in mm)

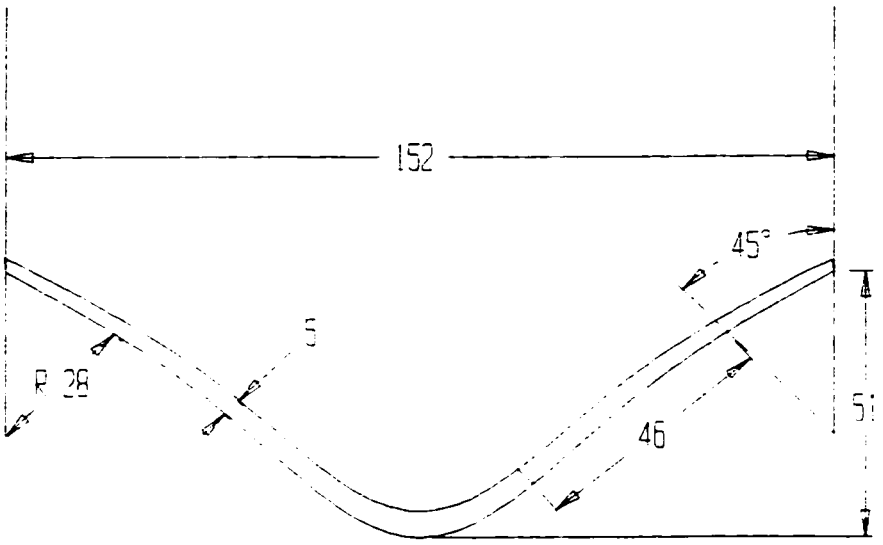

Figure 3.3 Prototype Pipe-Arch - Overall Dimensions (all in mm)

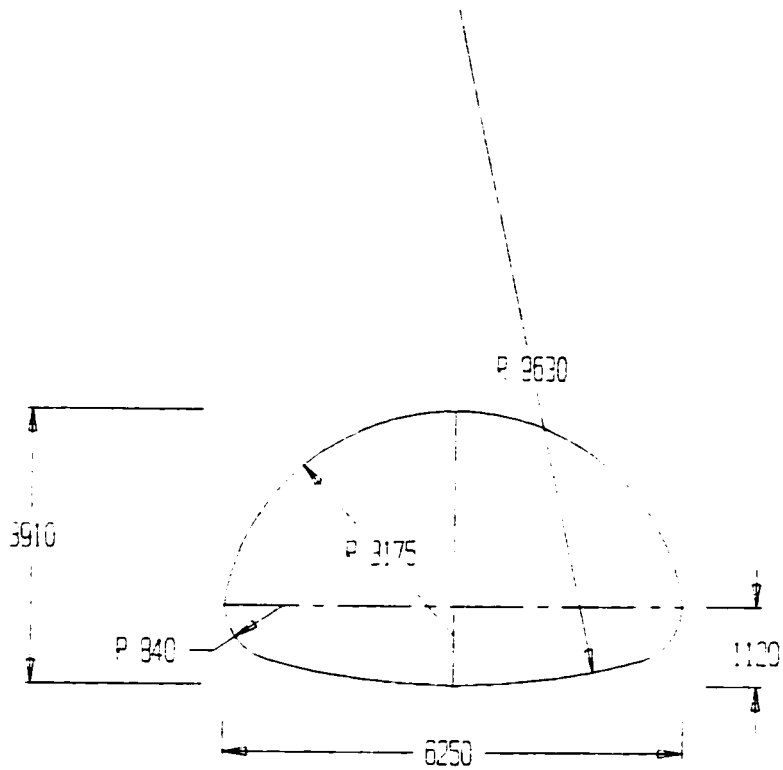

Figure 3.4 Corrugation Profile - Model Pipe-Arch (all in mm)

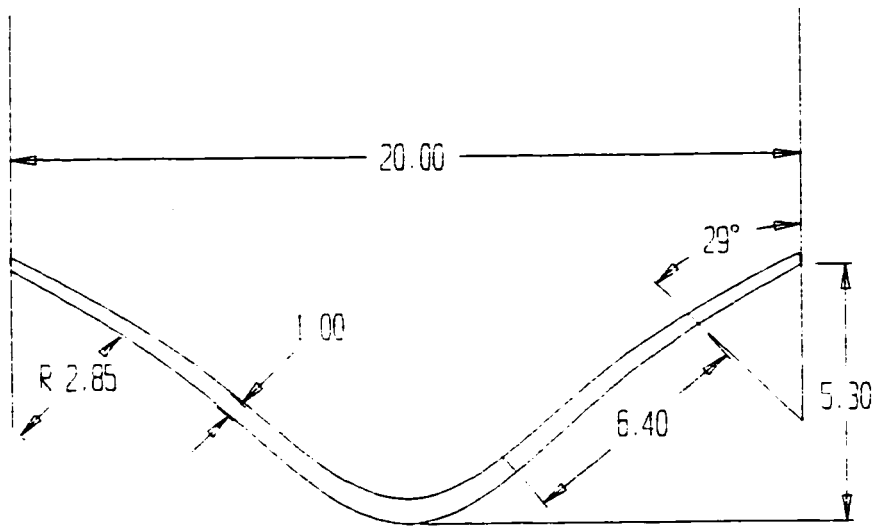

Figure 3.5 Model Pipe-Arch Overall Dimensions (all in mm)

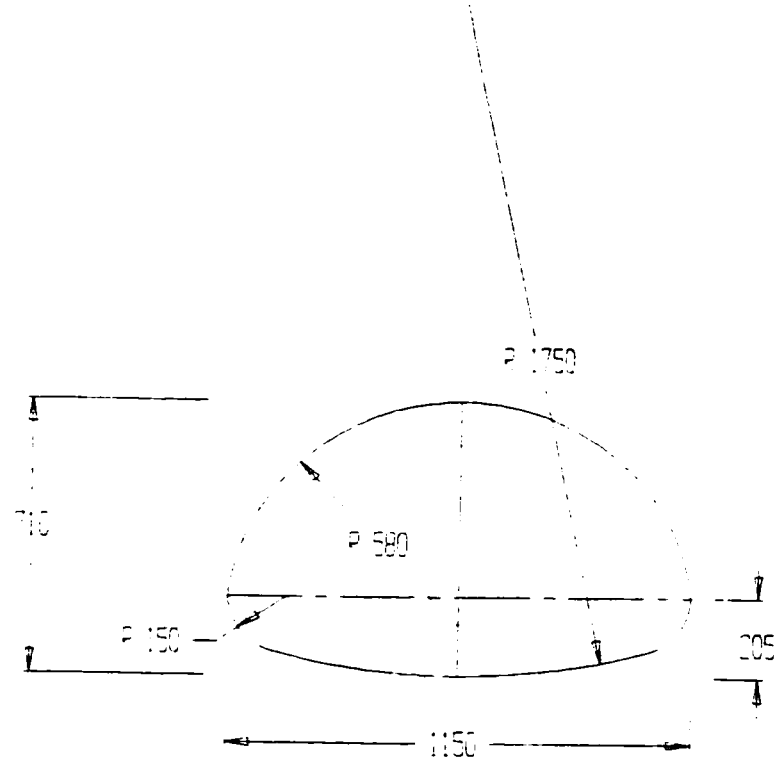

Figure 3.6 Plywood Template - Side View

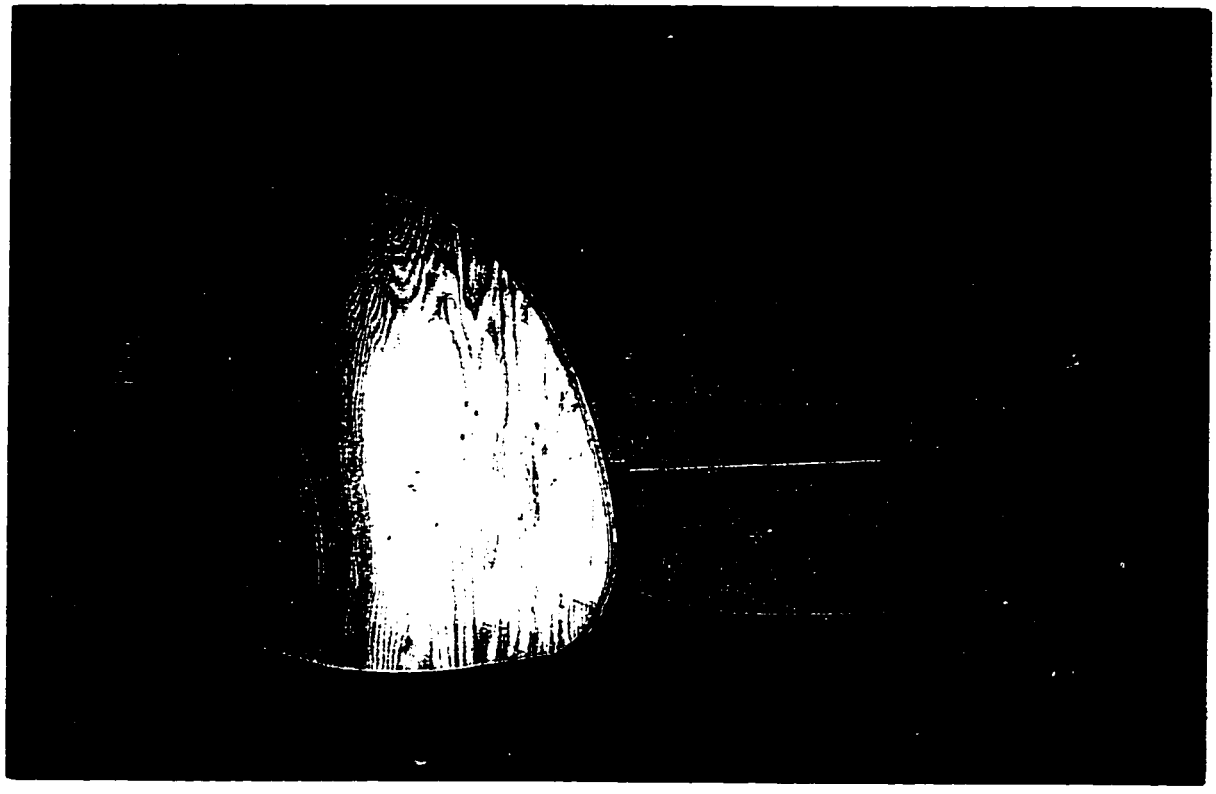

Figure 3.7 Corrugation Machine - Front View

Figure 3.8 Structural Sections - Haunches

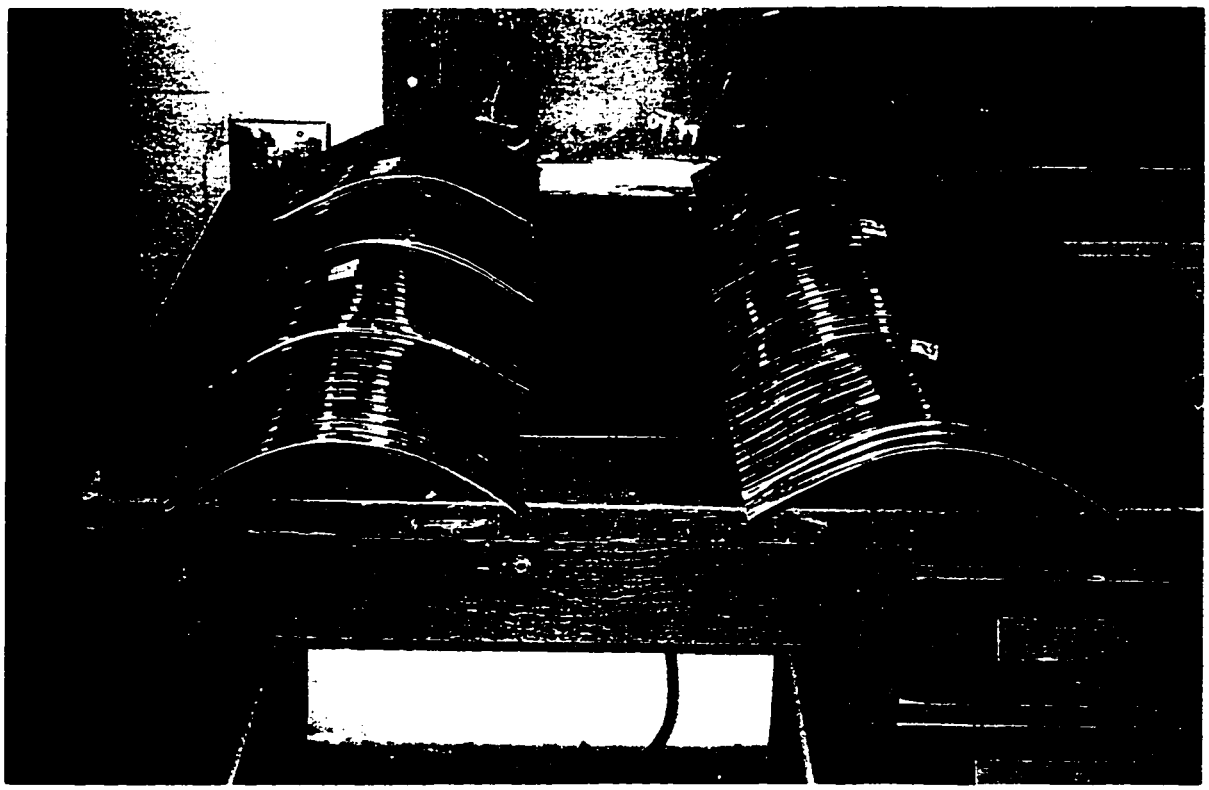

Figure 3.9 Finished Pipe-Arch

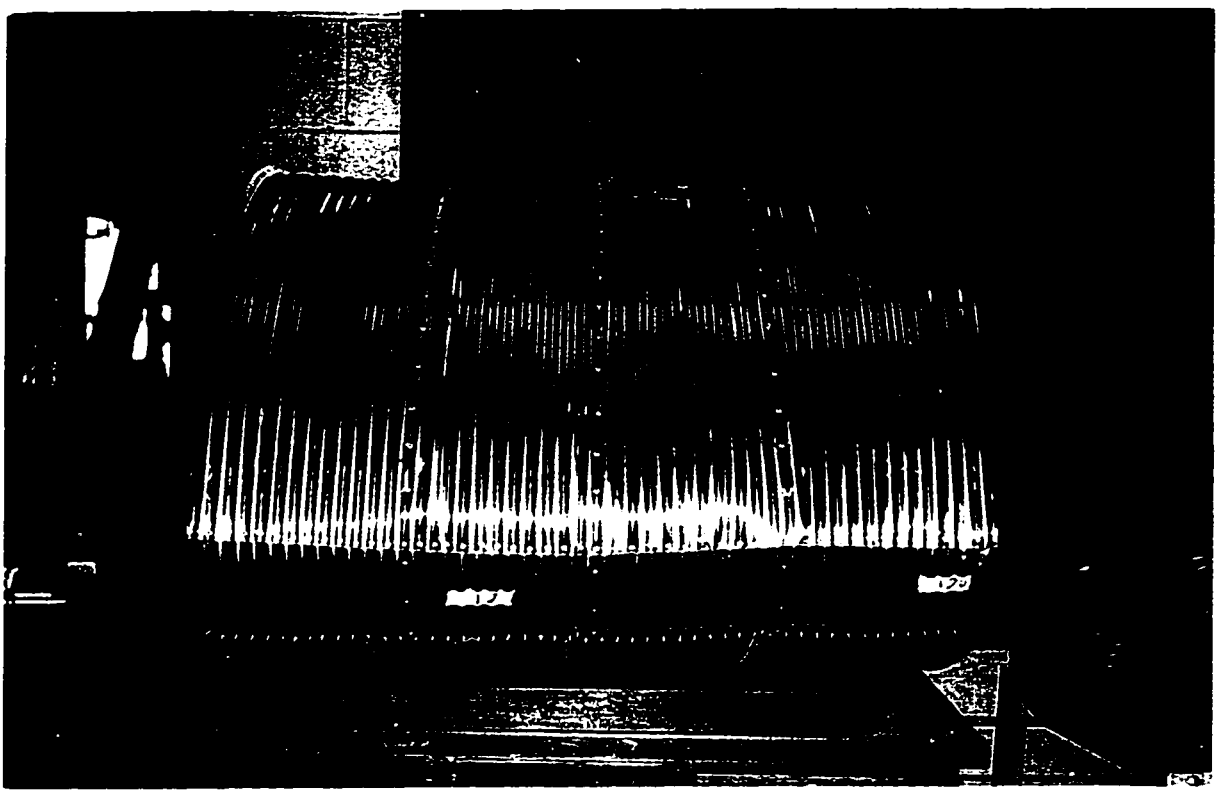

Figure 3.10 Sand Box - Overall Dimensions (all in mm)

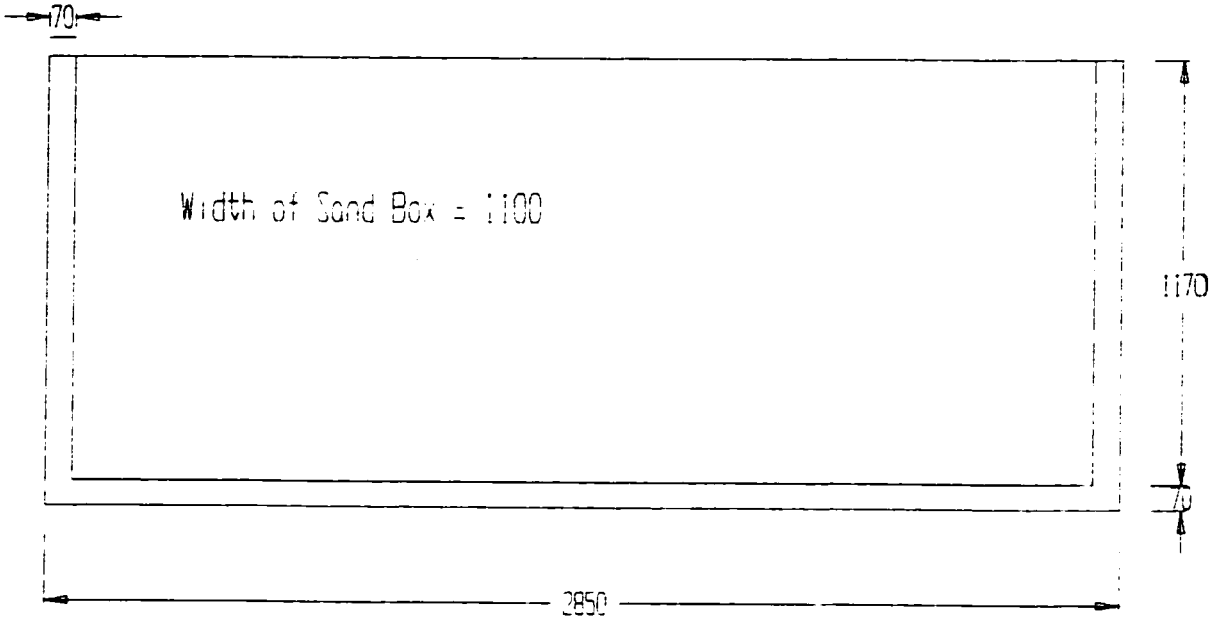

Figure 3.11 Loading Beam - Overall Dimensions (all in mm)

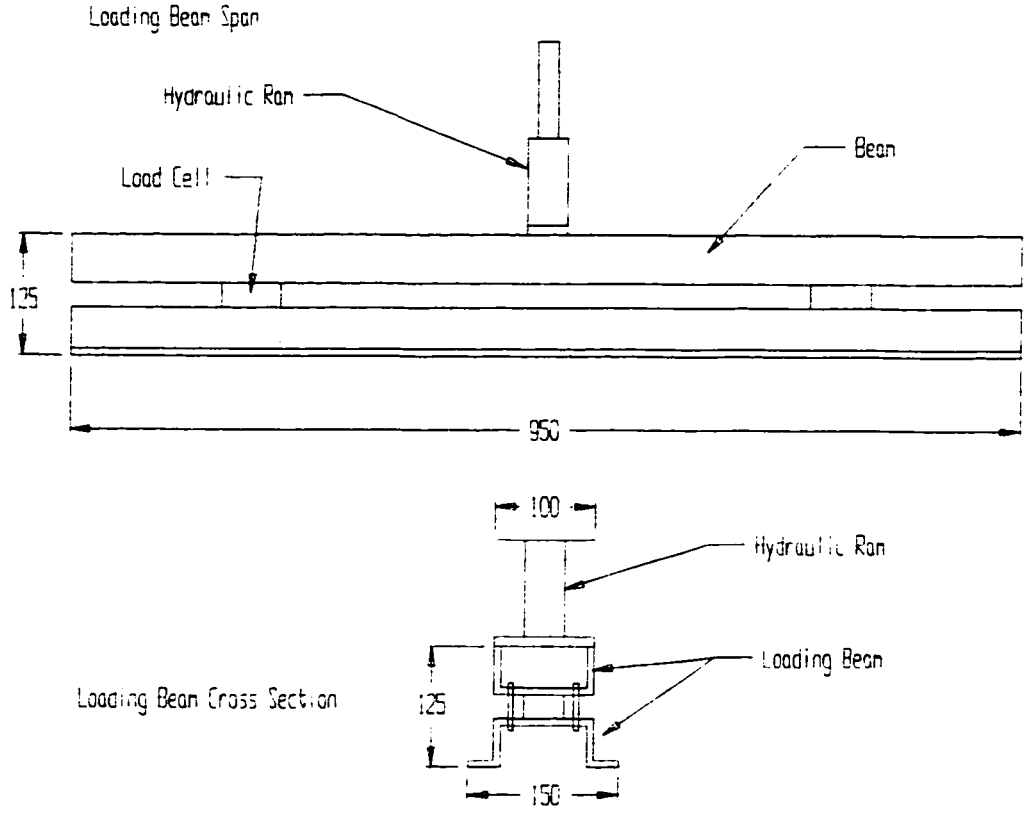

Figure 3.12 Location of Strain Gauges (all in mm)

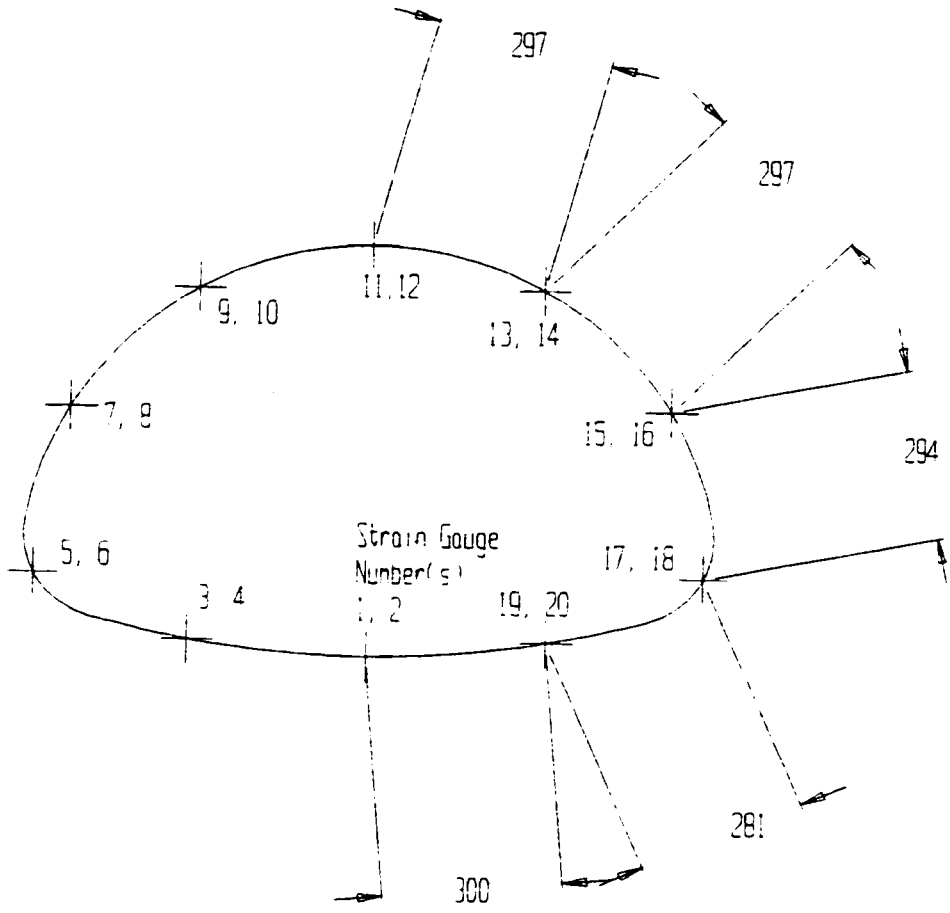

Figure 3.13 Arrangement of Strain Gauges

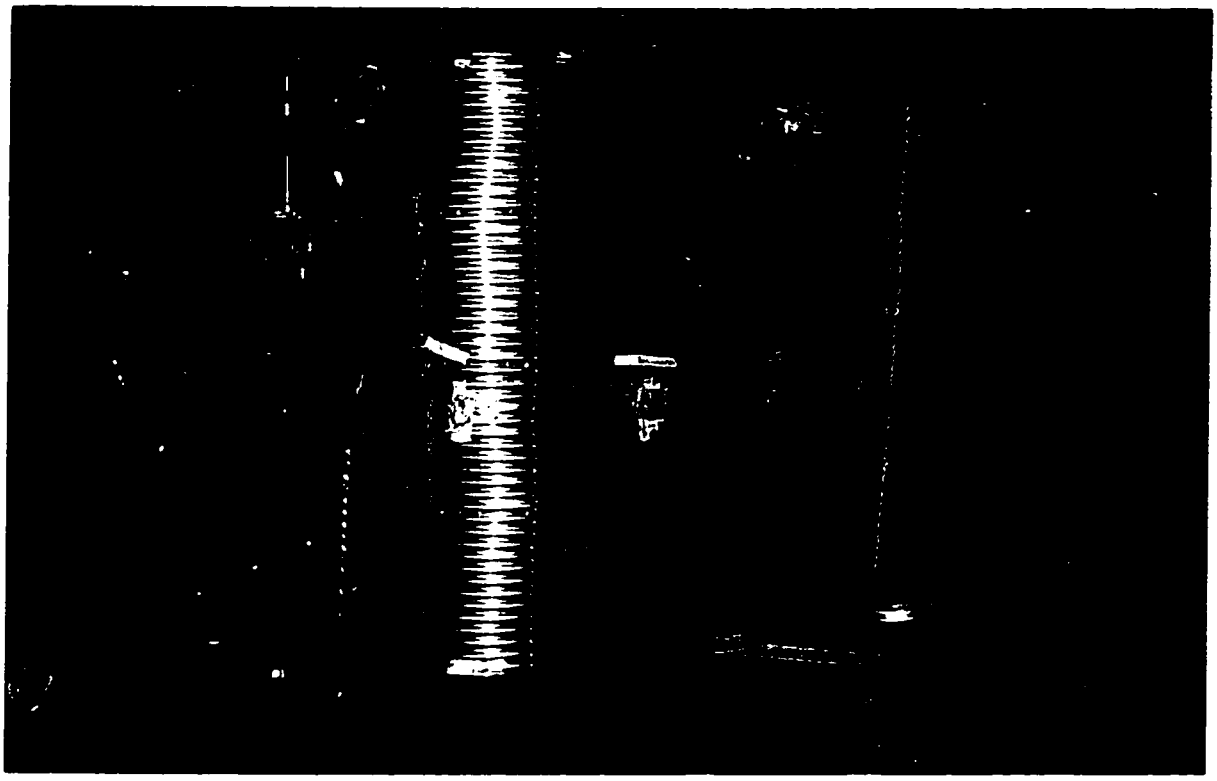

Figure 3.14 Location of Dial Gauges (all in mm)

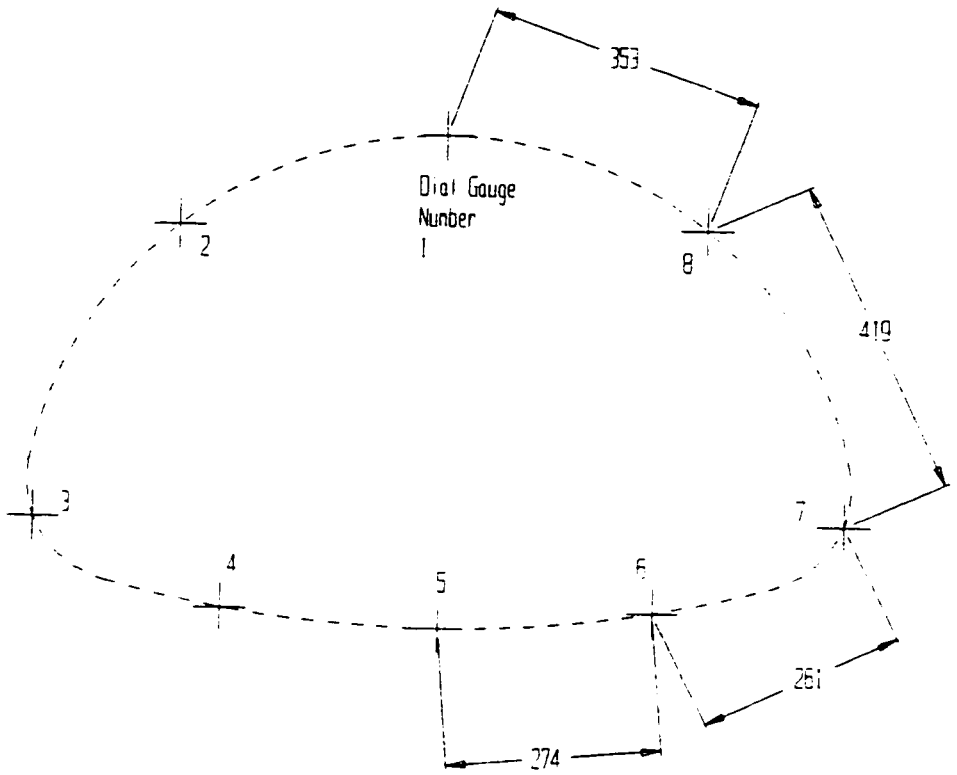

Figure 3.15 Arrangement of Dial Gauges

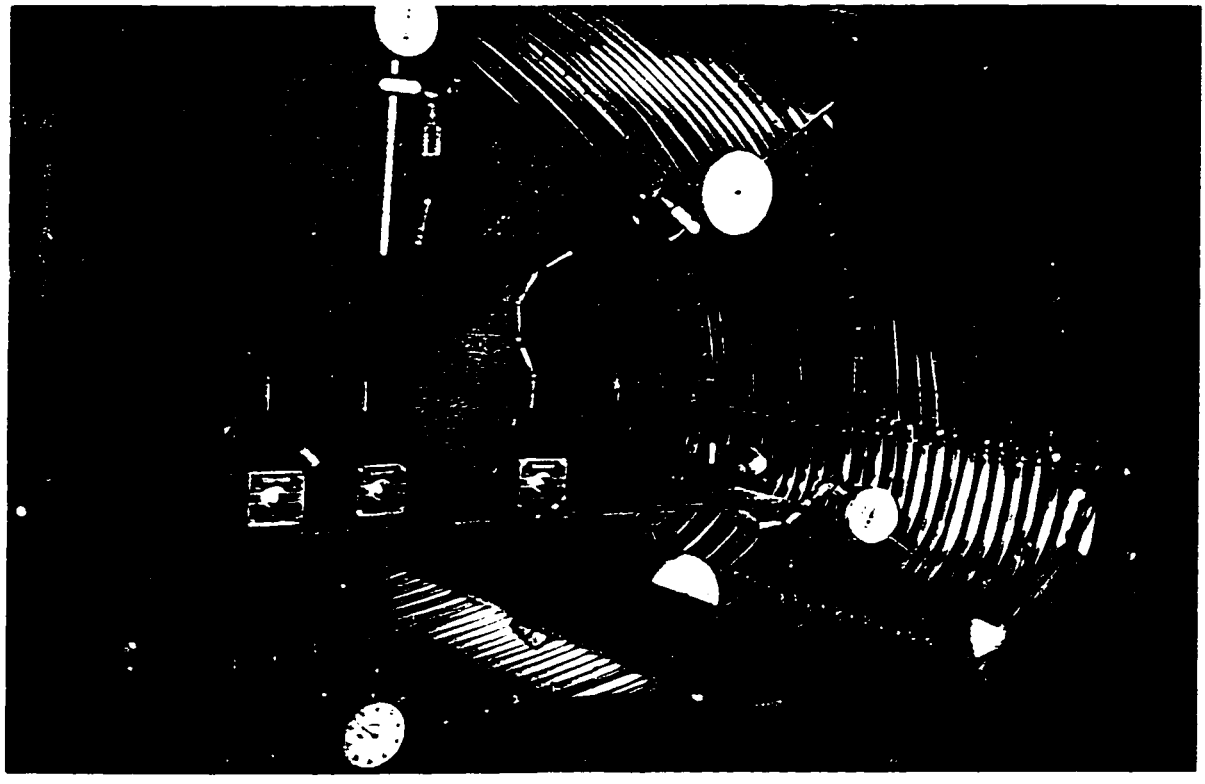

Figure 3.16 Load Cells and Loading Device

Figure 3.17 Automatic Strain Indicator

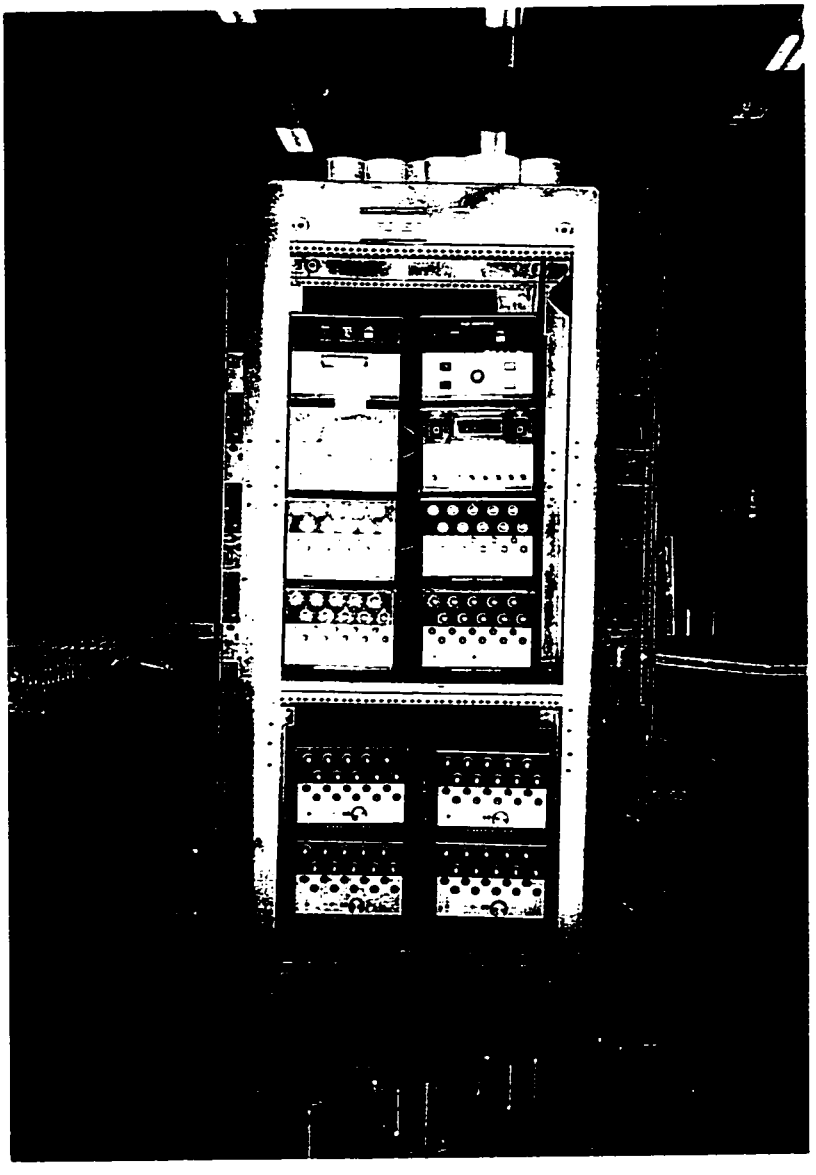

Figure 3.18 Components of Rubber Pressure Tubes

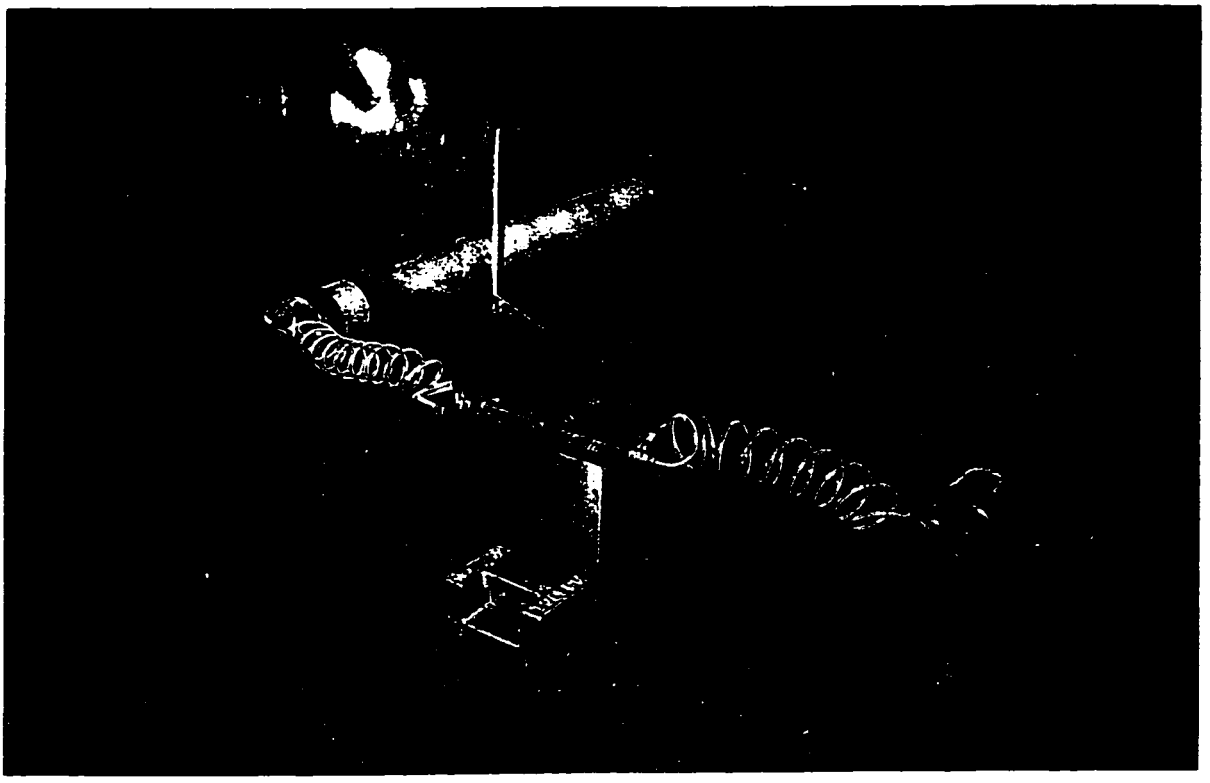

Figure 3.19 Spacing of Reinforcement (all in mm)

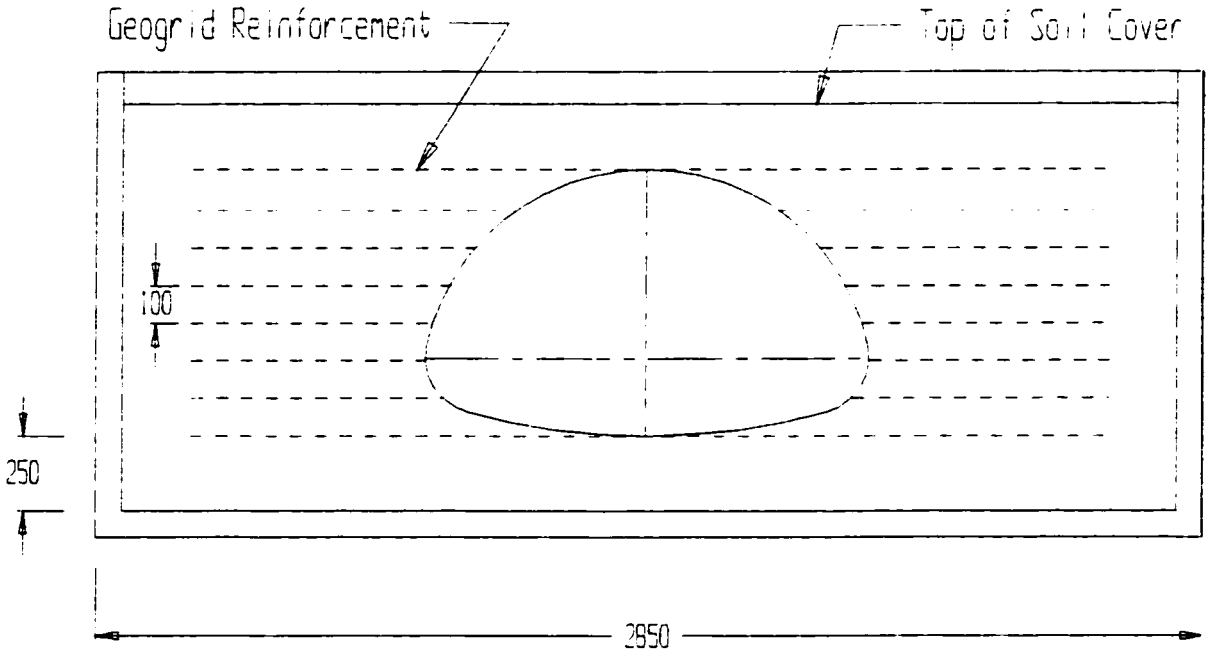

Figure 3.20 Length of Reinforcing Layers (all in mm)

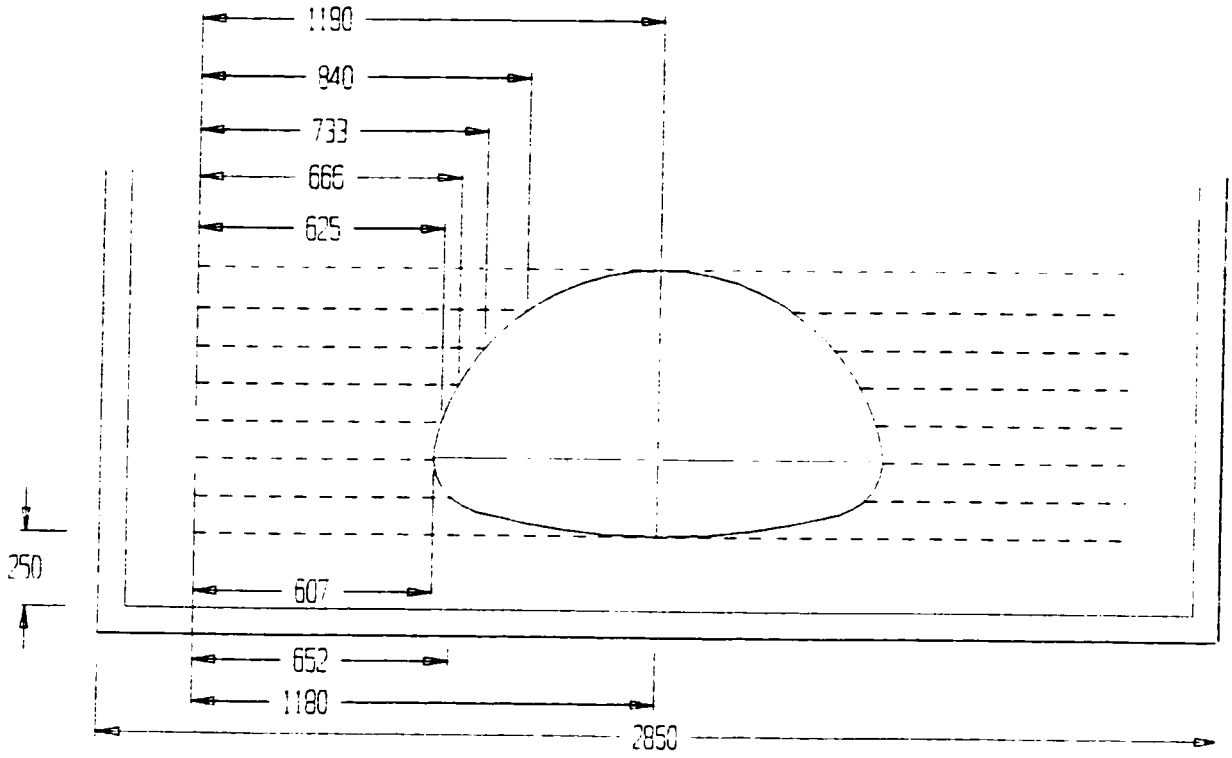

Figure 3.21 Tensile Test on Geogrid Sheets - Equipment Set-up (all in mm)

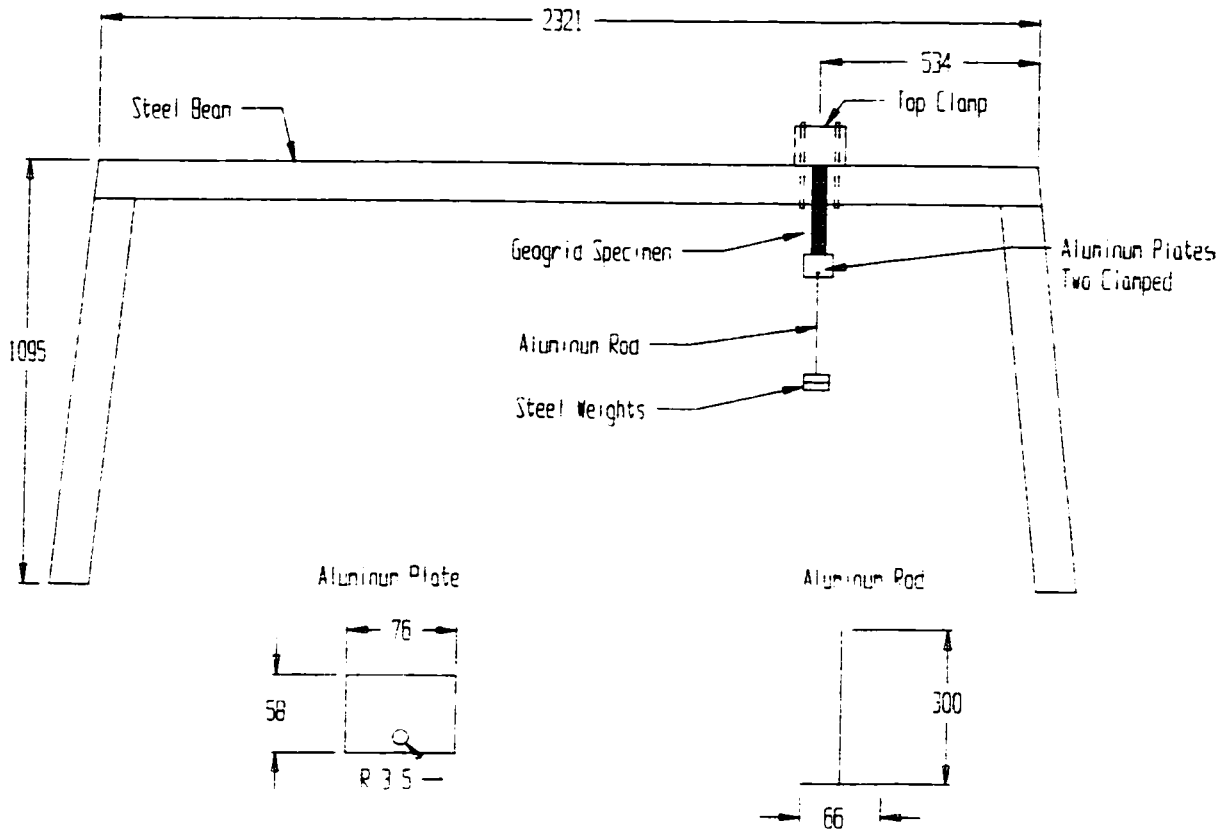

Figure 3.22 Geogrid Specimen (all in mm)

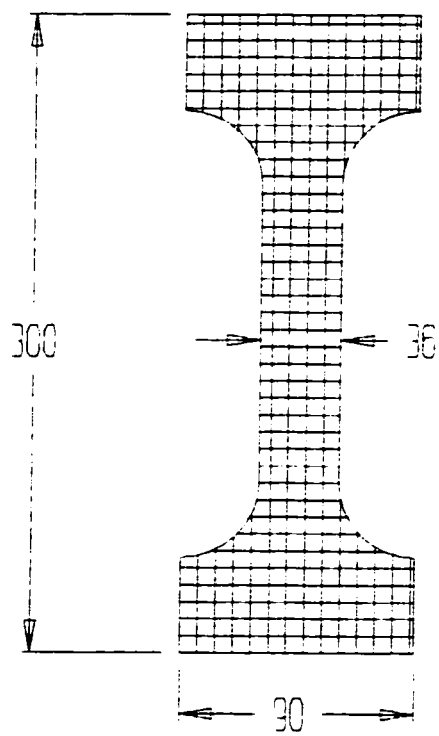

Figure 3.23
Load vs. Elongation (Geogrid Specimen)

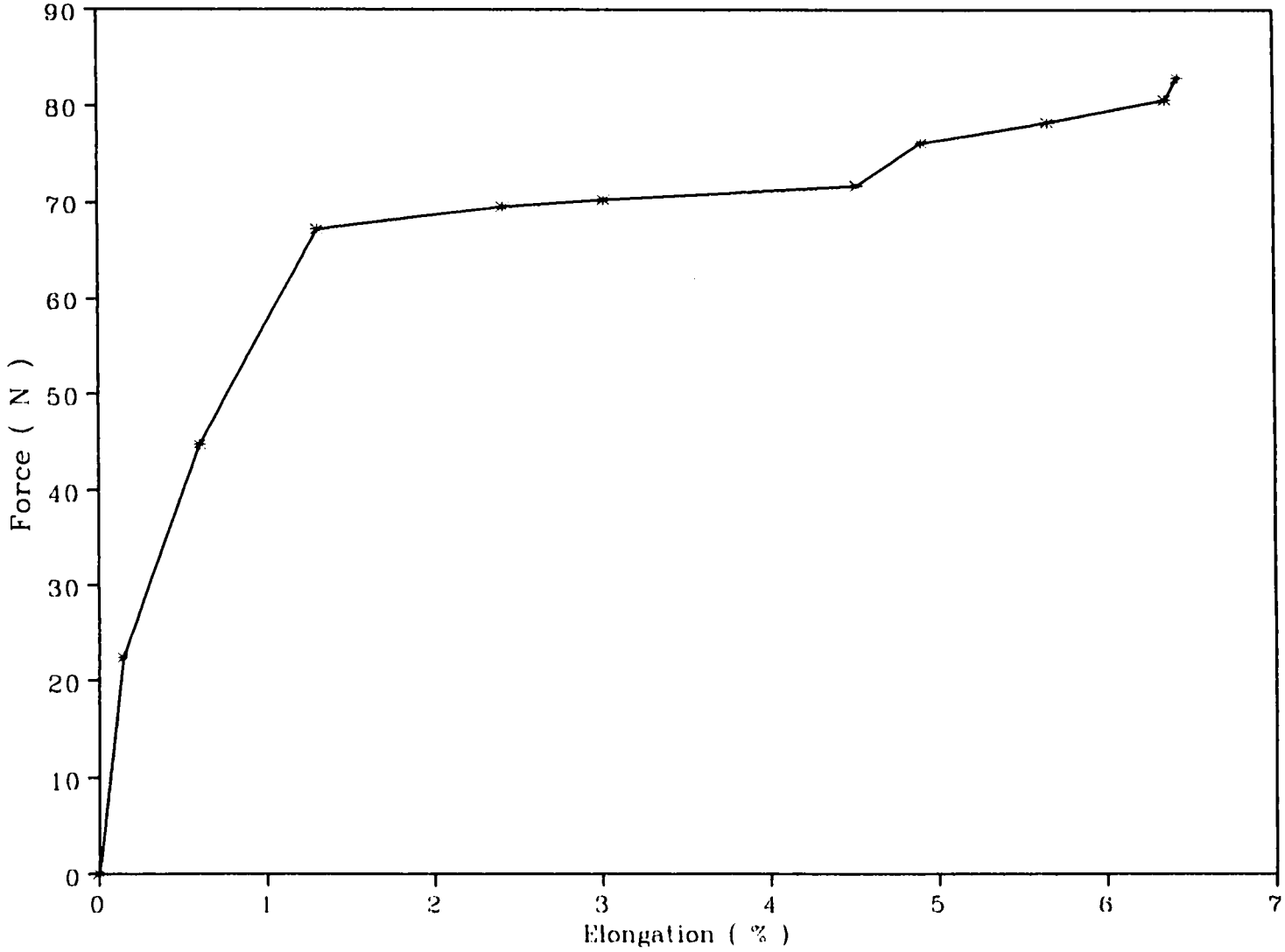

Figure 3.24 First Layer of Geogrid - At Haunch Level

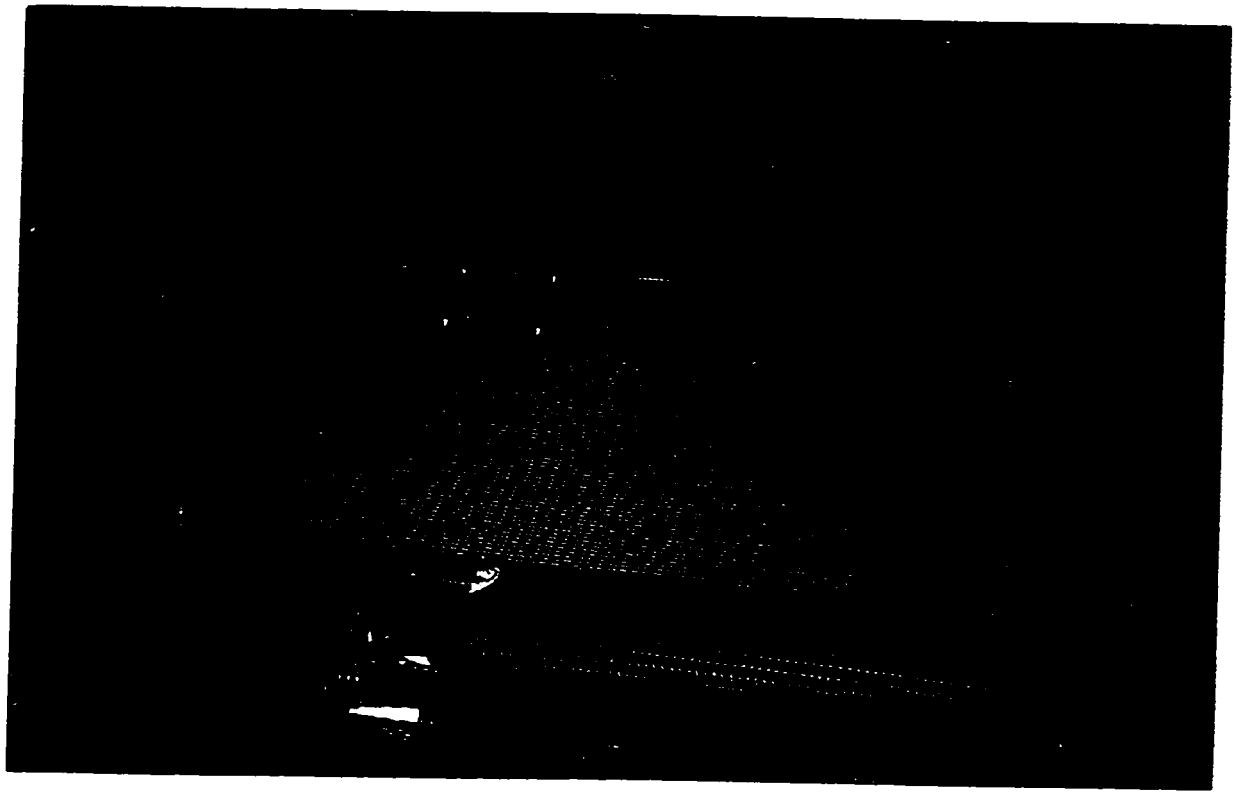

Figure 3.25 Sixth Layer of Geogrid - Below Crown Level

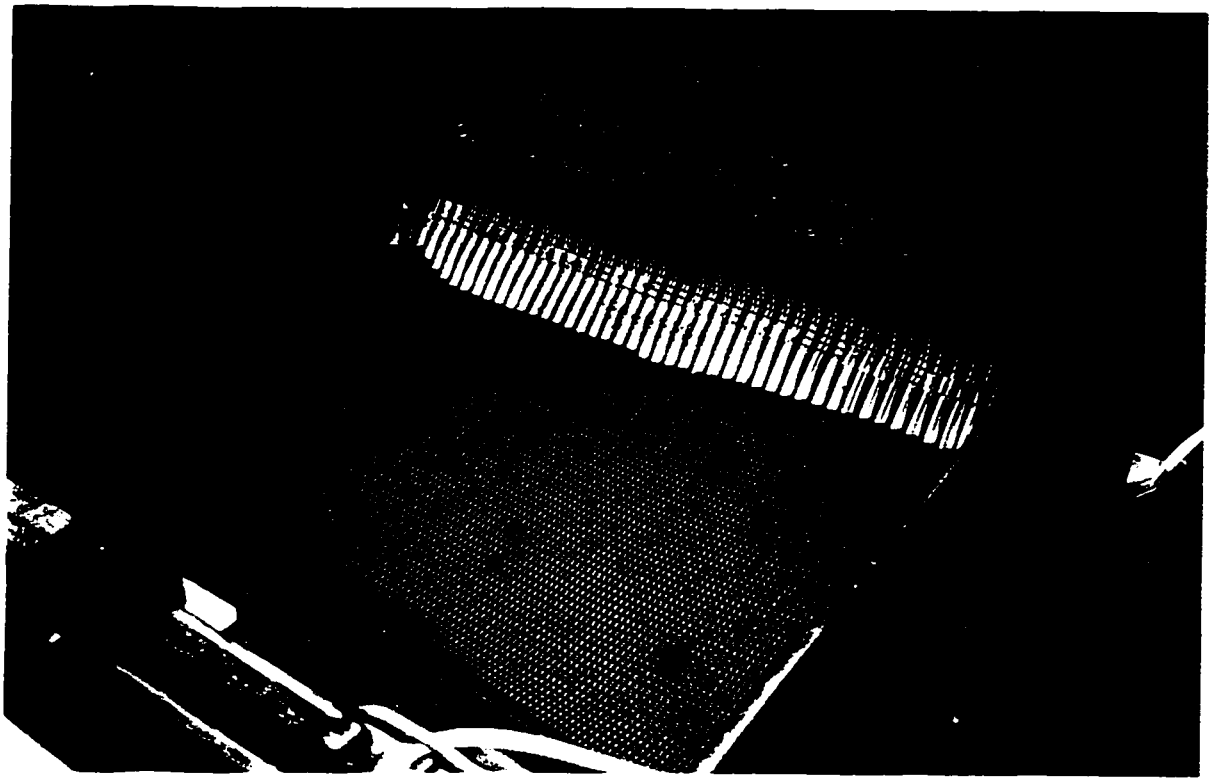

CHAPTER IV

DISCUSSION OF RESULTS

4.1 Unreinforced-Soil Structure

The first experimental model built and tested was the unreinforced-soil pipe-arch shown in Figure 4.1. During construction, readings for strain and deflection were taken after each layer of sand was compacted. The numerical results of the deformations are presented in Table 4.1. Here it can be observed that the maximum deflection experienced by the structure occurred at the crown and it was approximately equal to 47mm (outwards). On the other hand, the invert of the structure deformed little in comparison with the rest of the structure having a total deflection of approximately 2.5mm (outwards). The haunches of the structure, which are the most critical structural components of the pipe-arch, also experienced a maximum inward deformation of 8mm.

The deformations experienced during construction were anticipated based on field observations of pipe-arches and previous research available on this type of structures [23].

The strains recorded at this first stage served to calculate moments and axial forces experienced by the structure during construction. These are shown in Tables 4.2 and 4.3.

From these tables, it can be observed that the maximum moment producing compression at the inner fibers of the structure was equal to 79.6 N.m and it occurred at the crown of the structure. The invert of the structure experienced a moment of 7.1 N.m. in tension at the inner fibers. Finally, the haunches' moments were 48 N.m in compression

at the inner fibers. Similar results for axial force were obtained for the pipe-arch during construction and are presented in Table 4.3.

The second stage of the test involved the application of a live load of a magnitude equivalent to the standard live load required by the OHBDC [36] for these type of structures.

During loading of the structure, the deflection, bending moment, and axial force varied gradually as the load increased. (note that during this stage the soil surrounding the metal structure was kept undisturbed, by keeping the pressure inside the rubber tubes constant).

The deflection at the crown of the pipe-arch changed from approximately 4mm (inward) for an applied load of 1.2 kN to 62mm (inward) for an applied load of 8.7 kN. (8.7 kN was the maximum load experienced by the structure before the soil surrounding the structure failed). The haunches of the structure deformed little in comparison to the crown. They experienced deflections ranging from 0.08mm (outward) at a load of 1.2 kN to 0.76mm (outward) at a load of 8.7 kN Similarly, the invert of the structure only deflected 0.09mm (inward) at a load of 8.7 kN (see figure 4.2). Table 4.4 shows the deformation of the pipe-arch at different stages during loading.

The magnitude of the moment as well as the axial force were also calculated at different stages of loading. The moments at different loads are shown in Table 4.5 and the axial force in Table 4.6. Table 4.5 shows that during loading, the maximum bending moment was 61 N.m producing tension at the inner fibers as shown in Figure 4.3. The moment at the crown was equal to 38 N.m (tension at the inner fibers). Also, the moment

at the haunches and invert was determined to be 15 N.m (compression at the inner fibers) and 4.5 N.m (tension at the inner fibers), respectively.

These moments were all produced by an applied load of 8.7 kN, which was equal to the maximum applied live load on the unreinforced-soil structure.

The axial force was also determined in the same manner as the bending moments and deflections, Table 4.6 shows that the axial force at the crown for the structure was 90.2 kN for the same load described before. Also, results for the axial force at the haunches and invert of the structure have been included in this table. Figure 4.4 shows the axial load at different stages of loading.

Once the applied load reached 8.7 kN, the next step was to study the effect of disturbing the soil around the haunches of the pipe-arch. This was accomplished by reducing the pressure inside the rubber tubes. The pressure was reduced by letting air flow out from the rubber tubes in a gradual manner. Tables 4.7 through 4.9 show the variations in deflection, bending moment, axial force, rubber tube pressure, and applied load.

It can be readily observed from Table 4.7 and Figure 4.2 that the deflections at the crown, haunches and invert increased to maximum value of 73mm (inward), 3.5mm (outward) and 0.7mm (outward), respectively. Also the applied live load of 8.7 kN had to be reduced to a load of 6.8 kN, as a result of failure of the soil surrounding the structure. Notice that this load was recorded once the pressure inside the rubber tubes had reached zero.

Similar results for bending moment and axial force for the pipe-arch are described in Tables 4.8 and 4.9 and represented in Figures 4.3 and 4.4. The structure was able to carry the load successfully only after small reductions in the pressure inside the rubber tubes had occurred. However, once the soil completely lost its strength and the soil surrounding the critical areas (haunches) of the pipe-arch had completely failed, the metal in various parts of the structure started yielding, (see Tables 4.8 and 4.10) and the load carrying capacity of the structure decreased. The pipe-arch structure eventually failed and was no longer able to carry any load. A graphical history for the different stages of the test conducted on the unreinforced-soil structure is presented in Figures 4.5 through 4.7.

4.2 Reinforced-Soil Structure (Failure of the Soil Surrounding Both Corner Plates)

The experimental study of the horizontally reinforced-soil structure was conducted in a similar manner as the one for the unreinforced-soil pipe-arch. The difference was that geotextile material was used to horizontally reinforce the soil surrounding the pipe-arch.

During construction the deformation, bending moment, and axial force were monitored and measured. Tables 4.10 through 4.12 show the results obtained during construction. The maximum deflection, during backfilling, occurred at the crown of the structure and was equal to 25.1mm (outward), the haunches and the invert of the pipe-arch deformed 4mm (inward) and 1.3mm (outward), respectively.

The bending moments obtained are given in Table 4.11. The maximum bending moment recorded during construction was equal to 36.1 N.m (compression at the inner fibers) and it was calculated from the readings of the strain gauges located at the crown of the pipe-arch. The invert of the structure experienced a moment equal to 0.6 N.m (compression at the inner fibers) and the corresponding moments at the haunches were equal to 5.6 N.m (tension at the inner fibers). Likewise, results for the axial force are given in Table 4.12.

At the loading stage, the horizontally reinforced-soil pipe-arch was able to carry loads of up to 11.2 kN. The loading stage provided the following results (see Tables 4.13 through 4.15 and Figures 4.8 through 4.10): the deflection at the crown varied from 2mm (inward) at a initial applied load of 4.3 kN to 12.8mm (inward) at a maximum applied load of 11.2 kN. The corresponding bending moment at these two stages were, 24.4 N.m (tension at the inner fibers) at a load of 4.3 kN, and 15.9 N.m (tension at the inner fibers) at a load of 11.2 kN.

The haunches of the structure were also monitored and the results obtained were as follows: the deflection varied from 0.05mm (outward) at 4.3 kN to 0.23mm (outward) at a load of 11.2 N.m. The corresponding moments were: 6.63 N.m (tension at the inner fibers) at a load of 4.3 kN and 14.6 N.m (tension at the inner fibers) at a load of 11.2 kN.

The invert of the pipe-arch produced the following results: the deflection changed form 0.0mm at 4.3 kN. to 0.5mm (outward) at 11.2 kN. Also, the bending moment was calculated to be 0.6 N.m (tension at the inner fibers) at 4.3 kN and it varied to 0.89 N.m (tension at the inner fibers) at a load of 11.2 kN.

The results obtained for the axial force of the pipe-arch, are presented in Table 4.15 and graphically shown in Figure 4.10.

Next, the final stage of the experimental test (i.e.: when the soil is disturbed and the pressure inside the rubber tubes is decreased) produced the results given in Tables 4.16 through 4.18 and are graphically presented in Figures 4.8 through 4.10.

One important observation to notice from these results is that, small variations in the pressure inside the rubber tubes had almost no effect on the bending moment, deflection, and axial force for the reinforced-soil pipe-arch. Also, as the soil around the structure started to fail, the load carrying capacity of the pipe-arch began to decrease, but it became stable after a few seconds.

Finally, once the pressure in the rubber tubes was reduced considerably, the load carrying capacity of the structure remained almost unchanged. This can be readily observed from the results described in Tables 4.16 through 4.18. It is obvious from these results that the reinforcing material attached to the structure was still carrying load even at the last stage of testing, (i.e.: when the soil surrounding the structure had undergone a considerable amount of failure). The structure seems to recover its strength (load carrying capacity) after the load surrounding the haunches had failed (see Tables 4.16 through 4.18). Figures 4.11 shows the reinforced structure at yielding.

4.3 Reinforced-Soil Structure (Failure of the Soil Surrounding One Corner Plate)

The study of a reinforced-soil structure when uneven soil settlements occur was also carried out in the laboratory. The first two stages of testing (backfilling and loading before disturbing the soil) gave similar results as to the ones obtained in the previous test. The last stage of testing, when the pressure was reduced in one of the rubber tubes, provided similar results to the reinforced-soil pipe-arch subjected to even soil settlements.

Again, the strength and beneficial effects of the reinforcing material appear to be present even after the load carrying capacity of the soil had decreased considerably. These findings are summarised in Tables 4.19 through 4.21 and shown in Figures 4.12 through 4.14.

4.4 Comparison between Unreinforced-Soil and Reinforced-Soil Structures

In comparison, the total deflection at the crown for the unreinforced-soil model, after construction, was 48mm (outward) which is almost 25mm more that the one experienced for the reinforced-soil pipe-arch, similar comparisons can be made at the haunches, invert and sides of the structure. This difference proves to be a direct result from the introduction of the reinforcing sheets. Figures 4.15 through 4.17, compare the bending moment, deflection and axial force for both reinforced-soil and unreinforced-soil structures during construction.

The introduction of reinforcing sheets of geotextile material laid transversely to the axis of the pipe-arch, proved to be beneficial in increasing the load carrying capacity of the structure when temporary loads were applied to it. Since, this particular pipe-arch was under shallow soil cover conditions, temporary loads represent a great concern. The load carrying capacity of the structure was increased by almost 40% when reinforcing sheets of geotextile material were attached to the pipe-arch. The bending moments in the structure were almost eliminated, and the axial force and deflections greatly reduced. This can be readily observed in Figures 4.18 through 4.21.

As explained earlier, rubber tubes filled with air, located near to the haunches of the pipe-arch, were used to simulate the effect of freeze-thaw cycles which occur often in cold regions. Figures 4.22 and 4.23 show that the reinforced-soil structure suffers little deformations when the pressure inside the pressure tubes was decreased. On the other hand when no reinforcement was used the soil surrounding the structure move rapidly. This rapid failure of the soil surrounding the structure, produced a sudden and catastrophic failure of the unreinforced-soil structure, as shown in figure 4.7.

The axial forces and large bending moments accompanied with this effect (freeze-thaw cycle) were also reduced when a reinforced-soil system was used instead of an unreinforced-soil system. This is shown in Figures 4.24 through 4.27.

Table 4.1

Pipe-Arch Deflection (Unreinforced-Soil)
Stage 1: Construction and Backfilling

(mm)

Soil Height From Invert (mm) Dial Gauge Location	102	204	306	408	510	612	970
1 (crown)	0.5	-5.4	-13.0	-24.2	-32.9	-45.2	-47.5
2	0.4	-4.4	-1.5	-0.6	2.6	13.7	16.4
3 (Haunch)	0.2	9.3	5.5	5.6	5.6	4.9	7.9
4	-0.1	1.3	-0.1	-3.0	-4.4	-5.3	-6.1
5 (Invert)	0.3	0.8	-1.8	-2.0	-2.0	-2.3	-2.6
6	-0.5	-0.3	-3.8	-8.0	-9.5	-11.3	-12.1
7(Haunch)	-0.6	3.4	3.8	4.2	4.3	3.5	3.2
8	-1.0	-4.4	-1.5	-0.6	2.6	13.7	16.4

Table 4.2

Pipe-Arch Bending Moment (Unreinforced-Soil)
Stage 1: Construction and Backfilling

(N.m)

Soil Height From Invert (mm) Strain Gauge Location	102	204	306	408	510	612	970
1 (Invert)	-6.3	-11.3	-14.1	-12.4	-10.0	-8.8	-7.1
2	27.9	23.0	15.3	4.7	-3.0	-8.4	-8.9
3 (Haunch)	0.9	4.0	2.3	-3.1	-10.0	-12.3	-14.2
4	-9.0	-6.4	-26.1	13.1	29.4	51.6	48.0
5	2.6	2.3	2.1	1.7	1.5	1.2	2.5
6 (Crown)	-4.2	-8.4	-15.1	-27.8	-42.8	-60.1	-79.6
7	2.6	2.4	2.2	1.8	1.6	1.3	2.6
8	-8.9	-6.3	-26.1	13.1	29.4	51.6	48.0
9 (Haunch)	0.9	3.9	2.3	-3.1	-10.1	-12.3	-14.2
10	1.3	-1.8	-4.8	-8.0	-9.1	-8.8	-9.5

Table 4.3

Pipe-Arch Axial Force (Unreinforced-Soil)
Stage 1: Construction and Backfilling

(kN)

Soil Height From Invert (mm) Strain Gauge Location	102	204	306	408	510	612	970
1 (Invert)	36.4	37.2	37.5	37.1	36.7	36.5	35.9
2	-0.9	2.4	7.6	15.0	20.1	23.7	23.8
3 (Haunch)	33.2	32.6	33.1	34.7	36.6	37.2	37.0
4	28.0	28.3	0.2	30.2	30.6	31.2	31.0
5	-131.4	-131.4	-131.4	-131.3	-131.2	-130.9	-131.2
6 (Crown)	-52.1	-48.9	-43.7	-33.8	-22.3	-8.5	5.8
7	-131.4	-131.4	-131.4	-131.2	-131.2	-130.8	-131.2
8	28.0	28.4	0.3	30.3	30.6	31.2	31.1
9 (Haunch)	33.2	32.6	33.1	34.7	36.6	37.1	36.9
10	35.1	36.1	37.1	38.3	38.7	38.7	38.5

Table 4.4

Pipe-Arch Deflection (Unreinforced-Soil)
Stage 2: Application of an External Load

(mm)

Rubber Tubes - Pressure (kN/m^2)	2.9	2.9	2.9	2.9	2.9	2.9	2.9	2.9
Applied Load (kN)	1.2	1.7	2.4	4.0	5.7	7.0	8.4	8.7
Dial Gauge Location								
1 (crown)	4.2	8.3	14.4	18.3	34.6	39.8	47.4	62.1
2	-2.7	-2.8	-3.2	-4.7	-10.2	-11.7	-14.2	-19.6
3 (Haunch)	-0.1	-0.1	-0.1	-0.1	-0.2	-0.2	-0.4	-0.8
4	0.0	-0.1	-0.2	-0.2	-0.2	-0.2	-0.3	-0.5
5 (Invert)	0.0	0.0	0.0	-0.1	-0.1	-0.1	-0.1	-0.1
6	-0.1	-0.1	-0.1	-0.1	-0.1	-0.1	-0.3	-0.5
7(Haunch)	0.0	-0.1	-0.1	-0.1	-0.2	-0.2	-0.4	-0.7
8	-2.8	-2.8	-3.3	-4.7	-10.2	-11.8	-14.2	-19.6

Table 4.5

Pipe-Arch Bending Moment (Unreinforced-Soil)
Stage 2: Application of an External Load

(N.m)

Rubber Tubes - Pressure (kN/m^2)	2.9	2.9	2.9	2.9	2.9	2.9	2.9	2.9
Applied Load (kN)	1.2	1.7	2.4	4.0	5.7	7.0	8.4	8.7
Strain Gauge Location								
1 (Invert)	-6.6	-6.4	-5.8	-5.5	-5.0	-4.9	-4.6	-4.5
2	-8.7	-8.8	-8.8	-8.9	-8.8	-8.7	-8.7	-8.6
3 (Haunch)	-14.1	-14.1	-14.2	-14.5	-14.7	-14.9	-15.0	-15.1
4	50.2	50.7	53.0	55.1	57.4	59.2	61.0	61.5
5	1.7	1.5	0.4	-0.8	-2.4	-3.6	-5.0	-5.6
6 (Crown)	-49.2	-44.8	-26.7	-9.9	7.7	20.5	33.9	38.6
7	1.7	1.5	0.5	-0.8	-2.3	-3.6	-5.0	-5.5
8	50.2	50.7	53.0	55.2	57.5	59.3	61.0	61.5
9 (Haunch)	-14.1	-14.2	-14.2	-14.6	-14.7	-15.0	-15.1	-15.1
10	-9.7	-9.7	-9.9	-10.2	-10.3	-10.4	-10.5	-10.5

Table 4.6

Pipe-Arch Axial Force (Unreinforced-Soil)
Stage 2: Application of an External Load

(kN)

Rubber Tubes - Pressure (kN/m^2)	2.9	2.9	2.9	2.9	2.9	2.9	2.9	2.9
Applied Load (kN)	1.2	1.7	2.4	4.0	5.7	7.0	8.4	8.7
Strain Gauge Location								
1 (Invert)	35.5	35.4	35.2	35.0	34.9	34.8	34.7	34.6
2	23.7	23.6	23.6	23.6	23.4	23.3	23.2	23.2
3 (Haunch)	36.8	36.7	36.6	36.5	36.5	36.5	36.3	36.3
4	29.9	29.7	29.0	28.2	27.4	27.0	26.4	26.0
5	-131.4	-131.4	-131.0	-130.5	-129.6	-128.8	-127.8	-127.4
6 (Crown)	-20.4	-24.2	-39.3	-53.1	-67.1	-76.8	-86.8	-90.2
7	-131.4	-131.3	-131.0	-130.5	-129.6	-128.7	-127.8	-127.4
8	29.9	29.8	29.0	28.2	27.5	27.1	26.4	26.1
9 (Haunch)	36.8	36.7	36.6	36.5	36.4	36.4	36.3	36.3
10	38.5	38.5	38.5	38.4	38.4	38.4	38.4	38.4

Table 4.7

Pipe-Arch Deflection (Unreinforced-Soil)
Stage 3: Soil Failure

(mm)

Rubber Tubes - Pressure (kN/m^2)	2.61	2.32	1.74	2.61	2.03	1.45	1.45	0.58	0
Applied Load (kN)	8.7	8.7	8.7	8.2	8.2	8.2	8.3	8.3	6.8
Dial Gauge Location									
1 (crown)	62.1	62.2	62.3	64.3	64.3	65.3	69.5	69.9	73.0
2	-19.6	-19.6	-19.6	-19.9	-19.9	-20.5	-22.6	-22.9	-25.4
3 (Haunch)	-0.8	-0.8	-0.8	-0.9	-1.0	-1.2	-2.3	-2.3	-3.5
4	-0.5	-0.5	-0.5	-0.6	-0.6	-0.7	-0.9	-1.0	-2.2
5 (Invert)	-0.1	-0.1	-0.1	-0.1	-0.1	-0.1	-0.2	-0.3	-0.7
6	-0.5	-0.5	-0.5	-0.5	-0.5	-0.5	-0.7	-0.7	-1.2
7(Haunch)	-0.7	-0.7	-0.8	-0.9	-0.9	-1.1	-2.3	-2.3	-3.5
8	-19.6	-19.6	-19.6	-20.0	-20.0	-20.6	-22.6	-22.9	-25.4

Table 4.8

Pipe-Arch Bending Moment (Unreinforced-Soil)
Stage 3: Soil Failure

(N.m)

Rubber Tubes - Pressure (kN/m^2)	2.61	2.32	1.74	0.58	2.90	1.45	0.58	0
Applied Load (kN)	8.7	8.7	8.7	8.7	8.3	8.3	8.3	6.8
Strain Gauge Location								
1 (Invert)	-4.6	-4.7	-4.8	-4.9	-4.3	-4.3	-4.3	-4.1
2	-8.5	-8.5	-8.4	-8.2	-8.5	-8.3	-8.2	-8.4
3 (Haunch)	-15.2	-15.4	-15.7	-16.1	-16.5	-17.0	-17.3	-17.6
4	61.5	61.4	61.4	61.3	68.2	68.1	68.1	73.2
5	-5.6	-5.6	-5.5	-5.6	-11.7	-11.7	-11.7	-14.1
6 (Crown)	38.7	38.8	38.7	38.7	26.1	26.1	26.0	76.7
7	-5.5	-5.5	-5.5	-5.5	-11.7	-11.6	-11.7	-14.1
8	-15.2	-15.3	-15.7	-16.0	68.2	68.2	68.1	73.2
9 (Haunch)	-15.3	-15.4	-15.8	-16.1	-16.5	-17.0	-17.4	-17.7
10	-10.4	-10.5	-10.4	-10.4	-10.6	-10.5	-10.5	-10.4

Table 4.9

Pipe-Arch Axial Force (Unreinforced-Soil)
Stage 3: Soil Failure

(kN)

Rubber Tubes - Pressure (kN/m^2)	2.61	2.32	1.74	0.58	2.90	1.45	0.58	0
Applied Load (kN)	8.7	8.7	8.7	8.7	8.3	8.3	8.3	6.8
Strain Gauge Location								
1 (Invert)	34.7	34.7	34.7	34.8	34.6	34.5	34.6	34.4
2	23.1	23.1	23.0	22.9	22.9	22.8	22.7	22.8
3 (Haunch)	36.4	36.5	36.5	36.8	36.4	36.7	36.7	36.9
4	26.1	26.1	26.1	26.1	23.8	23.8	23.7	22.1
5	-127.4	-127.3	-127.3	-127.2	-122.5	-122.5	-122.5	-119.6
6 (Crown)	-90.3	-90.2	-90.2	-90.0	-43.5	-43.5	-43.5	-55.9
7	-127.4	-127.3	-127.2	-127.2	-122.5	-122.4	-122.4	-119.5
8	26.1	26.1	26.1	26.1	23.8	23.9	23.7	22.2
9 (Haunch)	36.4	36.4	36.5	36.7	36.4	36.7	36.7	36.9
10	38.3	38.3	38.3	38.3	38.2	38.3	38.1	38.3

Table 4.10

Pipe-Arch Deflection (Reinforced-Soil)
Stage 1: Construction and Backfilling

(mm)

Soil Height From Invert (mm) Dial Gauge Location	102	204	306	408	510	612	970
1(Crown)	0.2	-2.9	-6.9	-12.8	-17.4	-23.9	-25.1
2	-0.5	-2.3	-0.8	-0.3	1.4	7.3	8.7
3(Haunch)	-0.1	4.9	2.9	3.0	3.0	2.6	4.2
4	-0.1	0.7	-0.1	-1.6	-2.3	-2.8	-3.3
5(Invert)	0.2	0.4	-1.0	-1.1	-1.1	-1.2	-1.4
6	-0.3	-0.2	-2.0	-4.2	-5.1	-6.0	-6.4
7(Haunch)	-0.3	1.8	2.0	2.2	2.3	1.8	1.7
8	-0.5	-2.3	-0.8	-0.3	1.4	7.3	8.7

Table 4.11

Pipe-Arch Bending Moment (Reinforced-Soil)
Stage 1: Construction and Backfilling

(N.m)

Soil Height From Invert (mm) Strain Gauge Location	102	204	306	408	510	612	970
1 (Invert)	-5.6	-6.1	-4.0	-2.2	-1.1	1.6	0.6
2	2.3	1.0	-1.8	-3.3	-4.3	-5.7	-6.8
3 (Haunch)	11.6	13.2	4.1	-2.9	-6.6	-3.5	5.7
4	-3.4	-2.6	0.3	11.4	21.8	22.1	16.9
5	-2.6	-3.0	-4.6	-5.7	-5.2	-1.7	11.4
6(Crown)	-40.0	-41.4	-44.4	-51.0	-15.8	-27.7	-36.2
7	-2.6	-3.0	-4.6	-5.7	-5.2	-1.6	11.4
8	-1.7	0.7	12.9	37.3	50.6	47.1	38.7
9 (Haunch)	11.7	13.2	4.1	-2.9	-6.6	-3.5	5.7
10	2.225	1.005	-1.866	-3.373	-4.341	-5.741	-6.889

Table 4.12

Pipe-Arch Axial Force (Reinforced-Soil)
Stage 1: Construction and Backfilling

(kN)

Soil Height From Invert (mm) Strain Gauge Location	102	204	306	408	510	612	970
1 (Invert)	25.4	25.6	24.7	24.1	23.7	21.3	22.9
2	36.1	36.8	38.3	39.4	39.9	40.7	41.3
3 (Haunch)	-37.7	-38.9	-34.7	-31.0	-29.3	-31.0	-37.1
4	34.2	34.0	33.6	32.1	31.1	31.7	30.5
5	21.5	21.6	22.3	22.5	22.3	20.5	14.6
6(Crown)	-100.9	-101.2	-101.6	-102.3	-53.9	-49.8	-46.8
7	21.5	21.7	22.3	22.6	22.4	20.6	14.6
8	-31.3	-32.6	-37.2	-46.5	-51.8	-51.3	-49.7
9 (Haunch)	-37.7	-38.9	-34.6	-30.9	-29.2	-31.0	-37.1
10	36.1	36.8	38.3	39.3	39.9	40.6	41.3

Table 4.13

Pipe-Arch Deflection (Reinforced-Soil)
Stage 2: Application of an External Load

(mm)

Rubber Tubes-Pressure (kN/m^2)	2.9	2.9	2.9	2.9	2.9	2.9	2.9	2.9	2.9
Applied Load (kN)	4.3	5.9	6.2	7.1	8.1	9.4	10.4	11.1	11.2
Dial Gauge Location									
1(Crown)	2.1	3.9	4.2	5.0	6.9	8.6	10.7	12.2	12.8
2	-0.5	-1.1	-1.2	-1.5	-2.1	-2.7	-3.5	-4.0	-4.2
3(Haunch)	-0.1	-0.1	-0.1	-0.1	-0.1	-0.2	-0.2	-0.2	-0.2
4	0.0	0.0	0.0	0.0	-0.1	-0.1	-0.1	-0.1	-0.1
5(Invert)	0.0	0.0	0.0	0.0	0.0	0.0	0.0	-0.1	-0.1
6	0.0	0.0	0.0	0.0	-0.1	-0.1	-0.1	-0.1	-0.1
7(Haunch)	0.0	0.0	0.0	0.0	-0.1	-0.1	-0.1	-0.2	-0.2
8	-0.5	-1.2	-1.3	-1.5	-2.2	-2.8	-3.5	-4.0	-4.2

Table 4.14

Pipe-Arch Bending Moment (Reinforced-Soil)
Stage 2: Application of an External Load

(N.m)

Rubber Tubes-Pressure (kN/m^2)	2.9	2.9	2.9	2.9	2.9	2.9	2.9	2.9	2.9
Applied Load (kN)	4.3	5.9	6.2	7.1	8.1	9.4	10.4	11.1	11.2
Strain Gauge Location									
1 (Invert)	0.6	0.6	0.6	0.7	0.8	0.8	0.9	0.9	0.9
2	-6.9	-7.1	-7.2	-7.2	-7.4	-7.4	-7.6	-7.6	-7.7
3 (Haunch)	6.6	8.1	8.4	9.1	10.8	12.1	13.5	14.3	14.6
4	17.1	17.4	17.4	17.7	18.2	18.6	19.2	19.7	19.8
5	8.1	4.3	3.8	1.9	-2.9	-7.0	-12.3	-15.9	-17.4
6(Crown)	-24.4	-16.6	-15.1	-11.7	-4.5	1.5	8.8	13.9	15.9
7	8.2	4.3	3.8	1.9	-2.8	-7.0	-12.3	-15.9	-17.4
8	39.2	39.9	39.9	40.3	41.2	42.0	42.9	43.7	44.0
9 (Haunch)	6.7	8.2	8.4	9.1	10.8	12.1	13.5	14.3	14.6
10	-7.0	-7.1	-7.2	-7.2	-7.4	-7.5	-7.6	-7.7	-7.7

Table 4.15

Pipe-Arch Axial Force (Reinforced-Soil)
Stage 2: Application of an External Load

(kN)

Rubber Tubes-Pressure (kN/m^2)	2.9	2.9	2.9	2.9	2.9	2.9	2.9	2.9	2.9
Applied Load (kN)	4.3	5.9	6.2	7.1	8.1	9.4	10.4	11.1	11.2
Strain Gauge Location									
1 (Invert)	22.9	22.9	22.9	22.9	22.9	22.8	22.8	22.8	22.8
2	41.4	41.5	41.5	41.5	41.6	41.6	41.7	41.8	41.8
3 (Haunch)	-37.9	-39.0	-39.2	-39.7	-40.7	-41.5	-42.4	-42.9	-43.1
4	29.8	29.6	29.4	29.4	29.2	29.0	28.9	28.8	28.7
5	13.4	13.7	13.6	14.0	15.2	16.5	18.2	19.3	20.0
6(Crown)	-52.7	-56.0	-56.6	-58.0	-60.7	-63.0	-65.6	-67.5	-68.2
7	13.4	13.7	13.7	14.0	15.3	16.5	18.2	19.4	20.0
8	-51.3	-52.5	-52.8	-53.4	-54.4	-55.4	-56.4	-57.2	-57.5
9 (Haunch)	-37.8	-38.9	-39.1	-39.7	-40.7	-41.5	-42.4	-42.9	-43.1
10	41.3	41.4	41.5	41.5	41.6	41.6	41.7	41.7	41.7

Table 4.16

Pipe-Arch Deflection (Reinforced-Soil)
Stage 3: Soil Failure

(mm)

Rubber Tubes-Pressure (kN/m^2)	2.61	2.32	2.03	1.74	1.45	0.58	1.45	1.45	0
Applied Load (kN)	9.8	9.8	9.8	9.8	9.8	9.8	8.8	9.2	10.7
Dial Gauge Location									
1(Crown)	12.8	12.9	12.9	12.9	12.9	12.9	13.4	14.2	18.8
2	-4.2	-4.2	-4.2	-4.2	-4.2	-4.2	-4.3	-4.6	-6.3
3(Haunch)	-0.3	-0.3	-0.3	-0.3	-0.3	-0.4	-0.4	-0.5	-0.7
4	-0.1	-0.1	-0.1	-0.1	-0.1	-0.1	-0.1	-0.2	-0.2
5(Invert)	-0.1	-0.1	-0.1	0.0	0.0	0.0	-0.1	-0.1	-0.1
6	-0.1	-0.1	-0.2	-0.2	-0.2	-0.2	-0.2	-0.2	-0.3
7(Haunch)	-0.2	-0.3	-0.3	-0.3	-0.3	-0.3	-0.4	-0.5	-0.6
8	-4.2	-4.2	-4.2	-4.2	-4.2	-4.2	-4.4	-4.6	-6.3

Table 4.17

Pipe-Arch Bending Moment (Reinforced-Soil)
Stage 3: Soil Failure

(N.m)

Rubber Tubes-Pressure (kN/m^2)	2.61	2.32	2.03	1.74	1.45	0.58	1.45	1.45	0
Applied Load (kN)	9.8	9.8	9.8	9.8	9.8	9.8	8.8	9.2	10.7
Strain Gauge Location									
1 (Invert)	0.9	0.9	0.9	0.9	0.9	0.9	0.9	0.9	1.0
2	-7.6	-7.7	-7.6	-7.7	-7.6	-7.6	-7.8	-7.8	-8.1
3 (Haunch)	13.7	13.1	13.1	12.4	12.1	11.6	13.4	13.5	15.7
4	19.8	19.8	19.7	19.8	19.8	19.7	19.8	20.1	22.0
5	-17.5	-17.5	-17.5	-17.5	-17.5	-17.5	-18.5	-20.3	-33.2
6(Crown)	15.6	15.4	15.3	15.1	15.0	14.9	17.3	19.4	35.1
7	-17.5	-17.5	-17.5	-17.5	-17.5	-17.5	-18.5	-20.3	-33.1
8	44.0	44.0	44.0	44.0	44.0	44.1	44.2	44.8	48.5
9 (Haunch)	13.7	13.1	13.2	12.4	12.2	11.7	13.4	13.5	15.8
10	-7.6	-7.7	-7.6	-7.7	-7.6	-7.7	-7.8	-7.8	-8.1

Table 4.18

Pipe-Arch Axial Force (Reinforced-Soil)
Stage 3: Soil Failure

(kN)

Rubber Tubes-Pressure (kN/m^2)	2.61	2.32	2.03	1.74	1.45	0.58	1.45	1.45	0
Applied Load (kN)	9.8	9.8	9.8	9.8	9.8	9.8	8.8	9.2	10.7
Strain Gauge Location									
1 (Invert)	22.8	22.8	22.8	22.8	22.8	22.8	22.8	22.8	22.7
2	41.7	41.7	41.7	41.7	41.7	41.7	41.9	41.8	42.0
3 (Haunch)	-42.6	-42.3	-42.5	-41.9	-41.8	-41.6	-42.7	-42.9	-44.2
4	28.8	28.8	28.9	28.9	28.9	29.0	28.6	28.7	28.4
5	20.1	20.3	20.4	20.5	20.5	20.7	20.5	21.7	26.7
6(Crown)	-68.1	-68.0	-67.9	-67.9	-67.9	-67.8	-68.7	-69.4	-74.8
7	20.2	20.3	20.4	20.5	20.6	20.7	20.5	21.7	26.8
8	-57.2	-57.1	-57.0	-56.9	-56.9	-56.7	-57.7	-57.9	-60.3
9 (Haunch)	-42.6	-42.3	-42.5	-41.9	-41.8	-41.5	-42.7	-42.9	-44.2
10	41.7	41.7	41.7	41.6	41.7	41.7	41.8	41.7	41.9

Table 4.19

Pipe-Arch Bending Moment (Reinforced-Soil)
Uneven Soil Failure

(N.m)

Rubber Tube 1 - Pressure (kN/m^2)	2.9	2.9	2.9	2.9	2.9	2.9
Rubber Tube 2 - Pressure (kN/m^2)	2.03	1.45	0.58	0	0	0
Applied Load (kN)	10.7	10.7	10.7	10.7	12.0	12.7
Strain Gauge Location						
1 (Invert)	1.1	1.1	1.1	1.1	1.1	1.1
2	21.7	21.7	21.7	21.6	21.5	21.6
3 (Haunch)	-35.5	-35.5	-35.5	-35.5	-35.2	-35.0
4	22.4	22.4	22.3	22.3	23.2	24.1
5	-35.8	-35.8	-35.8	-35.9	-41.6	-47.6
6(Crown)	38.5	38.4	38.3	38.2	46.3	54.5
7	-29.0	-28.9	-28.8	-28.7	-35.4	-40.0
8	49.3	49.2	49.3	49.3	50.8	52.7
9 (Haunch)	16.8	16.3	15.8	15.5	16.5	16.9
10	-8.2	-8.1	-8.1	-8.1	-8.3	-8.3

Table 4.20

Pipe-Arch Axial Force (Reinforced-Soil)
Uneven Soil Failure

(kN)

Rubber Tube 1 - Pressure (kN/m^2)	2.9	2.9	2.9	2.9	2.9	2.9
Rubber Tube 2 - Pressure (kN/m^2)	2.03	1.45	0.58	0	0	0
Applied Load (kN)	10.7	10.7	10.7	10.7	12.0	12.7
Strain Gauge Location						
1 (Invert)	22.8	22.9	22.8	22.8	22.8	22.7
2	-3.7	-3.7	-3.7	-3.6	-3.6	-3.6
3 (Haunch)	0.3	0.4	0.5	0.5	0.3	0.4
4	28.3	28.3	28.3	28.3	28.2	28.3
5	28.2	28.3	28.4	28.4	30.7	33.5
6(Crown)	-75.8	-75.7	-75.7	-75.7	-78.2	-80.6
7	-74.1	-73.9	-73.9	-73.8	-75.1	-78.4
8	-61.2	-60.9	-60.7	-60.4	-61.6	-62.4
9 (Haunch)	-45.1	-44.8	-44.4	-44.2	-44.8	-45.0
10	42.0	41.9	41.9	41.9	42.0	42.1

Table 4.21

Pipe-Arch Deflection (Reinforced-Soil)
Uneven Soil Failure

(mm)

Rubber Tube 1 - Pressure (kN/m^2)	2.9	2.9	2.9	2.9	2.9	2.9
Rubber Tube 2 - Pressure (kN/m^2)	2.03	1.45	0.58	0	0	0
Applied Load (kN)	10.7	10.7	10.7	10.7	12.0	12.7
Dial Gauge Location						
1 (Crown)	13.7	13.7	13.7	13.7	14.8	17.9
2	-4.3	-4.3	-4.2	-4.2	-4.9	-5.7
3 (Haunch)	-3.9	-3.9	-3.9	-3.9	-3.8	-2.7
4	-3.7	-3.7	-3.7	-3.7	-3.8	-3.8
5 (Invert)	-1.6	-1.6	-1.6	-1.6	-1.6	-1.6
6	-6.4	-6.4	-6.4	-6.4	-6.4	-6.4
7 (Haunch)	1.6	1.6	1.6	1.6	1.5	1.5
8	-4.3	-4.3	-4.3	-4.3	-4.9	-5.5

Figure 4.1 Unreinforced-Soil Pipe-Arch Structure

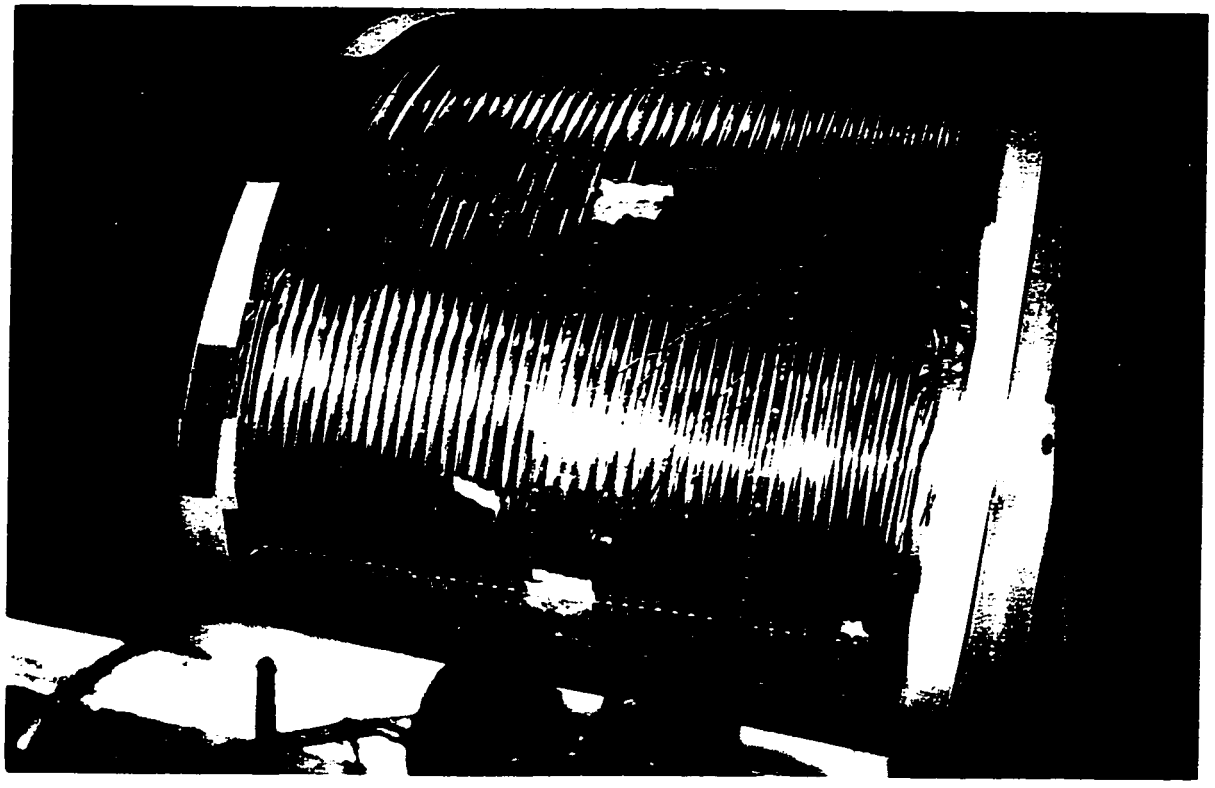

Figure 4.2 Unreinforced-Soil Pipe-Arch - Deflected Shape

A. Reference shape
B. Soil level at 510 mm from invert
C. Soil level 175 mm above crown - Applied load 7 kN - Rubber tube pressure of 2.9 kN/m^2
D. Soil level 175 mm above crown - Applied load 8.7 kN - Rubber tube pressure of 1.74 kN/m^2

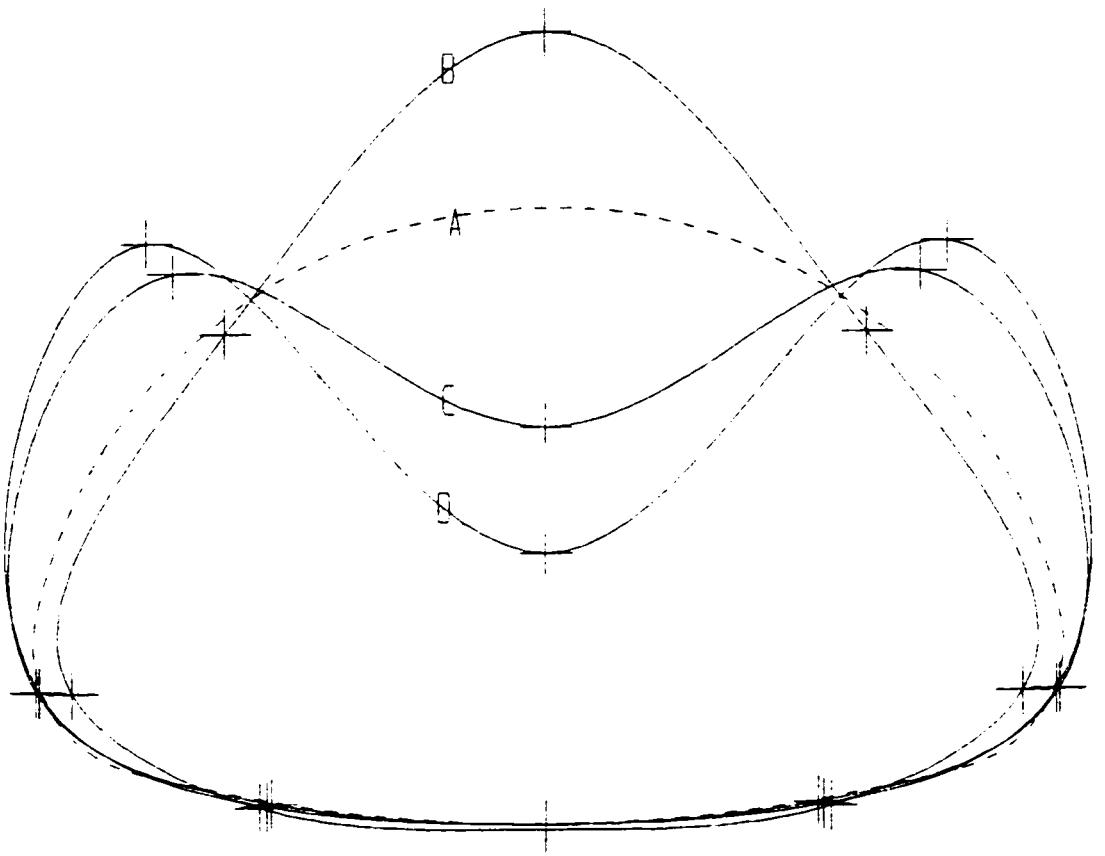

Figure 4.3 Unreinforced-Soil Pipe-Arch - Bending Moment Distribution

A. Reference shape

B. Soil level 175 mm above crown - Applied load 7 kN - Rubber tube pressure of 2.9 kN/m^2

C. Soil level 175 mm above crown - Applied load 8.7 kN - Rubber tube pressure of 1.74 kN/m^2

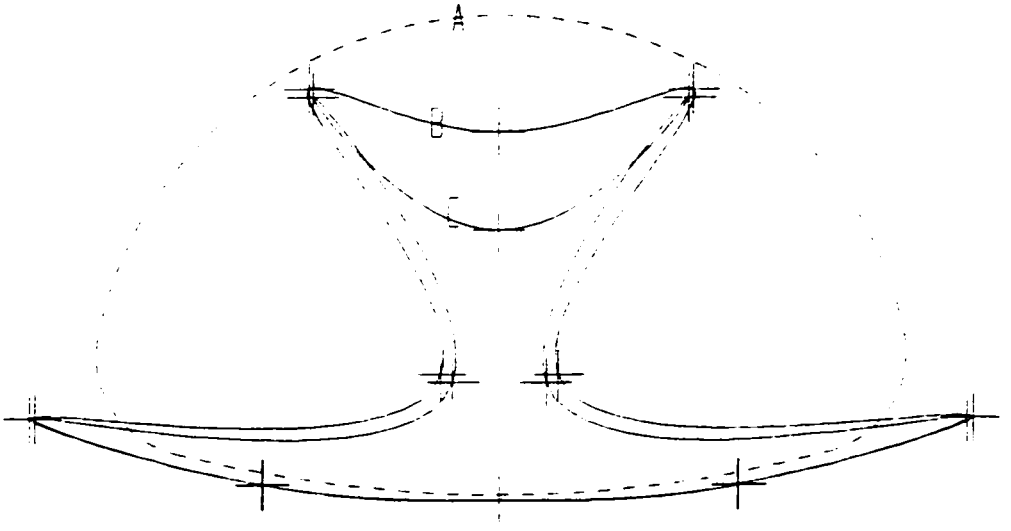

Figure 4.4 Unreinforced-Soil Pipe-Arch - Axial Load

A. Reference shape
B. Soil level 175 mm above crown - Applied load 7 kN - Rubber tube pressure of 2.9 kN/m^2
C. Soil level 175 mm above crown - Applied load 8.7 kN - Rubber tube pressure of 1.74 kN/m^2

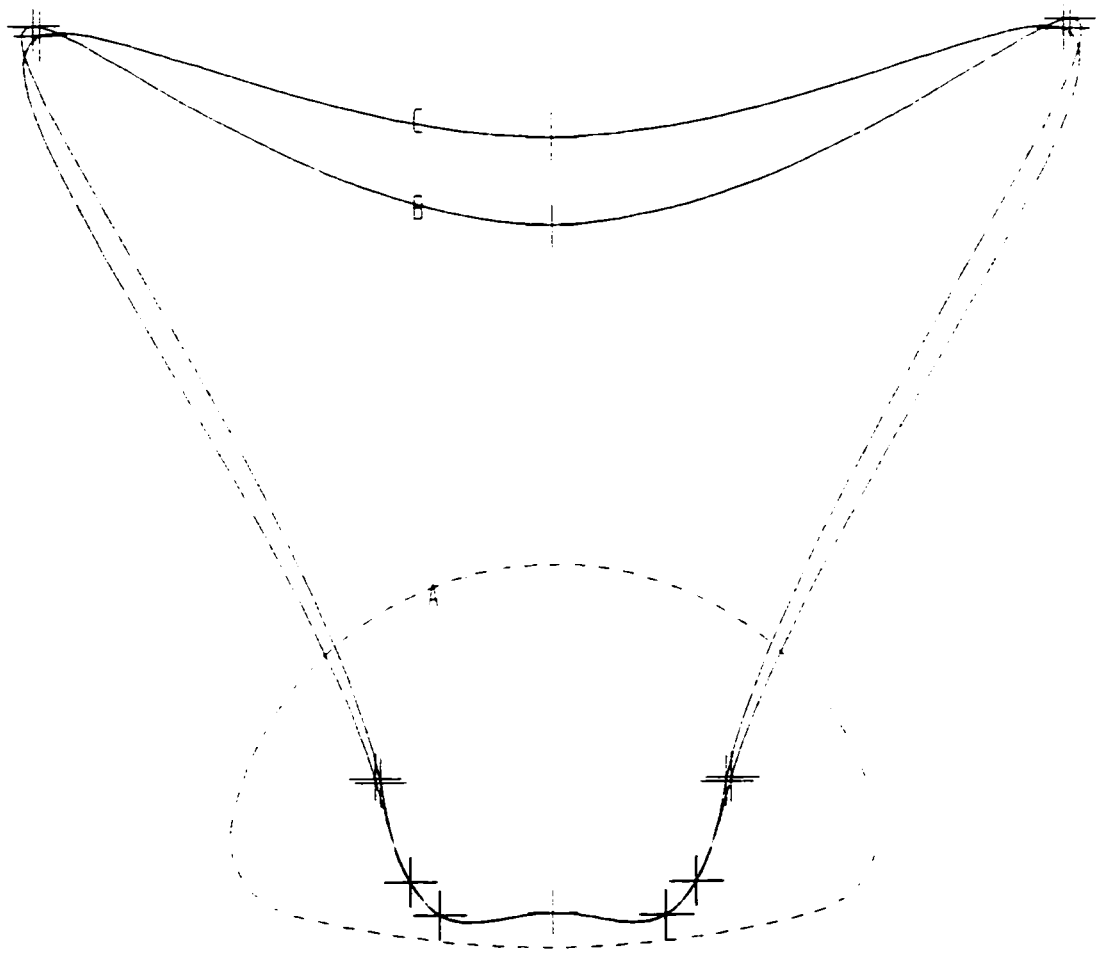

Figure 4.5 Failure of Soil at Invert and Haunches

Figure 4.6 Unreinforced-Soil Pipe-Arch - Yielding At Crown

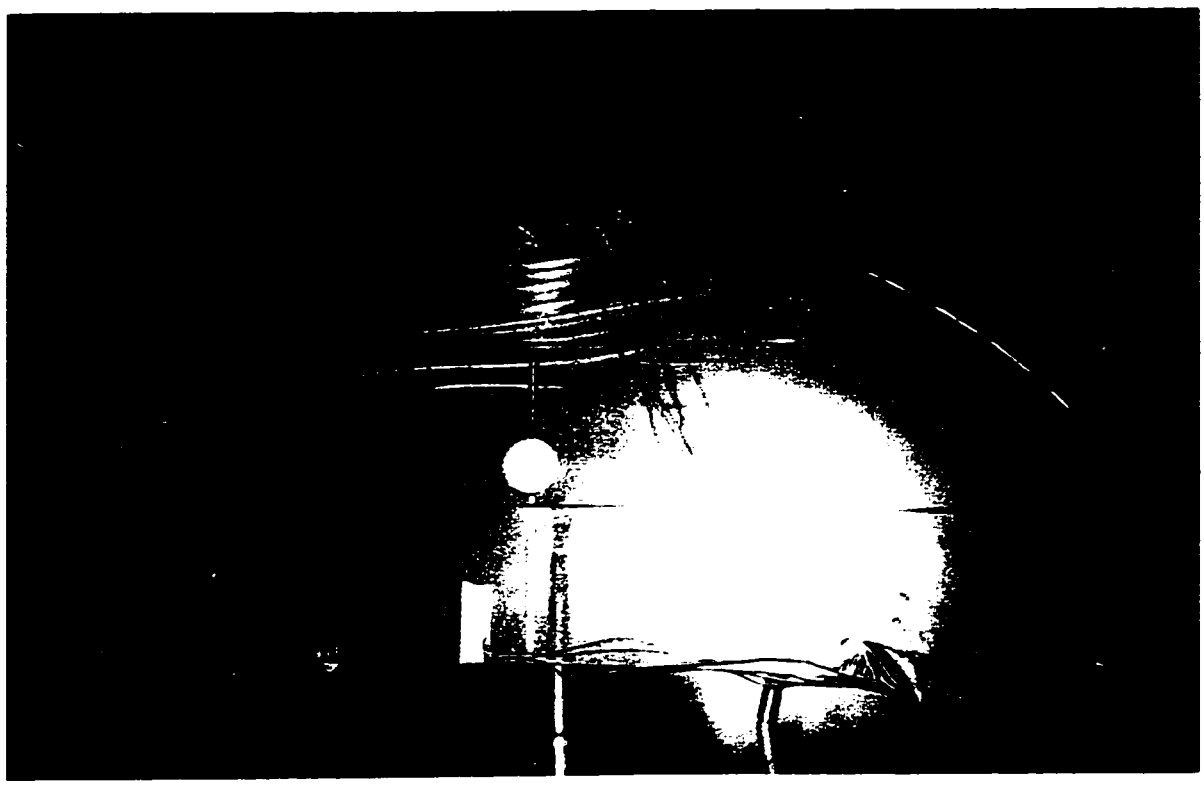

Figure 4.7 Catastrophic Failure of Unreinforced-Soil Pipe-Arch

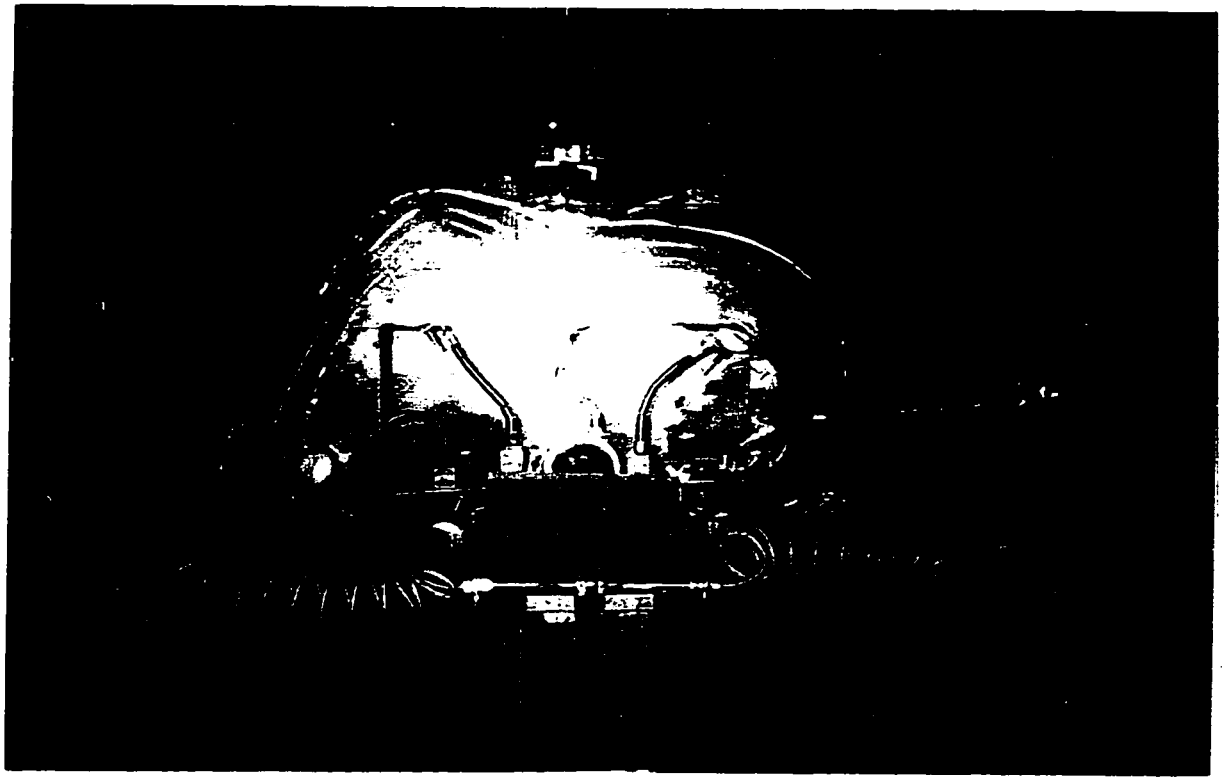

Figure 4.8 Reinforced-Soil Pipe-Arch - Deflected Shape

A. Reference shape
B. Soil level at 510 mm from invert
C. Soil level 175 mm above crown - Applied load 9.4 kN - Rubber tubes pressure of 2.9 kN/m^2
D. Soil level 175 mm above crown - Applied load 9.8 kN - Rubber tubes pressure of 1.45 kN/m^2

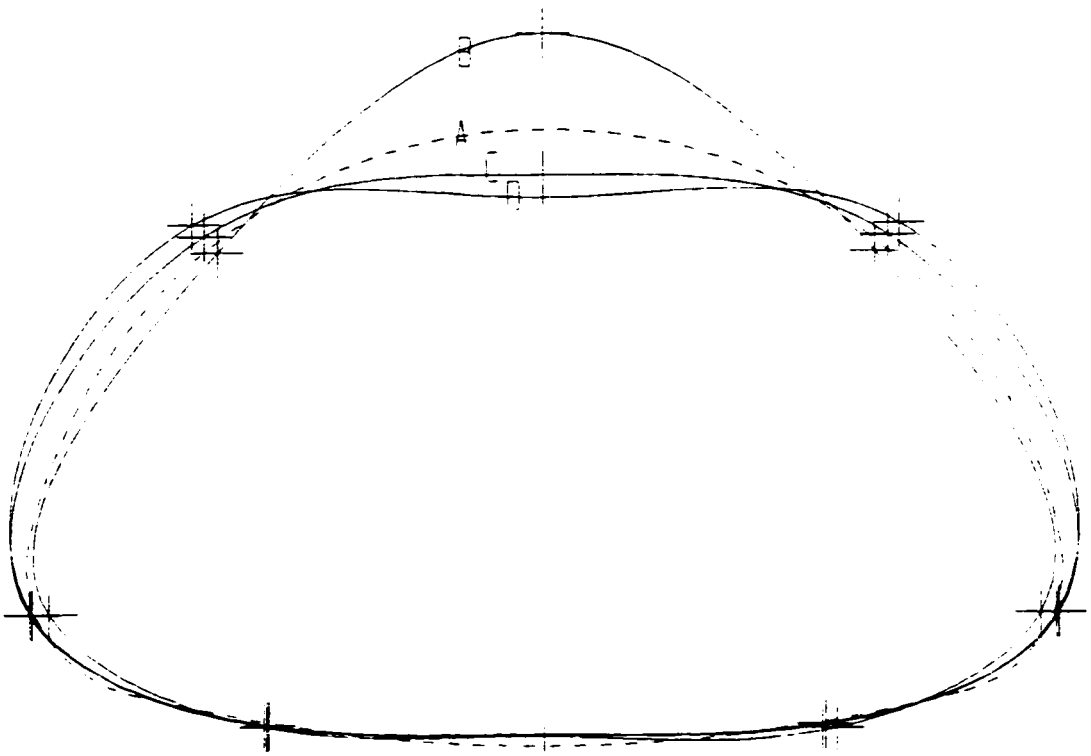

Figure 4.9 Reinforced-Soil Pipe-Arch - Bending Moment Distribution

A. Reference shape

B. Soil level 175 mm above crown - Applied load 9.4 kN - Rubber tubes pressure of 2.9 kN/m^2

C. Soil level 175 mm above crown - Applied load 9.8 kN - Rubber tubes pressure of 1.74 kN/m^2

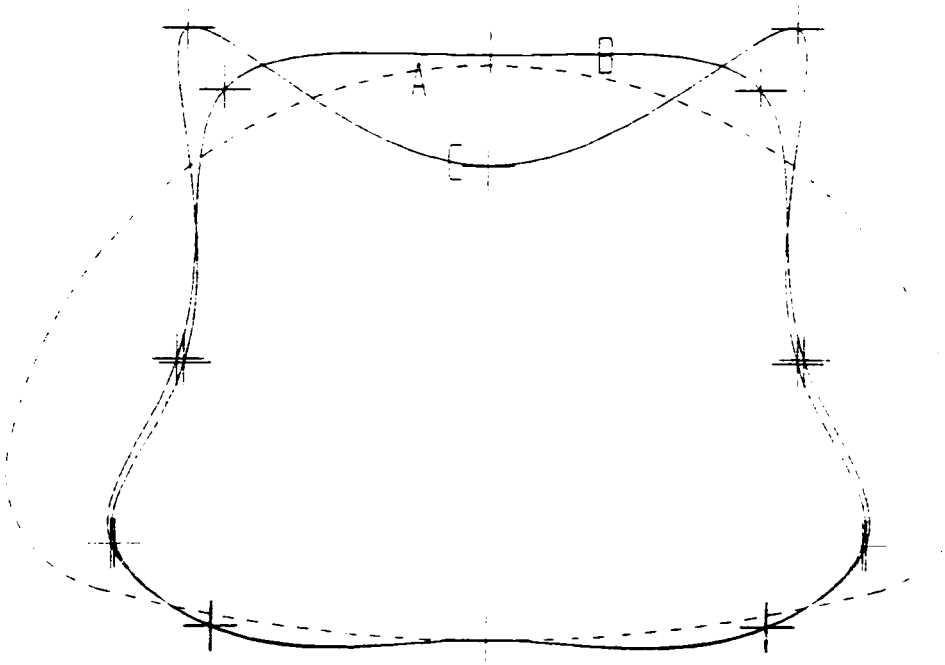

Figure 4.10 Reinforced-Soil Pipe-Arch - Axial Load

A. Reference shape
B. Soil level 175 mm above crown - Applied load 9.4 kN - Rubber tubes pressure of 2.9 kN/m^2
C. Soil level 175 mm above crown - Applied load 9.8 kN - Rubber tubes pressure of 1.74 kN/m^2

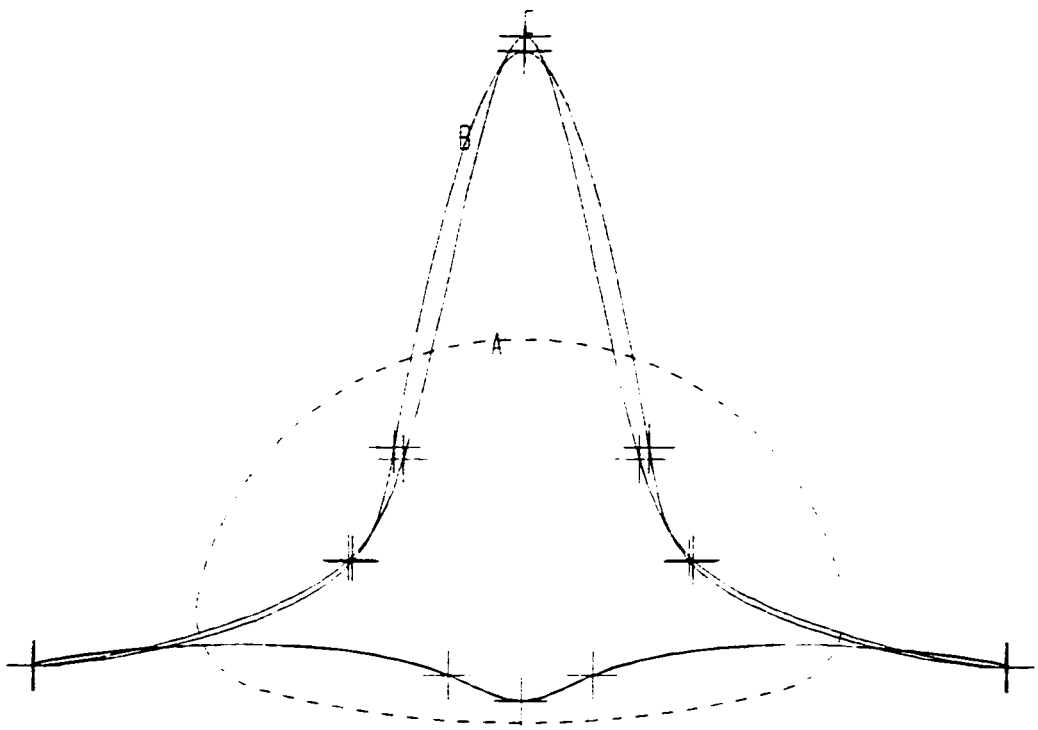

Figure 4.11 Reinforced-Soil Pipe-Arch - At First Sign of Yielding

Figure 4.12 Bending Moment Diagram for Pipe-Arch - Uneven Soil Failure

A. Reference shape

B. Soil level 175 mm above crown - Applied load 10.7 kN - Rubber tubes pressure of 2.9 kN/m^2 and 2.03 kN/m^2

C. Soil level 175 mm above crown - Applied load 12.7 kN - Rubber tubes pressure of 2.9 kN/m^2 and 0 kN/m^2

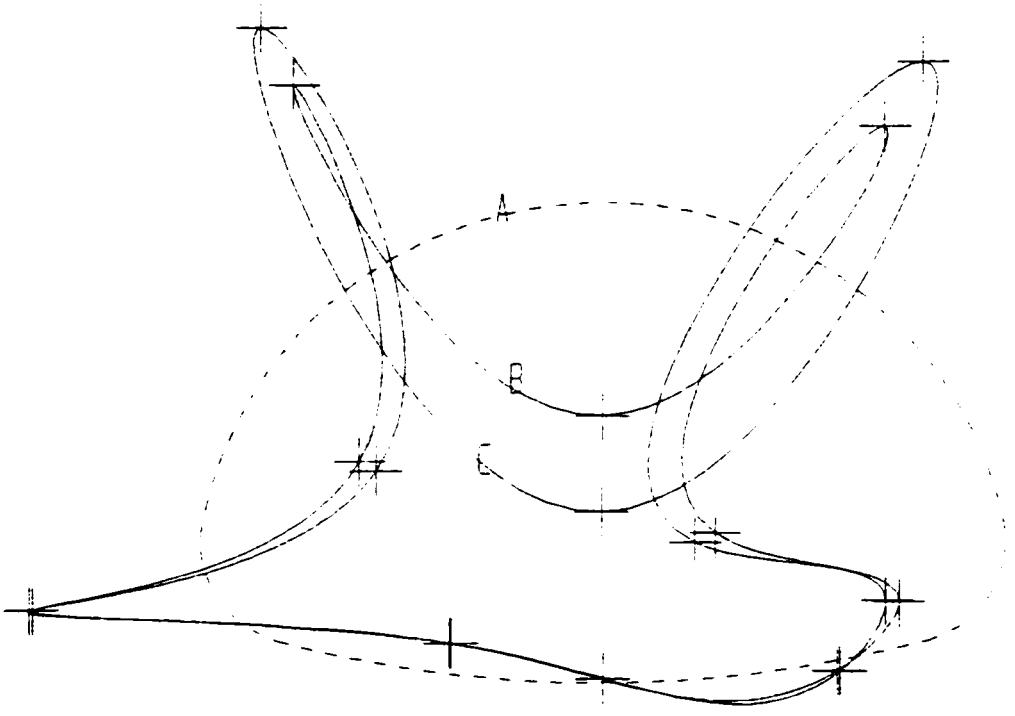

Figure 4.13 Axial Force Diagram for Pipe-Arch - Uneven Soil Failure

A. Reference shape

B. Soil level 175 mm above crown - Applied load 10.7 kN - Rubber tubes pressure of 2.9 kN/m^2 and 2.03 kN/m^2

C. Soil level 175 mm above crown - Applied load 12.7 kN - Rubber tubes pressure of 2.9 kN/m^2 and 0 kN/m^2

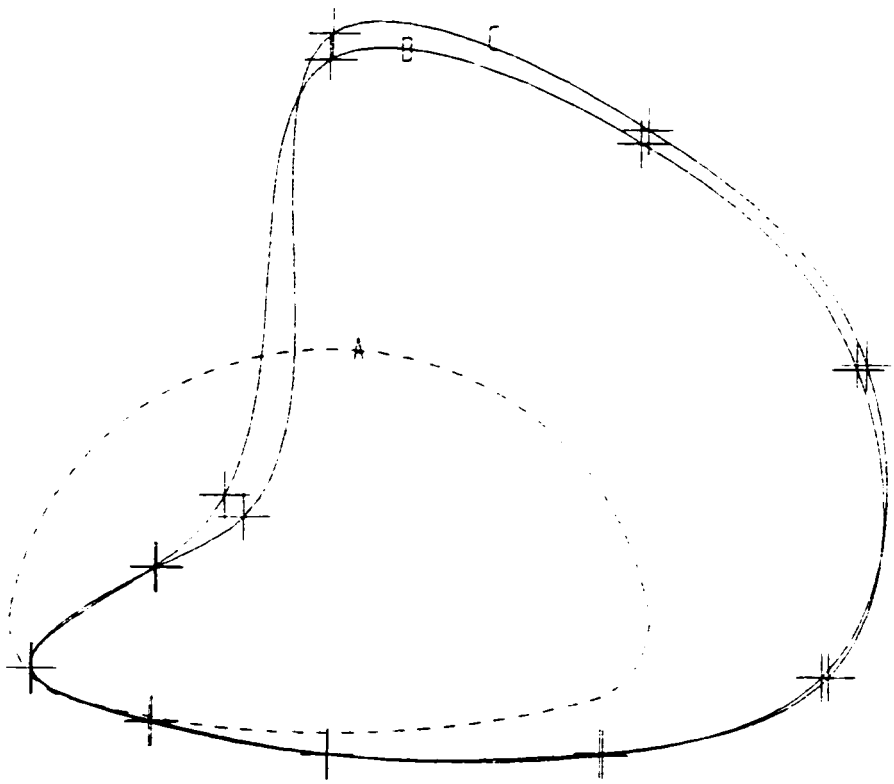

Figure 4.14 Deflected Shape for Pipe-Arch - Uneven Soil Failure

A. Reference shape

B. Soil level 175 mm above crown - Applied load 10.7 kN - Rubber tubes pressure of 2.9 kN/m^2 and 2.03 kN/m^2

C. Soil level 175 mm above crown - Applied load 12.7 kN - Rubber tubes pressure of 2.9 kN/m^2 and 0 kN/m^2

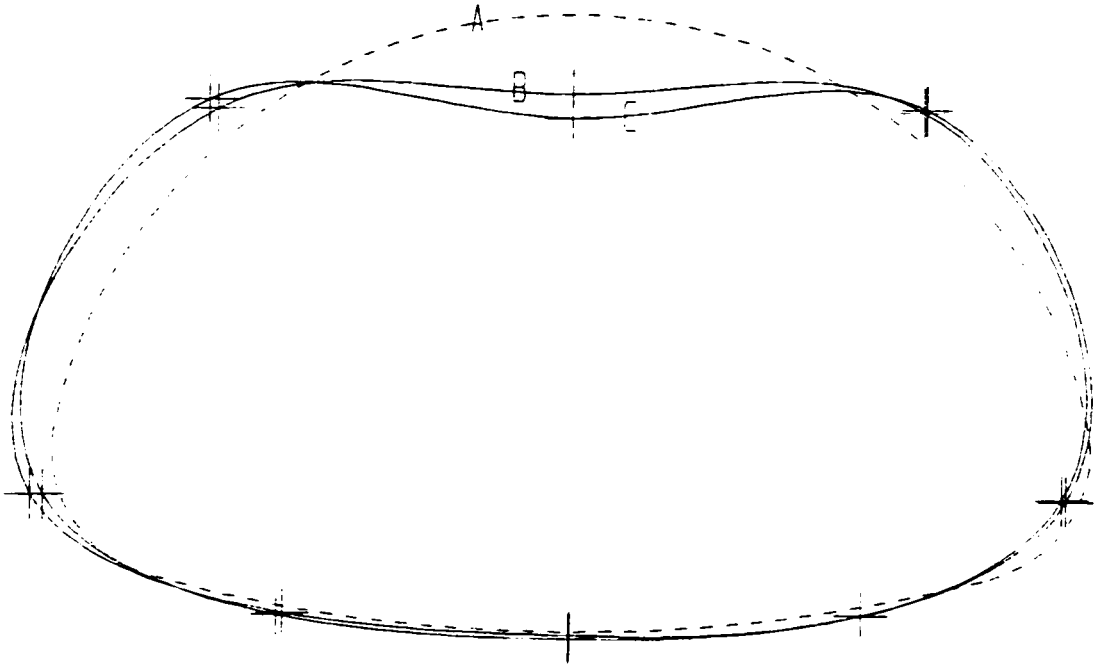

Figure 4.15 Deflected Shape for Pipe-Arch - Soil Level at 970 mm from Invert

A. Reference shape
B. Reinforced-soil
C. Unreinforced-soil

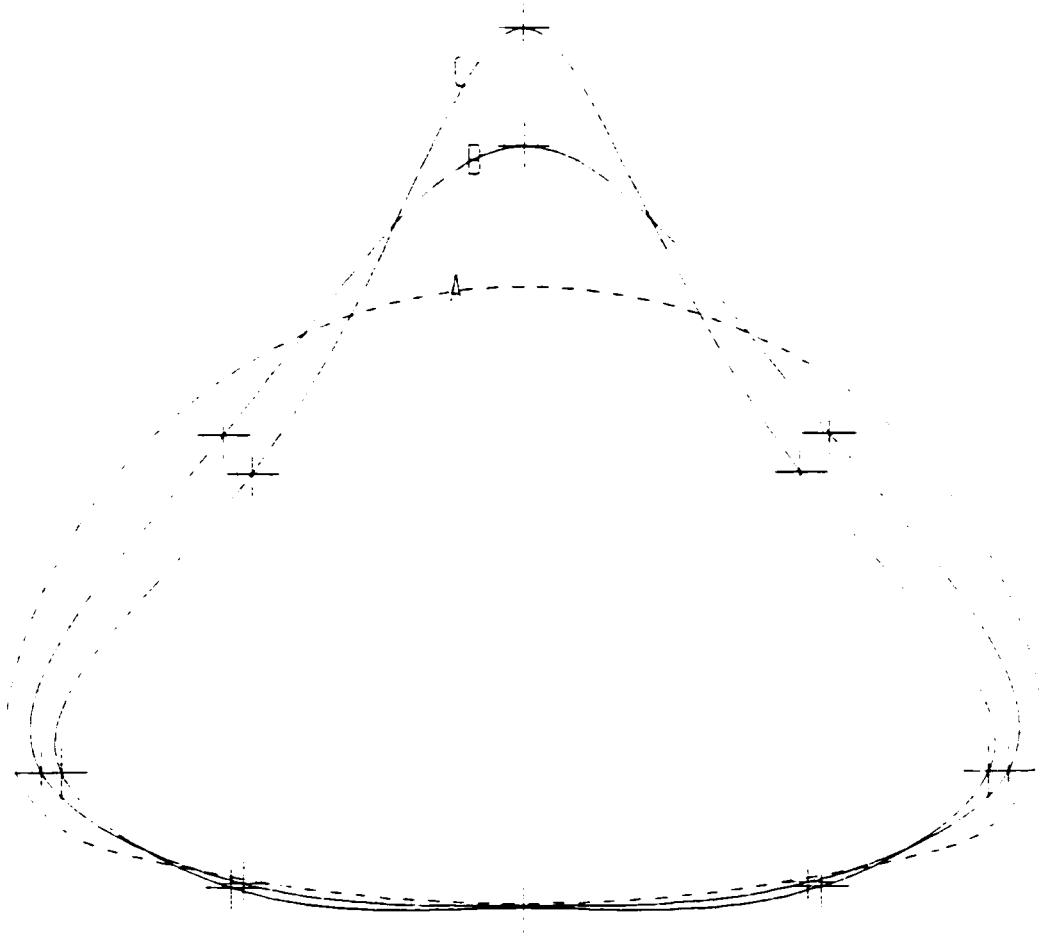

Figure 4.16 Bending Moment Diagram for Pipe-Arch - Soil Level at 970 mm from Invert

A. Reference shape
B. Reinforced-soil
C. Unreinforced-soil

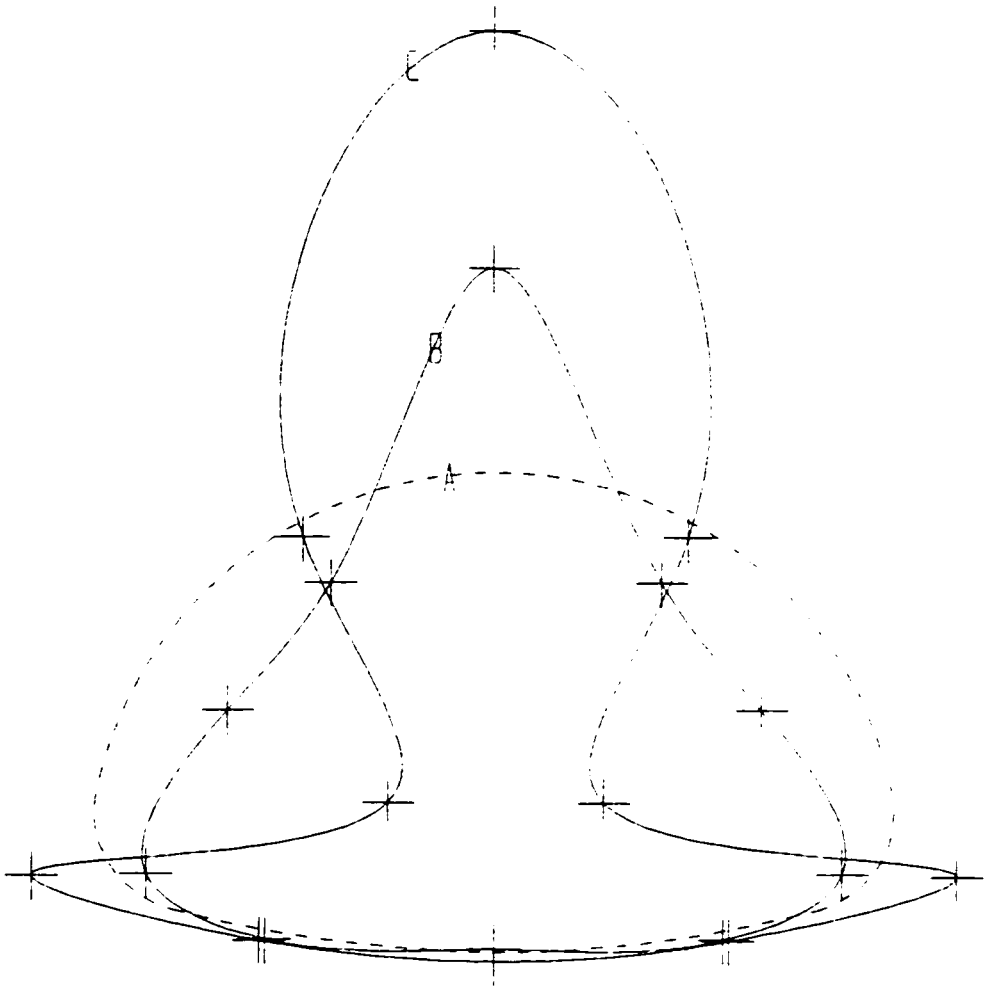

Figure 4.17 Axial Force Diagram for Pipe-Arch - Soil Level at 970 mm from Invert

A. Reference shape
B. Reinforced-soil
C. Unreinforced-soil

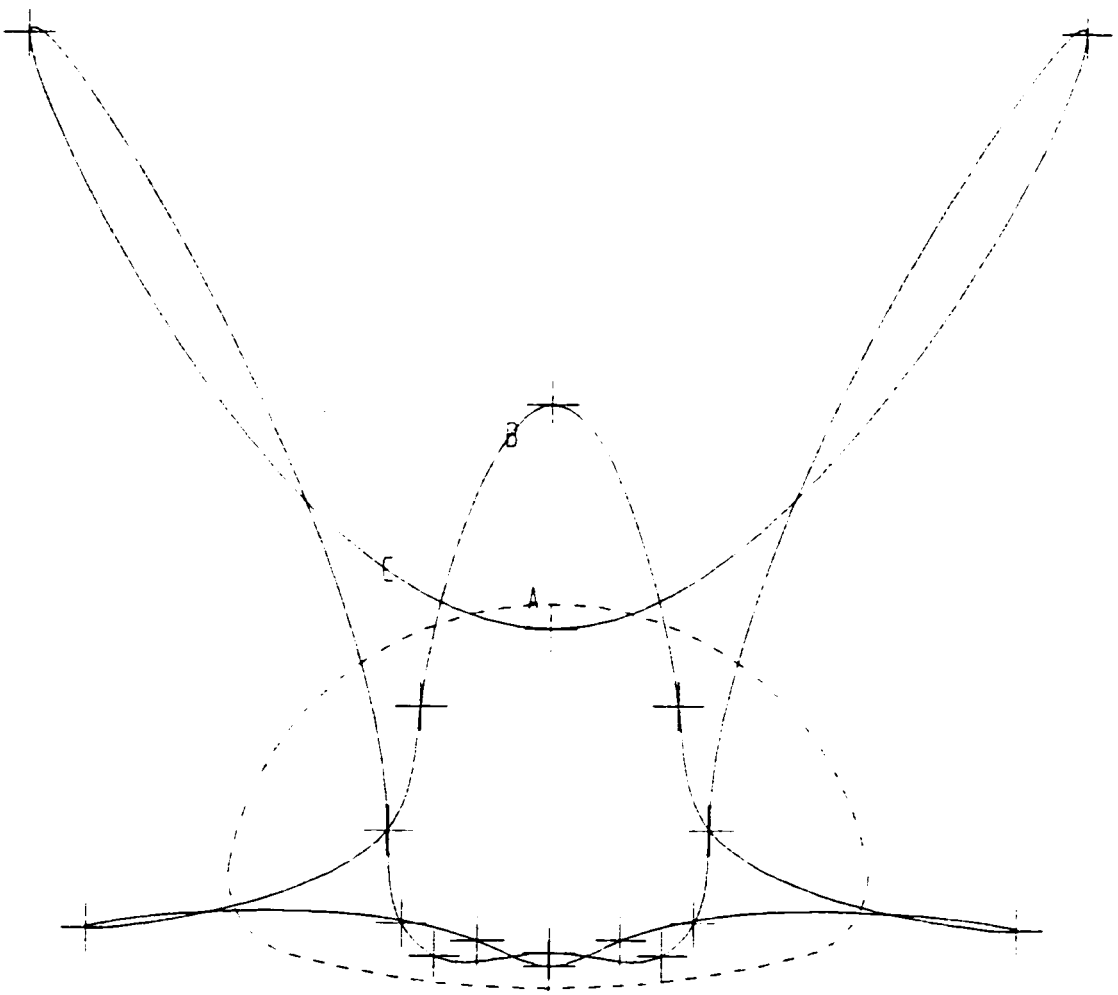

Figure 4.18 Deflected Shape for Pipe-Arch - Applied Load Range 6.9 kN to 7.1 kN

A. Reference shape
B. Reinforced-soil
C. Unreinforced-soil

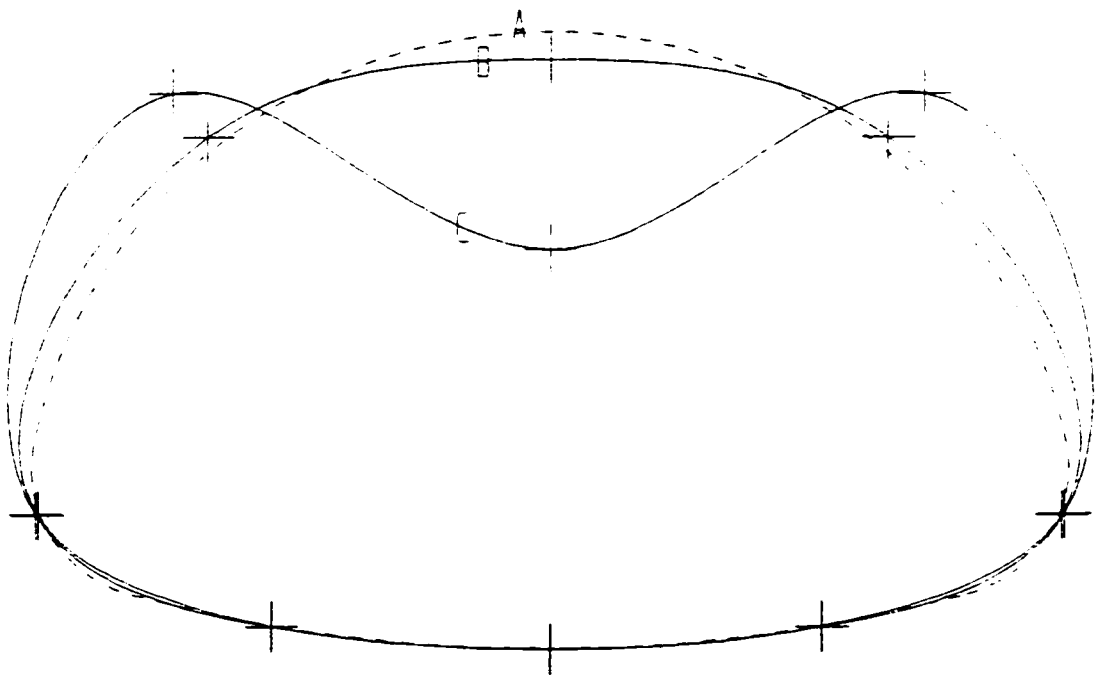

Figure 4.19 Deflected Shape for Pipe-Arch - Applied Load Range 8.7 kN to 9.4 kN

A. Reference shape
B. Reinforced-soil
C. Unreinforced-soil

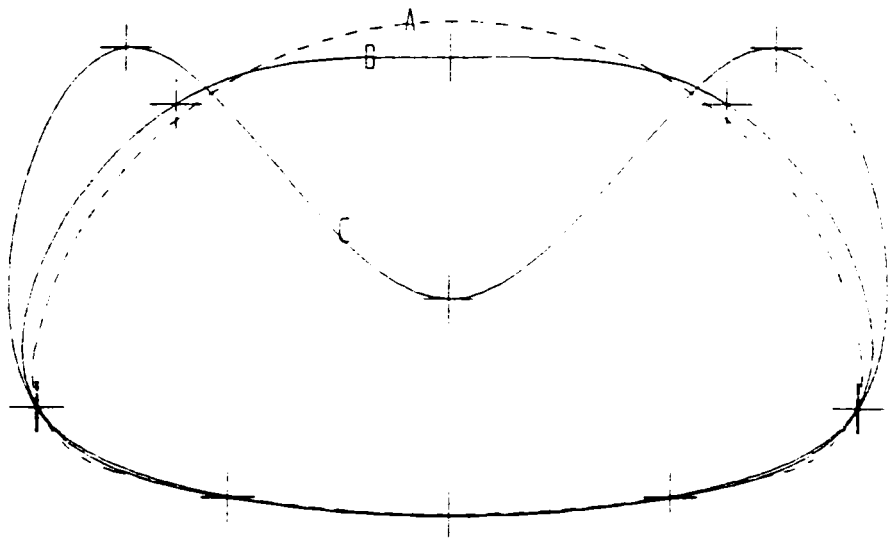

Figure 4.20 Axial Force Diagram for Pipe-Arch - Applied Load Range 5.6 kN to 5.9 kN

A. Reference shape
B. Reinforced-soil
C. Unreinforced-soil

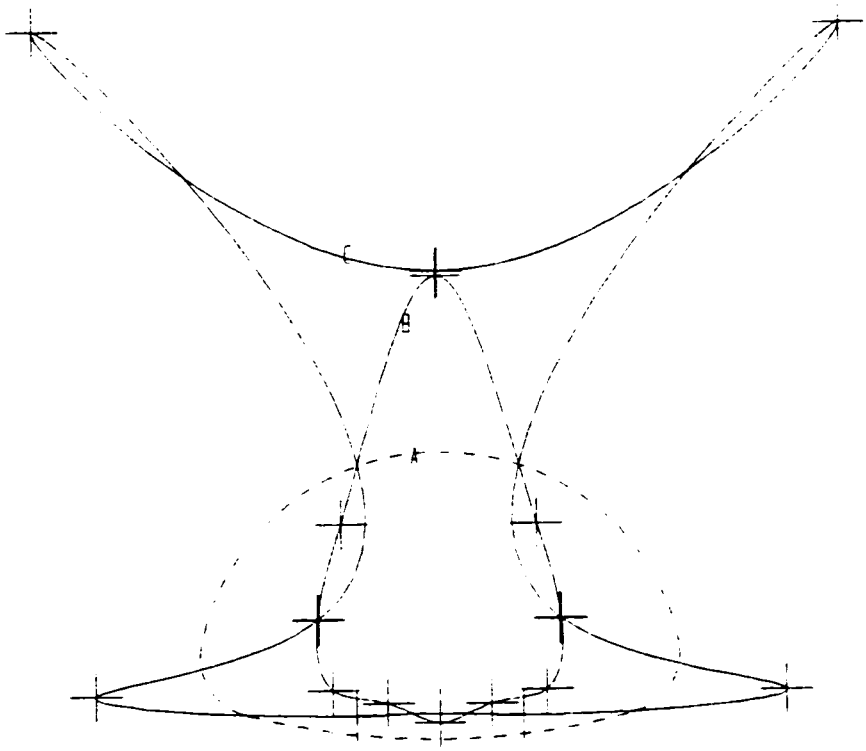

Figure 4.21 Bending Moment Diagram for Pipe-Arch - Applied Load Range 6.9 kN to 7.1 kN

A. Reference shape
B. Unreinforced-soil
C. Reinforced-soil

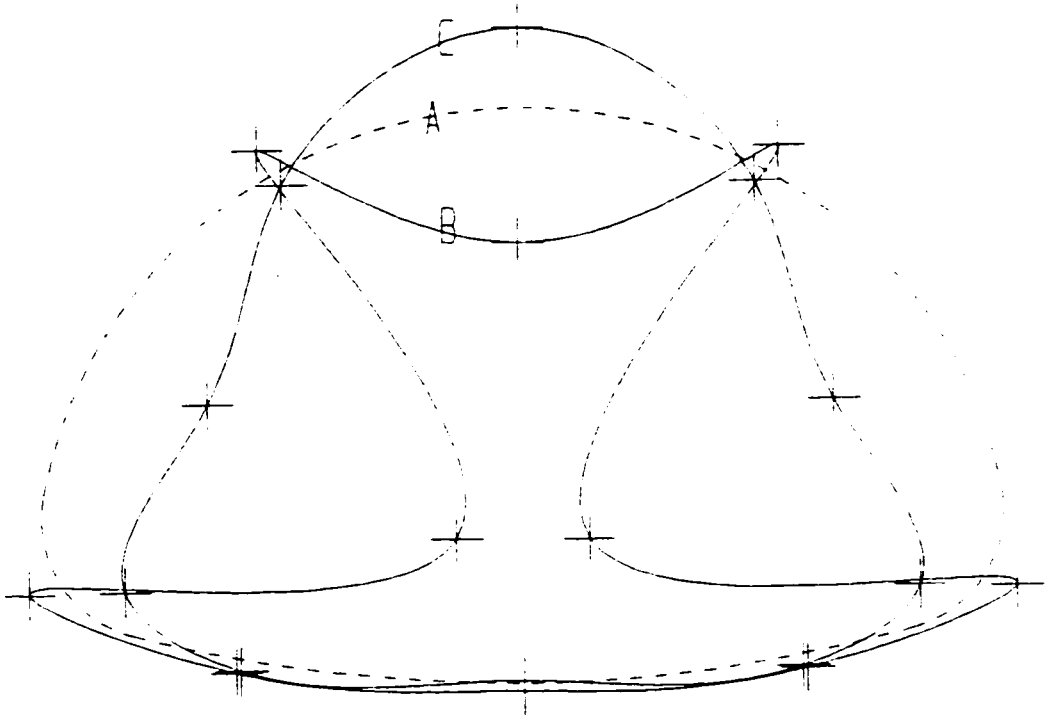

Figure 4.22 Deflected Shape for Pipe-Arch - Applied Load Range 8.3 kN to 8.8 kN - Rubber Tubes Pressure of 1.45 kN/m^2

A. Reference shape
B. Reinforced-soil
C. Unreinforced-soil

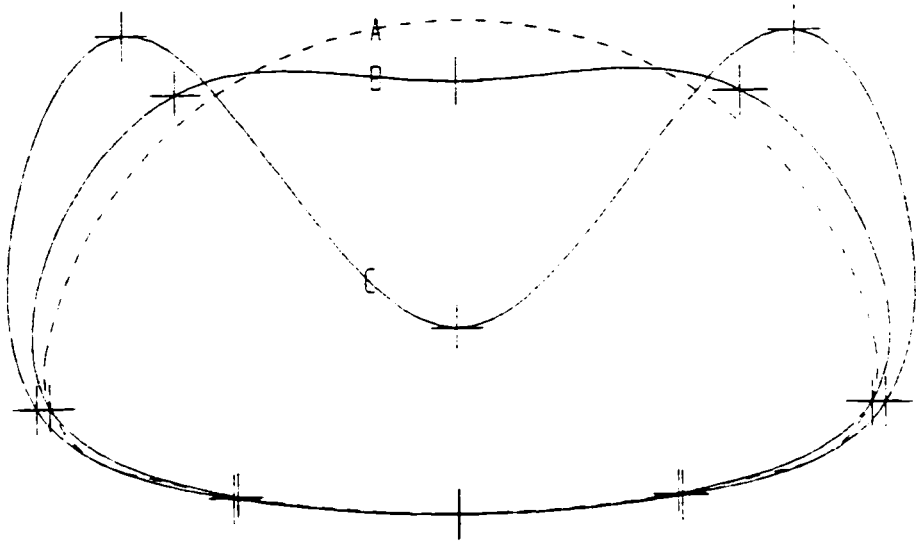

Figure 4.23 Deflected Shape for Pipe-Arch

A. Reference shape
B. Reinforced-soil - Applied load 10.7 kN - Rubber tubes pressure 0 kN/m^2
C. Unreinforced-soil - Applied load 6.8 kN - Rubber tubes pressure 0 kN/m^2

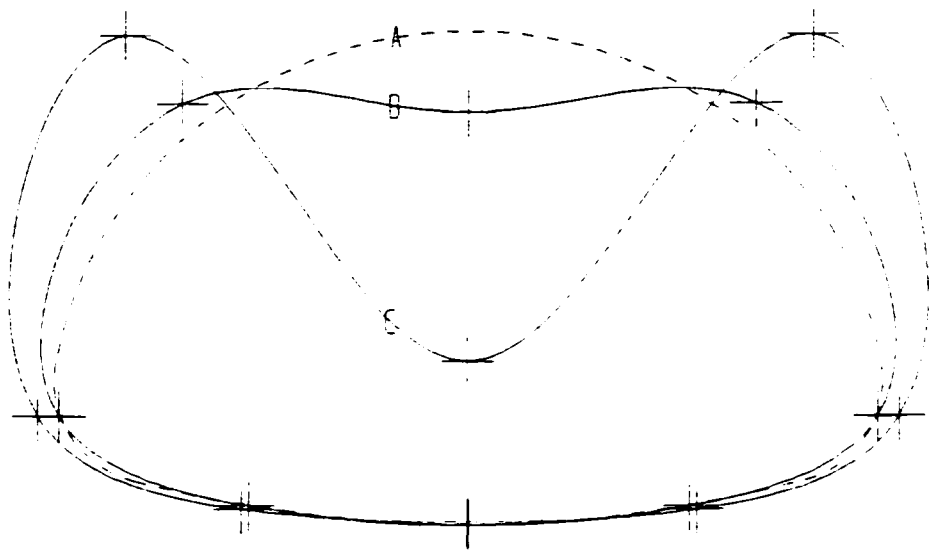

Figure 4.24 Bending Moment Diagram for Pipe-Arch - Applied Load Range 8.3 kN to 8.8 kN - Rubber Tubes Pressure 1.45 kN/m^2

A. Reference shape
B. Reinforced-soil
C. Unreinforced-soil

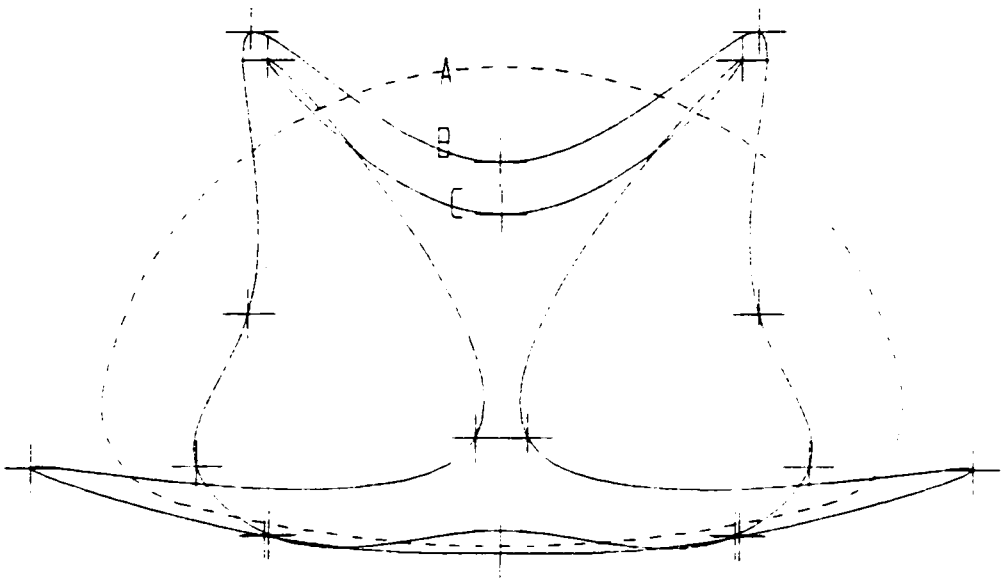

Figure 4.25 Bending Moment Diagram for Pipe-Arch

A. Reference shape
B. Reinforced-soil - Applied load 10.7 kN - Rubber tubes pressure 0 kN/m^2
C. Unreinforced-soil - Applied load 6.8 kN - Rubber tubes pressure 0 kN/m^2

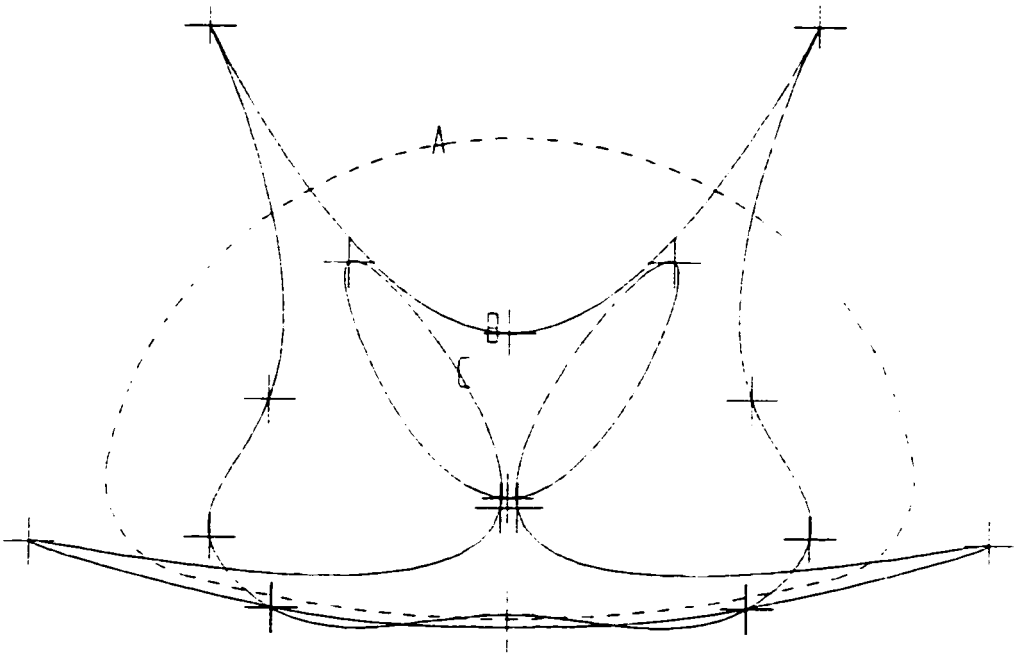

Figure 4.26 Axial Force Diagram for Pipe-Arch - Applied Load Range 8.3 kN to 8.8 kN - Rubber Tubes Pressure 1.45 kN/m^2

A. Reference shape
B. Reinforced-soil
C. Unreinforced-soil

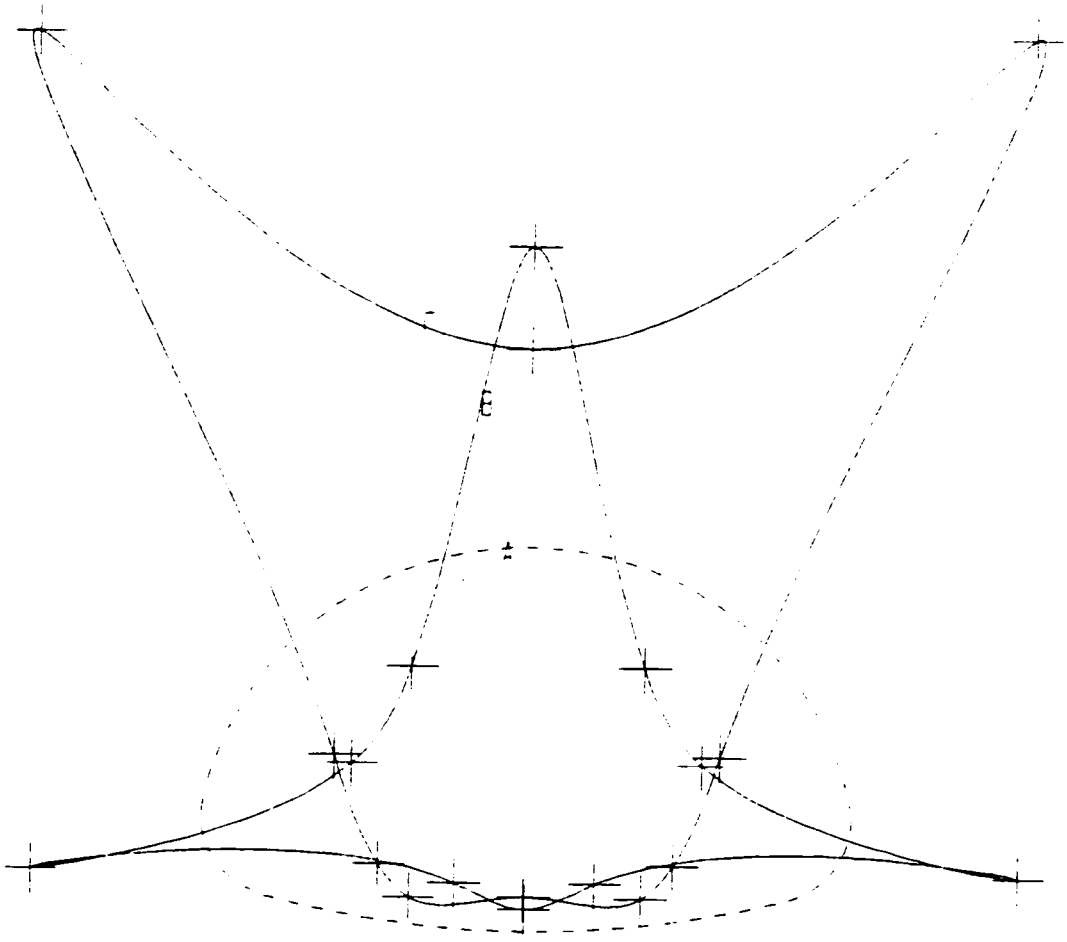

Figure 4.27 Axial Force Moment Diagram for Pipe-Arch

A. Reference shape

B. Reinforced-soil - Applied load 6.8 kN - Rubber tubes pressure 0 kN/m^2

C. Unreinforced-soil - Applied load 10.7 kN - Rubber tubes pressure 0 kN/m^2

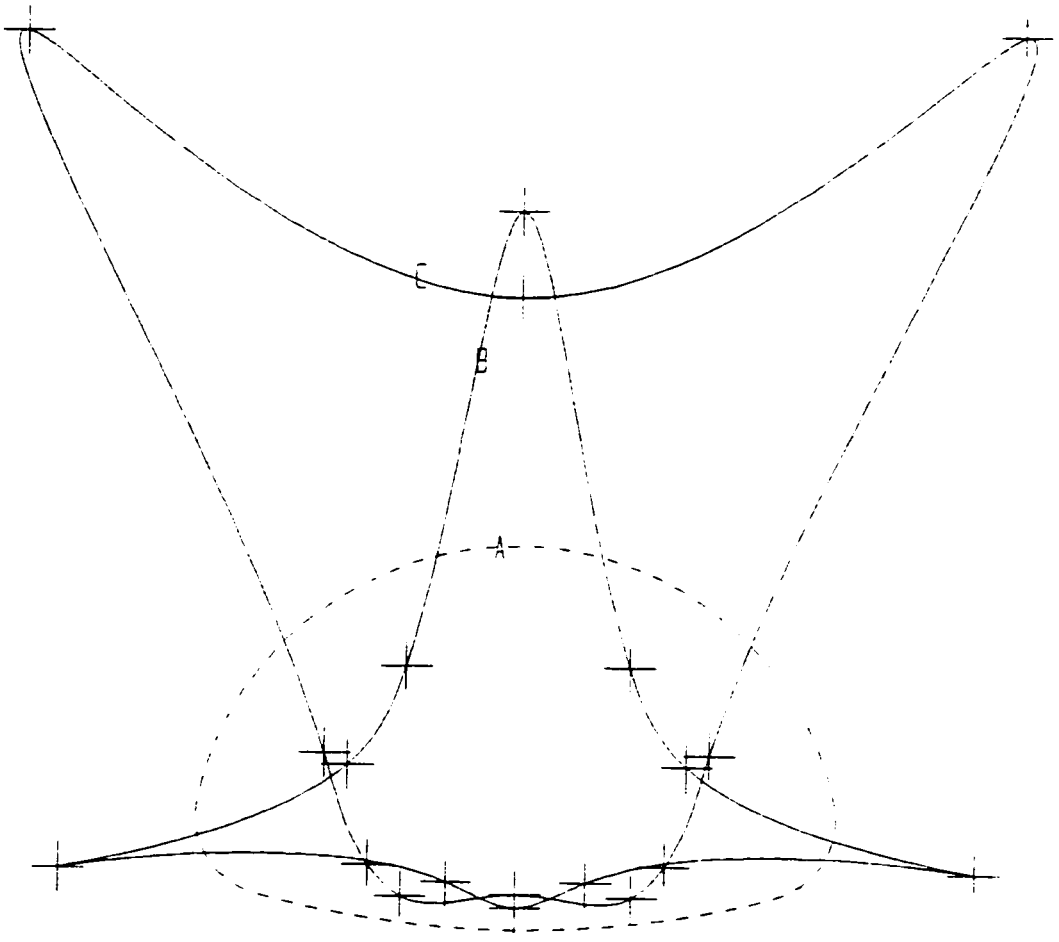

CHAPTER V

DESIGN

This chapter deals with the design of a reinforced-soil pipe-arch. The pipe-arch designed in this chapter is similar to the structure used as a prototype for obtaining the models tested in the laboratory. The properties of the corrugation profile for this structure as well as its overall dimensions are similar to the prototype structure described in chapter 3. The material assumed for reinforcement is standard geogrid material commonly used in practice.

Problem:

It is required to design a reinforced-soil pipe-arch that will carry a highway load equal to 7.7 kPa. The structure is to have a span S = 6250mm and a rise R = 3910mm. The suggested corrugation profile of the metal is 152 x 51mm (as described in chapter 3). The corner plate of the structure has a radius R_c = 840mm (see figure 5.1). The height of soil cover is required to be H = 2m. The properties of the soil are as follows: angle of internal friction $\phi_1 = 40°$; Weight of soil γ = 19 kN/m^3. The material to be used to reinforce the soil is BX100 Tensar biaxial geogrid. Such material is made out of polypropylene and has the following properties [14]: aperture size = 33mm; Open area = 70 % of total area; Thickness = 2.286mm; Tensile strength σ_G = 182 kN/m (minimum).

The elements required in the design are: the wall thickness of the metal structure, the bolting requirements, the corner plate pressure and the length and spacing of the layers of geogrid material.

The first step is to determine the backfill soil density required. For this case 85% minimum soil density is assumed.

Next, the design pressure [1] for this structure is obtained from:

$$P_v = K\,(DL + LL) \qquad (5\text{-}1)$$

where,

P_v = total vertical applied load, kPa

DL = dead load, kPa

LL = live load, kPa

H = height of cover, m

S = span, m

K = soil density factor:

for $S \leq H$	&	Standard Proctor soil density 85%	K = 0.86
for $S \leq H$	&	Standard Proctor soil density 90%	K = 0.75
for $S \leq H$	&	Standard Proctor soil density 65%	K = 0.65
for $S > H$	&	Any density	K = 1.0

By applying equation (5-1) the design pressure for the conditions described above is calculated as follows:

$$P_v = (1)\,\{(19)(2) + (7.7)\} = 45.7 \text{ kPa}$$

From the ring compression theory [48], the compressive thrust in the pipe-arch is determined by the following relation:

$$C = P_v \times S/2 \qquad (5\text{-}2)$$

where,

C = ring compression, kN/m

P_v = design pressure, kPa

S = span, m

Therefore, from equation (5-2) the compressive thrust in the conduit wall is determined as follows:

$$C = \{ 45.7 \times 6.25 \} / 2 = 143 \text{ kN/m}$$

The allowable wall stress, f_c, for this structure is determined by using the following relationship:

$$f_c = f_b / 2 \qquad (5\text{-}3)$$

where,

fc = design stress, MPa

fb = ultimate compressive wall stress, MPa

The ultimate compressive wall stress is calculated by using equations (2-5), (2-6), and/or (2-7), then by applying equation (5-3) the design wall stress is obtained and is given as:

$f_c = 202 / 2 = 101$ MPa for a 152 x 51mm corrugation

Next, the wall cross-sectional area, A, = 1.415 mm^2/mm, can be determined from the relationship between the compressive thrust and the allowable wall stress [1], as follows:

$$A = C / f_c \qquad (5\text{-}4)$$

where,

C = ring compression, kN/m

fc = wall design stress, MPa

Equation (5-4), gives a value of 1.415 mm^2/mm for the wall cross-sectional area. From design tables provided by the American Iron and Steel Institute [1], a specified wall thickness of 3.0mm provides a wall cross-sectional area of 3.522 mm2/mm with a moment

of inertia I = 1057.25 mm^4/mm. Since 3.522 mm^2/mm > 1.415 mm^2/mm required, the 3mm thickness is acceptable for this design.

Next, the handling stiffness [1], FF, for the pipe-arch it is found by trial and error as follows:

Iteration 1:

$$FF = S^2 / EI \qquad (5\text{-}5)$$

where,

S = span, mm

E = Young modulus of elasticity for steel = 200 x $(10)^3$, MPa

I = moment of Inertia, mm^4/mm

From equation (5-5):

$$FF = \{ (6250)^2 / (200 \times 10^3) (1057.25) \} = 0.185 \text{ mm/N}$$

For a pipe-arch the maximum allowable flexible factor, FF', is given by [1]:

$$FF' = 1.5\, FF_a \qquad (5\text{-}6)$$

where,

FF_a = recommended maximum flexible factor for ordinary installation, mm/N

Values for FF_a have been established through experience, based on minimum pipe stiffness requirements for practical handling and installation without undue care or bracing. These values are available through reference [1] for different corrugation profiles. From these reference for a pipe-arch with a corrugation profile of 152 x 51mm, FF_a is determined to be 0.114 mm/N. Therefore the maximum allowable flexible factor from (5-6) is:

$$FF' = 1.5\ (\ 0.114\ ) = \ 0.171 \text{ mm/N (maximum)}$$

Since $FF = 0.185 > FF' = 0.171$ the design is not acceptable

Iteration 2:

By increasing the thickness of the metal to 4.0mm, then the moment of inertia becomes $I = 1867.12$ mm^4/mm. Equation (5-5) can be tried again for this new cross-section:

$$FF = \{\ (\ 6250\ )^2 / (\ 200 \times 10^3\ )\ (\ 1867.12\ )\ \} = 0.134 < 0.171$$

Therefore this design is acceptable and 4.0mm thick plates for construction can be used.

Next, the corner bearing pressure on the soil must be determined; this can be estimated from [1]:

$$P_c = P_v \times R_t / R_c \qquad (5\text{-}7)$$

where,

P_c = pressure acting on soil at corners, kPa

R_t = radius at crown, mm

R_c = radius of corner, mm

P_v = design pressure, kPa

Thus,

$$P_c = 45.7 \times 3125 / 840 = 170 \text{ kPa}$$

Therefore, the allowable corner bearing pressure on the soil must be at least 170 kPa.

The reinforcement and its placement is designed by applying the equations formulated in section 2.4.2.1. First, the minimum required tensile strength of the geogrid must be checked, this is accomplished as follows [14]:

$$\sigma_a = \{ (1 - \sin\phi_1)(1 - z / H) + \tan^2 (45 - \phi_1 / 2)(z / H) \} \gamma_1 z \qquad (5\text{-}8)$$

where,

σ_a = Rankine's active pressure per meter, kN/m

ϕ_1 = angle of internal friction of the soil

γ_1 = Unit weight of soil, kN/m^3

z = depth from top of soil cover to the layer of reinforcement, m

H = total depth of excavation, m

For a maximum depth of 6 m (i.e.: at $z = H$) equation (5-8), becomes identical to equation (2-15):

$$\sigma_a = \{ \tan^2 (45 - \phi_1 / 2) \} \gamma_1 z \qquad (5\text{-}9)$$

or,

$$\sigma_a = \{ \tan^2 (45 - (40) / 2) \} (19) (6) = 24.8 \text{ kN/m}$$

Such value is compared to the specified tensile modulus for the geogrid available for design. The tensile strength for BX100 geogrid is σ_G = 182 kN/m, which is much larger than the minimum required. Therefore the strength of the geogrid mesh is adequate.

The spacing for the layers of the geogrid is determined as follows:

First Rankine's coefficient of active earth pressure is found from equation (2-15):

$$K_a = \tan^2 (45 - 40/2) = 0.217$$

Next the spacing (S_v) at different depths is found from the following equation [14]:

$$Sv = \frac{\sigma_G}{\gamma_1 z K_a [FS_{(B)}]} \qquad (5\text{-}10)$$

where,

σ_G = Allowable strength of geogrid per meter, kN/m

γ_1 = Unit weight of soil, kN/m^3

K_a = Rankine earth pressure coefficient

$FS_{(B)}$ = Factor of safety against tie breaking

The results obtained form this equation at different levels are summarised in Table 5.1.

Next, the length for each layer of reinforcement is determined for the most critical spacing between layers (i.e. 840mm). This is done by using equation (2-16).

The resulting lengths are as shown in table 5.1. From these results the length for each layer is chosen depending on the depth at which the geogrid is located.

For this particular structure a total of 7 layers per side are required. Table 5.2 shows the lengths rounded for each layer and its corresponding location with respect to the pipe-arch.

Table 5.1

Geogrid Soil-Reinforcement - Spacing and Horizontal Length
BX100 - Tensar Multinetting

z Depth of Soil m	S(v) Spacing m	L Length* mm	FS(b) Factor of Safety	K(a) Rankine Coefficient	FS(p) Factor of Safety
0	0.00	3071	1.5	0.217	1.5
0.5	10.19	2838	1.5	0.217	1.5
1.0	5.09	2605	1.5	0.217	1.5
1.5	3.40	2372	1.5	0.217	1.5
2.0	2.55	2139	1.5	0.217	1.5
2.5	2.04	1906	1.5	0.217	1.5
3.0	1.70	1673	1.5	0.217	1.5
3.5	1.46	1440	1.5	0.217	1.5
4.0	1.27	1207	1.5	0.217	1.5
4.5	1.13	974	1.5	0.217	1.5
5.0	1.02	741	1.5	0.217	1.5
5.5	0.93	508	1.5	0.217	1.5
6.0	0.85	275	1.5	0.217	1.5

* The length of reinforcement is based on the most critical spacing between layers (i.e. = 850 mm)

Table 5.2

Length of Geogrid Layers
BX100 - Tensar Multinetting

Location Distance from Invert of Structure m	L Length mm
5.100	2400*
4.250	1900*
3.400	1670
2.550	1200
1.700	740
0.850	510
At Invert	270

* Continuous layer laid on top of the structure multiply distance times two.

Figure 5.1 Overall Pipe-Arch Dimensions (all in mm)

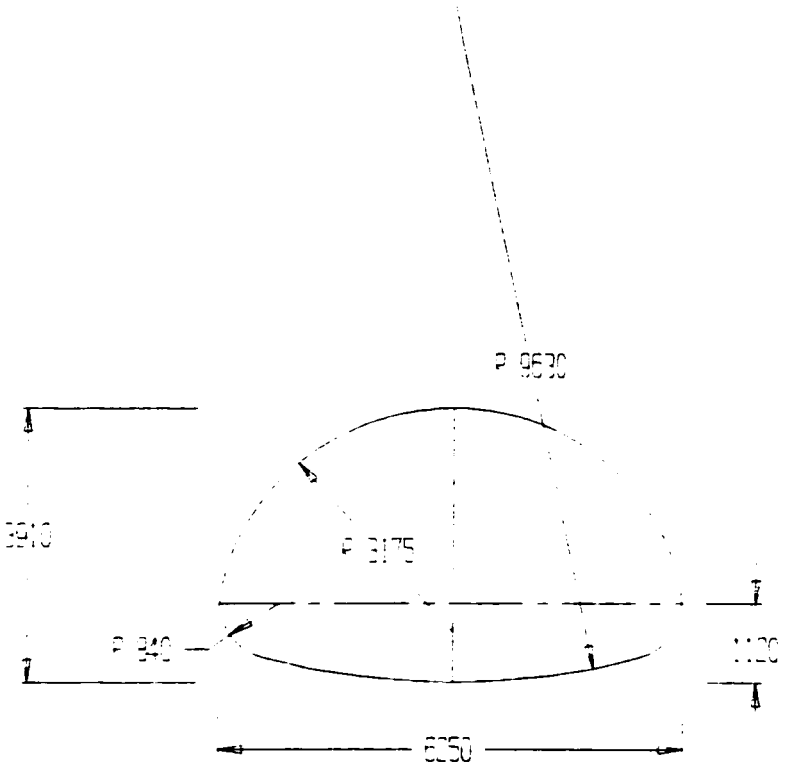

CHAPTER VI

CONCLUSIONS AND RECOMMENDATIONS

6.1 Conclusions

The following conclusions can be drawn from this investigation:

1. Large moments, axial forces and deflections were observed during construction when the unreinforced-soil structure was being backfilled. On the other hand when the horizontally reinforced-soil structures were backfilled, the moments, deflections and axial forces were reduced to a minimum. Thus, the shape of the structure was better controlled.
2. The advantage of the reinforced-soil system are: first, all the deflections that occur during backfilling are kept evenly distributed around the structure. Second, this system not only proves to be beneficial when compacting the soil, but also later on when the structure is being subjected to temporary construction loads.
3. The load carrying capacity of the structure was greatly increased when the soil was reinforced with layers of geogrid material.
4. The haunches and invert of the reinforced-soil pipe-arch experienced little or no deflections, moments, and/or axial forces when the surrounding soil first started to fail.
5. The friction developed along the mesh interfaces, made it possible to enhance the shear resistance of the soil.

6. Sudden and catastrophic failure, often found in unreinforced-soil pipe-arches can be eliminated when using reinforcement. Reinforcing the soil surrounding the pipe-arch changes the failure mode to a more predictable and progressive collapse.

6.2 Recommendations

Further research should be conducted. It is recommended that:

1. A study of the structural behaviour of a full scale model be conducted to further investigate the information obtained from small scale models.
2. Testing of additional models should be conducted to determine the beneficial effects of adding more reinforcing material to the critical components of the pipe-arch (invert and haunches).
3. More research be performed to study the effect of using geogrid/geotextile materials for other shapes of soil-metal structures.
4. A finite element analysis on the structural behaviour of full scale models should be conducted. Such an analysis can be verified by experimental testing of full scale models.

REFERENCES

1. American Iron Steel Institute (1995) "Handbook of steel drainage and highway construction products", 3rd. edition.
2. Abdel-Sayed, G. (1978) "Stability of flexible conduits embedded in soil", Canadian Journal of Civil Engineering, 5(3), pp. 324-333.
3. Abdel-Sayed, G., Bakht, B., and Jaeger, G.L. (1994) "Soil-steel bridges: design and construction", McGraw Hill, Inc., Chapter 8, pp. 237-239.
4. Abdel-Sayed, G., Bakht, B., and Jaeger, G.L. (1994) "Soil-steel bridges: design and construction", McGraw Hill, Inc., Chapter 4, pg. 118.
5. Al-Haussaini, Mosaid (1978) "Field Experiment of Reinforced Earth Wall", Journal of the Geotechnical Engineering Division, ASCE, March, 1978.
6. Bakht, B., and Knobel, Z. (1984) "Testing of a soil-steel structure with relieving slab", Ontario Ministry of Transportation, Report SRR-84-4, pp. 1-31.
7. Billard, J.W. and Wu, J.T.H. (1991) "Load test of a large scale geotextile-reinforced retaining walls", Proceedings, Geosynthetics '91, Atlanta, Volume 2, pp. 537-548.
8. Binquet, J. and Lee, K.L. (1975) "Bearing capacity analysis test on reinforced earth mass", Journal of Geotechnical Engineering Division, ASCE, Volume 101, No. GT12, pp. 1257-1276.
9. Booy, C. (1957) "Flexible conduit studies", Progress Report, Prairie Farm Rehabilitation Administration, Canada department of Agriculture, Saskatoon, Saskatchewan, Canada.

10. Brewer, W. (1990) "The design and construction of culverts using controlled low strength material-controlled density fill", In Structural Performance of Flexible Pipes, pp. 109-118, Netherlands.

11. Brockenbrough, R.L. (1964) "Influence of wall stiffness on corrugated metal culvert design", Highway Research Record, National Research Council/Highway Research Board, No. 56, pp. 71-82.

12. Bryne, P.M., Srithar, T., and Kern, C.B. (1990) "Field Measurements and analysis of large diameter flexible culvert", In structural Performance of flexible Pipes, pp. 27-37, Netherlands.

13. Carroll, R., Jr. (1988) "Specifying geogrids", Geotechnical Fabric Report, Industrial Fabric Association International, St. Paul, March/April.

14. Das, B.M. (1995) "Principles of foundation engineering", PWS Publishing Company, 3rd. edition, Chapter 11, pp. 667-719.

15. Das, B.M. (1995) "Principles of foundation engineering", PWS Publishing Company, 3rd. edition, Chapter 11, pp. 668-669.

16. Duncan, J.M. (1979) "Behaviour and design of long-span metal culverts", J. of Geotechnical Div., ASCE, Vol. 105(3), pp. 399-418.

17. Guido, V.A., Biesiadecki, G.L., and Sullivan, M.J. (1985) "Bearing capacity of geotextile reinforced foundations", Proceedings, Eleventh International Conference on Soil Mechanics and Foundation Engineering, San Francisco, Volume 3, pp. 1777-1780.

18. Guido, V.A., Knueppel, J.D., and Sweeny, M.A. (1987) "Plate load test on geogrid-reinforced earth slabs", Proceedings, Geosyntetics '87, pp. 216-225.

19. Juran, I. Schlosser, F., Long, N., and Leageay, G. (1978) "Full scale experiment on a reinforced earth bridge abutment I Lille", Procedure of the Symposium on Earth Reinforcement.

20. Kennedy, J., Laba, and Shaheen, H. (1986) "Soil-metal arch bridge on reinforced soil abutments", Proceeding, Second International Conference on Short and Medium Span Bridges, Volume 1, Ottawa, pp. 327-341.

21. Kennedy, J., Laba, J., and Mossaid, M. (1980) "Reinforced earth retaining walls under strip loading", Canadian Geotechnical Journal, Volume 17, No. 3, pp. 382-394.

22. Kennedy, J.B. and Laba, J.T. (1989) "Suggested improvements in designing soil steel structures", Transp. Res. Record, 1231, pp. 96-104.

23. Kloeppel, K. and Glock, D. (1970) "Theoretische und experimentelle untersuchugen zu den traglastproblemen biegeweiger, in die erde eingbetteten rohre", publication No.10, Institut fur Static and Stahlbau, T.H. Darmstadt, Germany.

24. Koerner, R.B. (1990) "Design with geosynthetics", Prentice Hall, 2nd. edition, Englewood Cliffs, NJ.

25. Laba J.T. and Kennedy J.B. (1986) "Reinforced earth retaining wall analysis and design", Canadian Geotechnical Journal, Vol. 23, No. 3, pp. 317-326.

26. Laba, J.T., Kennedy, J., and Seymour, P. (1984) "Reinforced earth retaining wall under vertical and horizontal strip loading", Canadian Geotechnical Journal, Volume 21, No. 3, pp. 407-418.

27. Lee, K.L., Adams, B.D., and Vagneron, J.J. (1973) "Reinforced earth retaining walls", Journal of the Soil Mechanics and Foundations Division, ASCE, Volume 99, No. SM10, pp. 745-763.

28. Lusher, U. (1966) "Buckling of soil-surrounded tubes", Journal of Soil Mechanics and Foundations Division, ASCE, 92(6), pp. 211-228.

29. Lusher, U. and Hoeg, K. (1994) "The beneficial action of the surrounding soil on the load carrying capacity of buried tubes", Procedure of the Symposium of Soil-Structure Interaction, University of Arizona, Tucson, Arizona, pp. 393-402.

30. Martin, J.P., Koerner, R.M., and Whitty, J.E. (1984) "Experimental friction evaluation of slippage between geomembranes, geotextiles and soils", Proceedings, International Conference on Geomembranes, Denver, pp. 191-196.

31. Martson, Anson (1930) "The theory of external loads on closed conduits", Bulletin No. 96, Iowa Engineering Experimental, Ames, Iowa, pp. 5-8.

32. Meyerhof, G.G. (1968) "Some problems in the design of shallow-buried steel structures", Proceedings of Canadian Structural Engineering Conference, Toronto, Ontario, pp. 57-63.

33. Moore, R.G. (1986) "Observed signs of distress in soil steel structures", Proceeding Second International Conference on Short and Medium Span Bridges, Ottawa, Canada, Vol. 1, Pg. 342-358.

34. Nicholsoon, P.J. (1986) "Soil nailing a wall", Civil engineering Magazine, pp. 37-39.

35. Omar, M.T., Das, B.M., Yen, S.C., Puri, V.K., and Cook, E.E. (1993) "Ultimate bearing capacity of rectangular foundations on geogrid reinforced sand", Geotechnical Testing Journal, ASTM, Volume 16, No. 2, pp. 246-252.

36. "Ontario Highway Bridge Design Code - Soil Steel Bridge Structures", Ministry of Transportation and Communication, Ontario, Section 12.

37. Playdon, D.K. and Symmonds, S.H. (1988) "Behaviour of slab-stiffened culvert structures", Canadian Journal of Civil Engineering, Vol. 15, pp. 726-731.

38. Schlosser, F. and Vidal, H. (1979) "Reinforced Earth", Liais. Labs. Points et Chausseess, pp. 1067-1087.

39. Sakti, J. and Das, B.M. (1987) "Model test for strip foundation on clay reinforced with geotextile layers", Transportation Research Record, No. 1153, National Academy of Sciences, Washington, DC, pp. 40-45.

40. Sprangler, M.G. (1941) "The structural design of flexible pipe culvert", Bulletin 153, Iowa State College engineering Experimental Station, Iowa.

41. Thamm, B.R., Kreiger, B., and Krieger, J. (1990) "Full-scale test on a geotextile-reinforced retaining structure", Proceedings, Fourth International Conference on Geotextiles, Geomembranes, and Related Products, The Haugue, Volume 1, pp. 3-8.

42. Timoshenko, S.P. and Gere, J.M. (1961) "Theory of elastic stability", McGraw Hill, New York.

43. Vidal, H. (1966) "The principle of reinforced earth", Highway Research Record 282, pp. 1-16.

44. Vidal, H. (1966) "The reinforced earth", Anuals de L'Institute Technique du Batiment et des Travaux, pp. 888-938.

45. Watkins, R.K. (1966) "Structural design of buried circular conduits", Highway Research Record, No. 145, pp. 1-16.

46. Watkins, R.K. (1964) "Structural design trends in buried flexible conduits", Procedure of the symposium on soil-structure interaction, University of Arizona, Tucson, Arizona, pp. 246-255.

47. White, H.L. (1960) "The corrugated Metal Conduit as compression ring", Armco Drainage and Metal Products, Inc.

48. Yu, Wei-Wen (1989) "Cold formed steel design", McGraw Hill, Inc., Chapter 3, pp. 49-52.

49. Yu, Wei-Wen (1989) "Cold formed steel design", McGraw Hill, Inc., Chapter 11, pp. 442-443.

50. Wolford, D.S. (1954) "Sectional properties of corrugated sheets determined by formula", Civil Engineering Magazine, Vol. 24, No. 2,pp. 103-104.

VITA AUCTORIS

The author was born on March 3, 1972 in San Salvador, El Salvador. In 1989, the author completed secondary school at the Externado San Jose secondary school in San Salvador city. The author arrived to Canada in 1989 and lived in Chatham, Ontario, Canada for two years. In 1991, the author joined the Faculty of Engineering at the University of Windsor, Windsor, Ontario, Canada. Then, in 1995 he graduated with a Degree of Bachelor of Applied Science in Civil Engineering ("Second Class Honours").

In 1996, he joined the Civil and Environmental Engineering Department at the University of Windsor as a Research and Teaching assistant. Finally, the author prepared this thesis in partial fulfilment of requirements for the Degree of Master of Applied Science in Civil Engineering

TEST TARGET (QA-3)

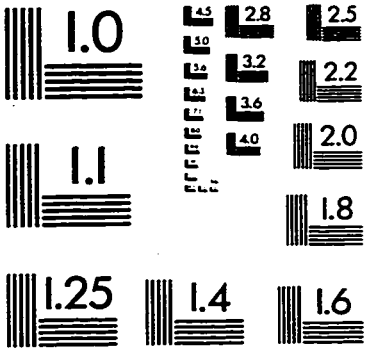

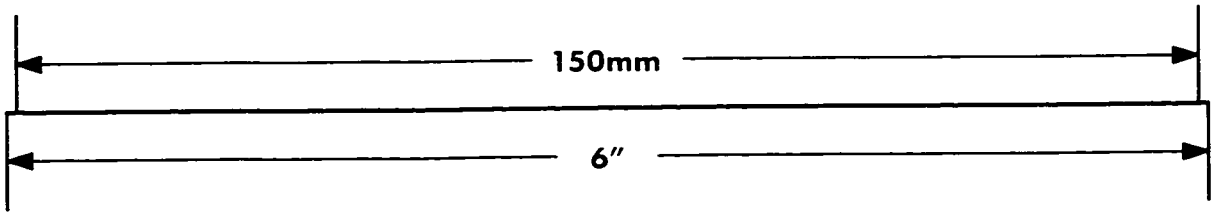

APPLIED IMAGE, Inc
1653 East Main Street
Rochester, NY 14609 USA
Phone: 716/482-0300
Fax: 716/288-5989

© 1993, Applied Image, Inc., All Rights Reserved